MASTER

FE-1514-57
UC-90c

Advanced Coal Gasification System for Electric Power Generation

WESTINGHOUSE ELECTRIC CORPORATION
GENERATION SYSTEMS DIVISION
LESTER, PENNA. 19113

RESEARCH AND DEVELOPMENT REPORT NO. 81

INTERIM REPORT NO. 5

FOR THE PERIOD JULY 1, 1976 - SEPTEMBER 30, 1976

PREPARED FOR:

U.S. ENERGY RESEARCH AND DEVELOPMENT ADMINISTRATION
FOSSIL ENERGY
GASEOUS FUELS
WASHINGTON, D.C. 20545

DISTRIBUTION OF THIS DOCUMENT IS UNLIMITED

DISCLAIMER

This report was prepared as an account of work sponsored by an agency of the United States Government. Neither the United States Government nor any agency thereof, nor any of their employees, makes any warranty, express or implied, or assumes any legal liability or responsibility for the accuracy, completeness, or usefulness of any information, apparatus, product, or process disclosed, or represents that its use would not infringe privately owned rights. Reference herein to any specific commercial product, process, or service by trade name, trademark, manufacturer, or otherwise does not necessarily constitute or imply its endorsement, recommendation, or favoring by the United States Government or any agency thereof. The views and opinions of authors expressed herein do not necessarily state or reflect those of the United States Government or any agency thereof.

DISCLAIMER

Portions of this document may be illegible in electronic image products. Images are produced from the best available original document.

ADVANCED COAL GASIFICATION SYSTEM FOR ELECTRIC POWER GENERATION

Report E(49-18)-1514-57

Research and Development Report No. 81 - Interim Report
No. 5
Report for the Transition Quarter
Period July 1 - September 30, 1976

Prepared for
ENERGY RESEARCH AND DEVELOPMENT ADMINISTRATION
FOSSIL ENERGY - GASEOUS FUELS
Contract No. E(49-18)-1514

"This report was prepared as an account of work sponsored by the United States Government. Neither the United States nor the United States ERDA, nor any of their employees, nor any of their contractors, subcontractors, or their employees, makes any warranty, express or implied, or assumes any legal liability or responsibility for the accuracy, completeness, or usefulness of any information, apparatus, product or process disclosed, or represents that its use would not infringe privately owned rights."

NOTICE
This report was prepared as an account of work sponsored by the United States Government. Neither the United States nor the United States Energy Research and Development Administration, nor any of their employees, nor any of their contractors, subcontractors, or their employees, makes any warranty, express or implied, or assumes any legal liability or responsibility for the accuracy, completeness or usefulness of any information, apparatus, product or process disclosed, or represents that its use would not infringe privately owned rights.

Prepared By
GENERATION SYSTEMS DIVISION
WESTINGHOUSE ELECTRIC CORPORATION
LESTER, PA. 19113

DISTRIBUTION OF THIS DOCUMENT IS UNLIMITED

BIBLIOGRAPHIC DATA SHEET	1. Report No. FE-1514-57	2.	3. Recipient's Accession No.
4. Title and Subtitle Advanced Coal Gasification System for Electric Power Generation, Research and Development Report No. 81 - Interim Report No. 5			5. Report Date October 15, 1976 6.
7. Author(s) L. A. Salvador and D. Keairns			8. Performing Organization Rept. No.
9. Performing Organization Name and Address Westinghouse Electric Corporation Generation Systems Division P.O. Box 9175 - Lester Branch Philadelphia, PA 19113			10. Project/Task/Work Unit No. WG-45930-T3 11. Contract/Grant No. ERDA E(49-18)-1514
12. Sponsoring Organization Name and Address U.S. Energy Research and Development Administration CCU-Fossil Energy Washington, D.C. 20545			13. Type of Report & Period Covered Transition Qtr July 1 - Sept. 30, 1976 14.

15. Supplementary Notes

16. Abstracts

A unique coal gasification system employing multiple fluidized beds has been embodied into a Process Development Unit located at Waltz Mill, Pa. The two main process loops are at present arranged for independent operation. The devolatilizer/desulfurizer subsystem has been under test on coal since October, 1975. That program ended during this quarter after a 168-hour continuous run processing two highly-caking Pittsburgh seam coals. The gasifier/agglomerator subsystem is now being prepared for test operation.

17. Key Words and Document Analysis. 17a. Descriptors

Fluidizing	Synthesis Gas Generators*	Exhaust Emissions
Fluidized Bed Processing	Gas Purification	Erosion Corrosion
Fluidized Bed Processors	Dolomite	Agglomeration
Coal Gas	Combustion	Gasifier Agglomerators*
Manufactured Gas	Combustion Deposits	Devolatilizer/Desulfurizers*
Gasification	Exhaust Gases	Gas Turbine Power Generation
Gas Generators	Desulfurizer	

*New Term (not in Thesaurus)

17b. Identifiers/Open-Ended Terms

Advanced Coal Gasification
Process Development Units

17c. COSATI Field/Group 0701, 0704, 0807, 1001, 1113, 1307, 1308, 1309, 1407, 2102, 2104

18. Availability Statement	19. Security Class (This Report) UNCLASSIFIED	21. No. of Pages 189
	20. Security Class (This Page) UNCLASSIFIED	22. Price 7.50

ABSTRACT

A unique coal gasification system employing multiple fluidized beds has been embodied into a Process Development Unit located at Waltz Mill, Pa. The two main process loops are at present arranged for independent operation. The devolatilizer/desulfurizer subsystem has been under test on coal since October, 1975. That program ended during this quarter after a 168-hour continuous run processing two highly-caking Pittsburgh seam coals. The gasifier/ agglomerator subsystem is now being prepared for test operation.

TABLE OF CONTENTS

TABLE OF CONTENTS

(Continued)

LIST OF TABLES

LIST OF FIGURES

1.0 OBJECTIVE AND SCOPE OF WORK

The overall objective of the Westinghouse coal gasification program is to produce a clean low-Btu gas from high-caking, sulfur coal that will meet environmental standards but yet have enough heating value to drive a turbine that will produce electrical energy. In order to achieve this goal, the program is divided into several areas of development, each with individual goals but all working toward the same end result.

1.1 PHASE I, TASK 2 - OPERATION OF THE PDU

Before adequate and reliable designs for a large-scale generating plant can be achieved, a combination of analytical studies, bench-scale experiments and semi-works or pilot scale evaluations are essential, particularly for areas of new technology. The Westinghouse PDU program provides this bridge in knowledge and experience between small scale operations and a scaled-up plant.

The objective of Task 2 is operation of the PDU to evaluate the process feasibility and operability of the Westinghouse coal gasification process as it is currently conceived with the devolatilization and in situ desulfurization of coal in one fluidized bed and with complete combustion and gasification of the char along with agglomeration of the ash in a second fluidized bed reactor.

The initial work in this task involved the evaluation of the devolatilizer subsystem. Shakedown and operating tests, reactor design tests, and feasibility demonstrations were conducted with a variety of coal feedstocks. The present work involves evaluation of the gasifier-agglomerator subsystem through a series of tests similar to those conducted in the devolatilizer. Eventually, the two reactors will be integrated and operated together.

1.2 PHASE I, TASK 2A - MODIFICATIONS TO THE PDU

This task deals with modifications to reactor piping and controls to achieve integrated operation. The objectives are to design, procure and install piping and controls for series operation of the devolatilizer and gasifier.

1.3 PHASE I, TASK 3 - LABORATORY SUPPORT STUDIES

Support studies are being conducted to provide background information on process technology, to provide PDU design data, to project operating

conditions for the PDU, to provide troubleshooting capability during PDU operation and to develop design data for larger plants. Primary areas of investigation include: fluidization and fluid-particle systems, coal behavior, ash agglomeration, sorbent behavior and reactor analysis.

Fluidization studies are directed toward development of the devolatilizer and the combustor-gasifier units. Test facilities include a flexible, one-foot diameter semi-circular unit which operates at atmospheric pressure and ambient temperature, a four-inch scale pressurized unit and atmospheric pressure units. The semi-circular unit has been used for investigation of important devolatilizer design parameters (area ratio of downcomer/draft-tube, draft tube height, distributor plate design, methods of solid feeding); operating parameters (flow ratio of downcomer/draft-tube, amount of downcomer aeration); and startup and shutdown procedures in relation to solid circulation rate, jet penetration length, solids mixing and gas bypassing. A pneumatic transport line of 2.54 cm I.D. is an integral part of this experimental system so that concentric solid feeding into the reactor similar to that of the PDU can be simulated.

The semi-circular model was modified during this reporting quarter such that it simulates the PDU combustor-gasifier unit. Operation will be initiated in the next quarter to investigate design parameters, operating procedures, and startup and shutdown procedures.

The coal behavior program complements the fluidization model studies and includes coal behavior in the devolatilizer, char behavior in the gasifier and ash behavior in the agglomerating combustor. Data are obtained on kinetic rates, product gas composition, tar formation and char characteristics. A fluidized bed test unit, operating at design temperature and pressure, is being used for the supporting investigations. An ash agglomeration test unit is being constructed for investigation of ash agglomeration.

The calcium-based sorbent studies provide data to support PDU, to recommend process options for first generation plants, to project operating conditions for investigation in the PDU, to develop design and operating criteria and to evaluate the potential for advanced systems. Work was previously conducted to develop sorbent selection criteria, a once-through process, regenerative process options, spent sorbent disposition options, and to provide technical and economic assessment of the alternatives. A pressurized thermogravimetric analysis system, differential thermal analysis and a pressurized, high-temperature fluidized bed test unit have been used to conduct these investigations. The primary objectives during this quarter were to support the PDU operation during the tests using dolomite sorbent.

Mathematical analyses are performed on the gasification process using the collected data and the reactor performance at different reactor configurations and at different operating conditions.

Solids fluidization and transport investigations are conducted as needed to provide data to complement information from the PDU. Objectives are to provide a basis to develop models and scaling relationships to design and predict performance of the PDU and larger scale fluidized bed gasification plants.

2.0 SUMMARY OF PROGRESS TO DATE

2.1 PHASE I, TASK 2 - OPERATION OF THE PDU

A feasibility demonstration test with two highly-caking coals from the Pittsburgh area was successfully completed. TP-010 was conducted with and Upper Freeport seam coal from the Renton Mine and with a Pittsburgh seam coal from the Champion Plant of Consolidation Coal Company. Both of these coals had Gieseler plasticity indices of over 25,000 ddm and free-swelling indices of 7 to 9, placing them amongst the potentially most highly-caking varieties of Eastern U.S. coals.

Renton coal was successfully processed in the devolatilizer for 115 hours and Champion coal for about 72 hours prior to a planned, normal shut-down. About 34 tons of Renton and 17 tons of Champion coal were processed to produce 31 tons of devolatilized char. Nominal conditions for the test were as follows:

Coal Feed Rate	500 - 700	lb/hr
Freeboard Velocity	2.3 - 2.5	fps
Inlet Gas Temperature	2050 - 2150	°F
Reactor Bed Temperature	1450 - 1600	°F
Reactor Pressure	225	psi
Bed Height	16 - 18	feet
Gas Throughput	5000 - 5400	lb/hr
Char Production Rate	250 - 420	lb/hr

The run was considered a successful demonstration of the recirculating draft tube concept in processing caking coals without pretreatment. This test is the last test of the devolatilizer reactor for these initial evaluation tests. Attention will now focus on the gasifier-agglomerator subsystem.

2.2 PHASE I, TASK 3 - LABORATORY SUPPORT STUDIES

Support work on fuel processing was conducted to investigate operating conditions for the PDU test program, provide troubleshooting capability for PDU operation, obtain data for PDU modifications, analyze and interpret results from the PDU operation and develop information for future process development. Primary effort was providing support for the PDU in areas of fluidization and fluid-particle systems, coal behavior, ash behavior, sorbent behavior, and reactor analysis.

1. Fluidization and Fluid-Particle Systems: Experimental results and analysis of simulated devolatilizer performance using the semi-circular model were conducted. Emphasis was on the develop-

ment of startup and shutdown procedures and the effect of draft tube diameter on performance. The semi-circular model was modified such that it now simulates the PDU combustor-gasifier unit. A test program was developed which will be implemented during the next quarter. Results are presented on the simulation of the separation of agglomerated ash from the agglomerating combustor. Experimental results indicate that >95% separation of the agglomerated ash can be achieved. An alternative technique to pressure drop measurements for monitoring the char-ash interface is being investigated. Data for the design of an electrical conductivity probe are presented.

2. Coal Behavior: A report summarizing the coal devolatilization studies was completed and an experimental procedure for studying the effect of char dust on coal agglomeration was developed. In devolatilization experiments in which fuel gas was used as the fluidizing agent in place of nitrogen, substantial increases in methane and ethylene production were observed.

   The experimental program on the gasification rate of PDU chars with steam and carbon-dioxide was continued and a reaction model was developed.

3. Ash Behavior: Assembly of the ash agglomeration combustor is underway and should be completed in September, 1976.

4. Reactor Analysis: Material and energy balances on the gasifier-combustor are in progress. Results of char gasification studies will be used in the balances.

2.3 SUMMARY SCHEDULES

2.3.1 PHASE I, TASK 2 - OPERATION OF THE PDU

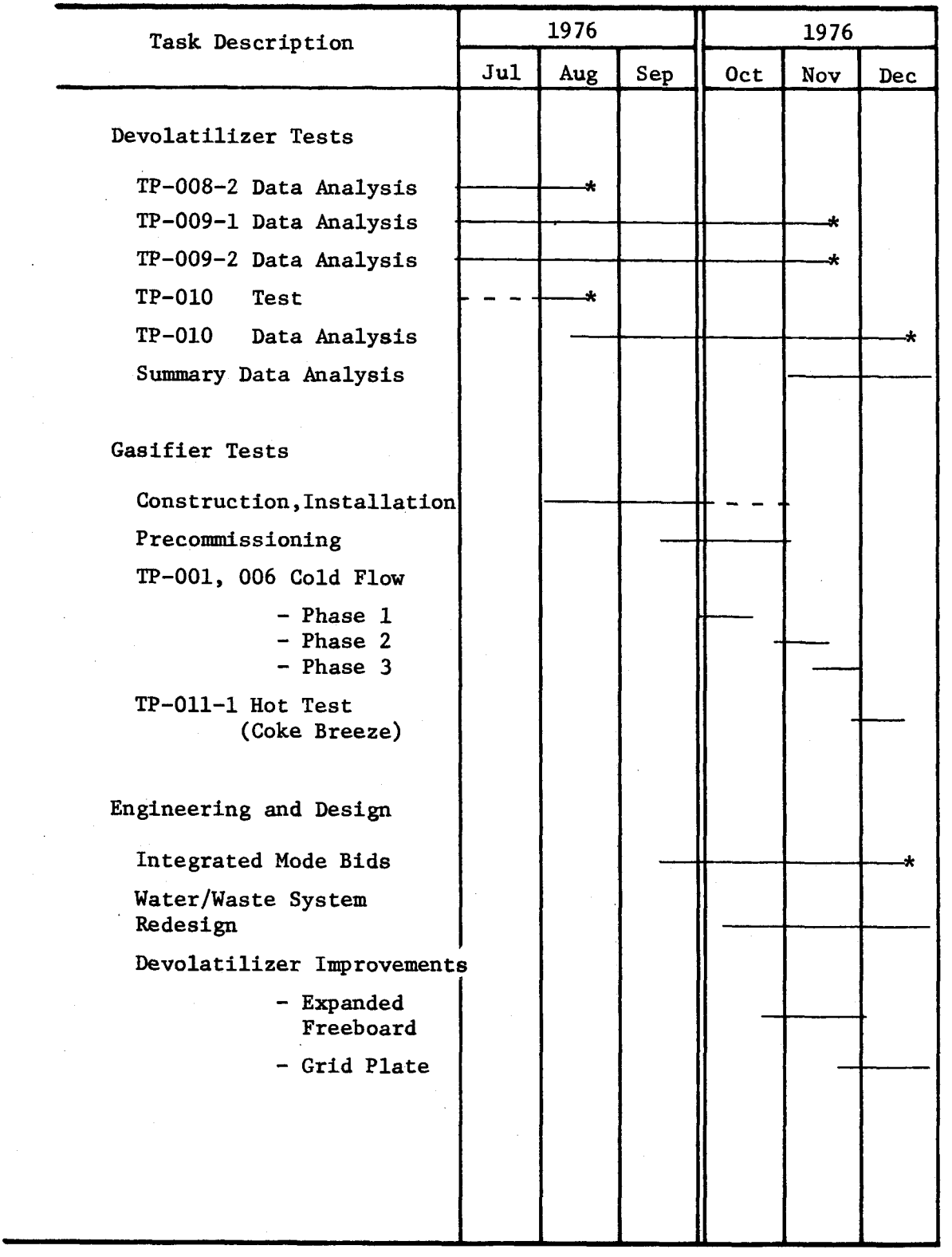

2.3.2 PHASE I, TASK 3 - LABORATORY SUPPORT STUDIES

Task Description	1976			1976		
	Jul	Aug	Sep	Oct	Nov	Dec
Fluidization & Fluid-Particle						
Devolatilizer Hydrodynamics	———	———				
Combustor-Gasifier Hydrodynamics			▽1 ———	———	———	———
PDU Operation Interfaces	———	———	———	———	———	———
Instrumentation	———	———	———	———	———	———
Coal Behavior						
Devolatilization	———	———	———	———	———	
PDU Char Gasification Kinetics			———	———	———	———
Ash Behavior						
Ash Agglomeration Behavior	———	———	———	———	▽2 ———	———
Sorbent Behavior						
PDU Support						
Reactor Analysis						
Devolatilizer Modeling	———	———	———	———	———	———
Combustor-Gasifier Material/ Energy Balance Projections	———	———	———	———	- - -	- - -
Combustor-Gasifier Modeling					———	———

▽1 Initiate Semi-Circular Model tests simulating PDU combustor -gasifier.

▽2 Initial operation of ash agglomeration test unit.

3.0 DETAIL DESCRIPTION OF TECHNICAL PROGRESS

3.1 PHASE I, TASK 2 - OPERATION OF THE PDU

3.1.1 Devolatilizer Tests

3.1.1.1 Work Accomplished

Plans were reviewed with ERDA for a demonstration test with highly-caking coals, and a final decision was made on the coal selection and test conditions. Discussions were also held with Bert Forney, ERDA consultant, and with Mr. Baumburger of Consolidation Coal Company. Test conditions specified were:

Coal Feed Rate	700 lb/hr
Duration of Test	7 days
Coals Selected	Renton (Upper Freeport) - 4 days Champion (Pittsburgh#8) - 3 days
Freeboard Velocity	2.2 fps
Inlet Temperature	2000-2200°F

The final test plan document and detailed operating procedures were released for TP-010. Meetings were held with all operating and engineering test personnel to instruct them on test objectives and test run details. Raw materials were ordered from Consolidation Coal Company and were processed by Penn-Rillton Company to a size distribution of 6x100 mesh. Approximately 44 tons of Renton coal and 30 tons of Champion coal were received from Penn-Rillton. Properties of these coals are shown in Table 3.1-1.

After the TP-010 test plan was released, conversations were held with ERDA concerning a study of char particle size during this run. A test plan Addendum was issued to provide for an experimental run to determine the effect of inlet flow ratio, coal feed rate, freeboard velocity, bed height, and temperature on bed and overhead particle size and rate. Test points in this plan were:

Test Point	1	2	3	4	5	6	
Coal Feed Rate	700	700	500	700	700	700	lb/hr
Freeboard Velocity	2.2	2.2	2.2	2.2	2.2	1.9	fps
Inlet Temperature	2150	2150	2150	2150	1950	2150	°F
Bed Height	16	20	16	16	16	16	feet
F-111/F-110 Flow Ratio	0.75	0.75	0.75	1.00	0.75	0.75	

TABLE 3.1-1 PROPERTIES OF COALS USED IN TEST TP-010

	Renton	Champion
Size, Wt. Mean, Micron	1000	700
Bulk Density, Lb/Ft^3	43.63	43.55
Percent Volatiles	35.56	35.00
Percent Carbon	53.86	49.00
Percent Moisture	1.68	6.50
Percent Ash	8.90	9.50
Percent Sulfur	1.42	1.90
Ash Fusion Reducing, I.D., °F	2510	2440
Ash Fusion Reducing, H=W, °F	2570	2560
Ash Fusion Reducing, H=1/2W, °F	2600	2610
Ash Fusion Reducing, Fluid, °F	2650	2640
Free Swelling Index	8 - 9	7 - 9
Gieseler Plasticity, ddm	30,000	25,000
Gieseler Softening °F	725	732
Gieseler Max. Fluidity, °F	814	822
Solidification, °F	895	895
Heating Value, Btu/Lb	13,650	12,570

Systems preparations were completed and TP-010 was initiated on July 22, 1976. During heatup, a high pressure drop was observed across the quenched product gas line between the quench scrubber and the contact cooler. Efforts to clear the line were unsuccessful, and a decision was made to remove the line from the structure and replace it with a new line. Upon inspection, it was found that the line's 4-inch I.D. was reduced to one inch by deposits of char and fines from previous tests. A new line was fabricated and installed, and testing resumed on July 28.

Test TP-010 was successfully conducted from July 28 through August 9, 1976 using two highly-caking coal feedstocks.

Hot air dryout of the reactor and pressurization of the plant systems was completed by July 30 when the heatup phase was completed by obtaining test data to establish heat loss from an empty reactor. Following heatup, char feed to the reactor was initiated. The startup phase was modified to include an 18-hour reactor stabilization period using char feed to build and establish a bed. Then, a 12-hour Minnehaha coal feed period was initiated at 400 lb/hr to stabilize reactor temperatures and to establish operation of the drawoff systems before initiating Renton coal feed.

Renton coal feed was successfully initiated on August 1, at a feed rate of 650 lb/hr. Thirty-four tons of Renton coal, having a Gieseler plasticity of 30,000 ddm and a free-swelling index of 8 to 9, were processed for 115 hours, yielding 21 tons of char and fines before changing over to Champion coal feedstock. Champion coal feedstock (Gieseler plasticity of 25,000 ddm and free-swelling index of 7 to 9) was initiated on August 6 and was continued for 72 hours before implementation of a planned shutdown. Char and fines produced during the Champion portion of this test run equaled about 10 tons. During operation with Renton and Champion coal feeds, several 10-hour steady-state test periods were established at various operating conditions to investigate particle size and elutriation rates. Preliminary data defining nominal test conditions for these periods are shown in Table 3.1-2. Figure 3.1-1 is a comparison of the planned and actual test run history.

Two major disruptions were experienced in normal operation during the 217 hours of continuous operation.

On August 2, a delay in delivery of CO_2 disrupted operation for ten hours. Conservation of CO_2 consumption was accomplished by discontinuing purge flows to pressure taps, with the exception of those in the reactor, and CO_2 was exchanged by steam in synthesis gas generator operation to maintain reactor temperatures. Bed height was maintained by intermittently feeding char from the dolomite lockhopper. During resumption of CO_2 usage, on August 2, the synthesis gas generators were shut down when a high-pressure excursion was noted on the reactor pressure indicator. It was realized later that this was apparently a false reading based on the manipulation of valves for re-introducing CO_2 to the purge taps. The burners were restarted within minutes of the shutdown and the bed was refluidized.

TABLE 3.1-2 TEST CONDITIONS FOR TP-010 STEADY-STATE PERIODS

	Renton Feedstock			Champion Feedstock		
Test Period	#1	#2	#3	#4	#5	#6
Coal Feed Rate, Lb/Hr	648	530	531	456	562	584
Transport Gas , Lb/Hr	501	470	794	786	1091	1019
Freeboard Velocity, Ft/Sec	2.31	2.37	2.40	2.44	2.38	2.43
F-110 Gas Inlet Temperature, °F	2104	2128	2100	2043	2043	2076
F-111 Gas Inlet Temperature, °F	2105	2106	2120	2164	2148	2208
Flow Ratio (F-111+RGS)/F-110	0.77	1.00	0.78	0.95	0.93	0.71
Reactor Bed Temperature, °F	1520	1552	1500	1520	1512	1527
Reactor Exit Temperature, °F	1504	1522	1480	1498	1440	1443
Reactor Pressure, Psig	222	225	225	225	225	230
Bed Height, Feet	16-18	16-18	16-18	16-18	15-17	15-17
Total Exit Gas Rate, Lb/Hr	5080	5130	5331	5348	5244	5320
Char Withdrawal Rate, Lb/Hr	234	153	158	74	113	32
Fines Withdrawal Rate, Lb/Hr	183	190	191	207	230	235
Steady-State Periods, Hours	18	10	16	8	4	7
Bed Density from PDT-48, Lb/Ft^3	10.5	13.5	9.0	17.7	26.0	24.0
Bed Density from PDT-47, Lb/Ft^3	10.5	17.0	18.0	24.4	24.7	27.0
Bed Density from PDT-46, Lb/Ft^3	9.5	14.5	15.3	26.2	24.7	25.0
Bed Particle Size, Wt.Mean, Micron	1180	--	1420	--	1250	1260
Bulk Density of Char, Lb/Ft^3	22.3	--	22.7	--	28.5	27.0

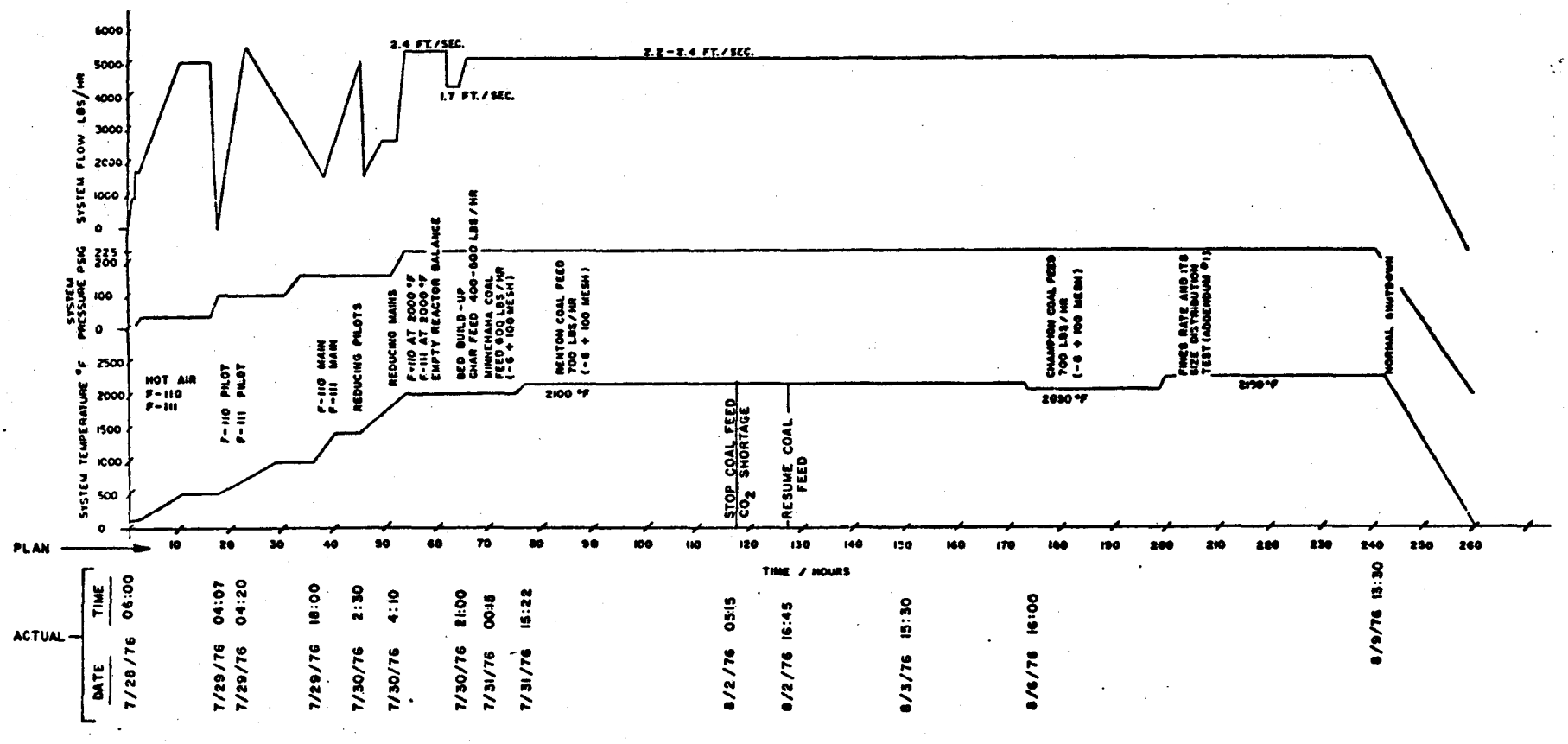

Figure 3.1-1 Comparison of the Planned Vs. Actual TP-010 Test History

On August 4, the F-122 heater, used to heat recycle gas for transporting the feed coal, became inoperative. Plugging of the coal feed line was experienced due to a low transport velocity. Six hours of interrupted coal feed were accumulated before this problem was resolved by increasing the mass flow rate through the line by the addition of CO_2 makeup flow. Unfortunately, with an added heat load of cold CO_2, the reactor could not be maintained at a temperature of 1500°F or greater at the higher planned coal feed rate of 700 lb/hr. Lower values of 450 to 600 lb/hr were subsequently used.

Temperature profiles were stable during the test and showed less of a gradient axially along the bed than in some previous tests. Figures 3.1-2 and 3.1-3 illustrate these trends. Differential pressure data indicate that bed densities for Renton coal were on the order of 10 to 20 lb/ft^3 and on the order of 25 to 30 lb/ft^3 for Champion coal. Both coals produced spherical, free-flowing particles of char with a bulk density of 20 to 25 lb/ft^3. Typical gas analyses during a typical material balance period are shown in Table 3.1-3.

TABLE 3.1-3 TP-010 TYPICAL GAS ANALYSES

	August 1, 1976, 11:30 AM, Data Point #1		
	F-110, Dry	F-111, Dry	Product Gas, Wet
CO	15.87	12.01	15.50
H_2	5.94	4.66	8.79
CO_2	14.56	27.27	15.20
CH_4	--	--	2.50
N_2	62.75	55.30	54.93
O_2	0.85	0.75	0.73
H_2O	--	--	2.40
	99.97	99.99	100.05

Following termination of test TP-010, the PDU was inspected for component damage, and results of this inspection and a summary of anomalies were discussed at a post-test debriefing of all management, engineering and technician personnel.

The reactor was in good condition as far as refractory was concerned, however, some carbon deposits were observed in the outlet pipe and near the reactor exit. Additional carbon buildup was noted downstream of the

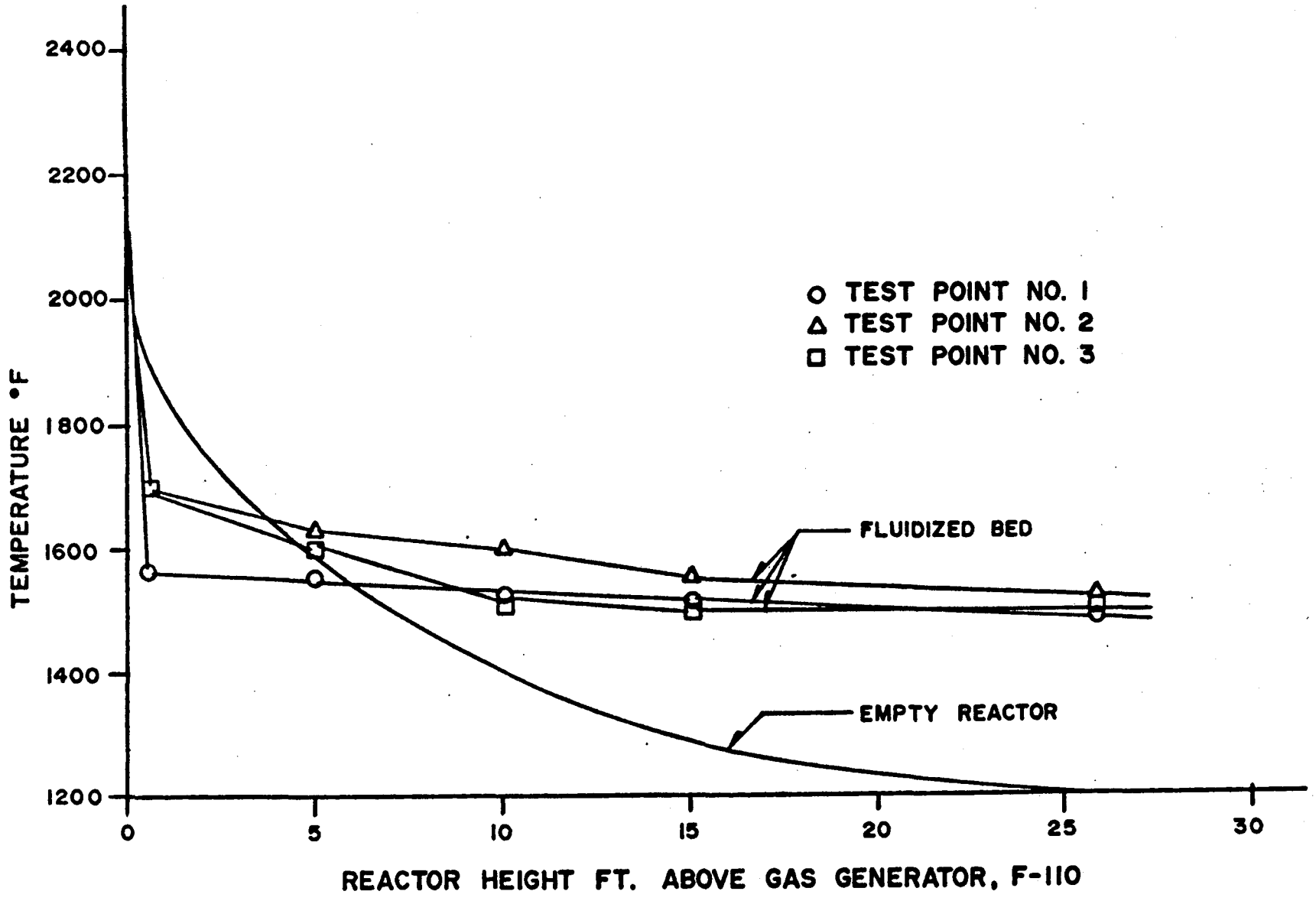

Figure 3.1-2 TP-010 Reactor Temperatures for Renton Coal

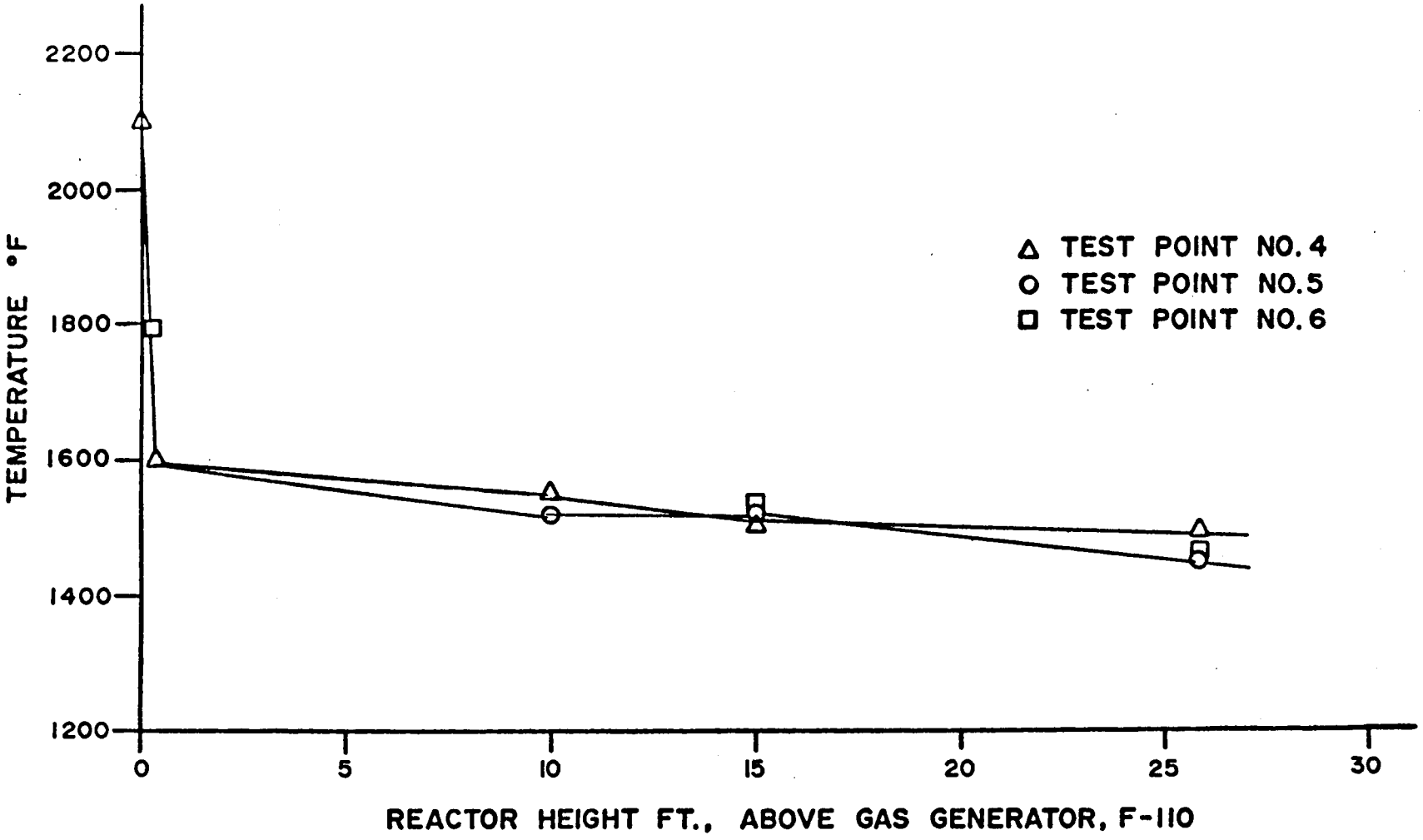

Figure 3.1-3 TP-010 Reactor Temperatures for Champion Coal

cyclone and in the quenched product gas line from the quench scrubber to the first contact cooler. The buildup of material in the exit piping from the cyclone was probably the result of carbon laydown at temperatures of 1200°F and less, due to high heat losses in the exit piping. The buildup in the quenched product gas line was a result of fines entrainment from the quench scrubber due to relatively high gas velocities in the unit. A small plug was observed near the top of the draft tube. As in the previous test with highly-caking coal, test data is being reviewed to determine when this plug developed. It is unlikely that the plug developed during early portions of the test with Renton coal; however, it is possible that it developed later in the test with Champion coal or during shutdown.

During post-test debriefing, a partial list of components were identified that operated inadequately during TP-010 and will require engineering, maintenance, modification or repair effort. These include: belt weighers, transport gas heaters, transport gas valves, Starwheel feeders, heater temperature controls, pressure instruments, and water and waste handling valves. Items that will be disassembled for thorough inspection and maintenance check prior to plant restart include: synthesis gas generators, fines cyclone, contact cooler, quench scrubber, char drawoff pot, all pumps and controls on the cooling water system, process air compressor, glycol cooling system and recycle gas compressor.

Playback of TP-010 data was completed and data analysis was initiated. Analyses of solids samples and of data from various gas characterization apparatus were given high priority. Final analyses of data, including heat and material balances, will be completed in the next quarter.

Test TP-010 was the last run in this initial series of PDU evaluations of the Westinghouse coal gasification process. Attention will now focus on evaluation of the gasifier-agglomerator.

TP-010 was a significant milestone in the program because it demonstrated operability of the process with highly-caking, Eastern U.S. coals without pretreatment with air or oxygen. Since pretreatment processes are inherently costly and inefficient (they consume some carbon from the coal and require additional reactors), TP-010 accomplishments are significant. It offers an option for handling caking coals at greater overall process efficiency. Table 3.1-4 summarizes the important accomplishments and problems encountered during TP-010.

Reduction of data on tests TP-009 and TP-010 continued, and a meeting was held with all test coordinators (Tests TP-007, TP-008-1, TP-008-2, TP-009-1, TP-009-2 and TP-010) to outline requirements for a summary analysis of all results from the devolatilizer tests that were conducted in the past year. This work was initiated at a low level of effort but will be emphasized when the data reduction and analysis for tests TP-009 and TP-010 are completed. A final summary is scheduled to be completed by January 1977.

TABLE 3.1-4 TEST TP-010 ACCOMPLISHMENTS AND TECHNICAL PROBLEMS

ACCOMPLISHMENTS

- 186 Hours of Devolatilizer Operation with Highly-Caking Coals:
  - 115 Hours of Renton Coal Feed at 500-650 lb/hr
  - 71 Hours of Champion Coal Feed at 450-600 lb/hr
- Produced 21 Tons of Renton Char and Fines
- Produced 10 Tons of Champion Char and Fines
- Attained 10 Steady-State Periods with 6 Points Designated as Variable Operating Conditions for Reactor Evaluations
- Performed Particle Size Test against Reactor Parameters
- Demonstrated Ability to Process Fresh, Caking Coals without Pretreatment
- Determined Heat and Material Balances, Reactor Temperature and Pressure Profiles and Other Operating Parameters for Three Eastern Coals
- Planned, Normal Shutdown

TECHNICAL PROBLEMS

- Heater in Coal Feed Line Failed Resulting In:
  - Limitation in coal feed rate to 600 lb/hr.
  - Increased elutriation rate into the cyclone.
  - Increased freeboard velocity and F111 burner temperature to compensate for cooling effect by increased cold transport gas.
- Product Gas Scrubbing System Plugged with Entrained Solids
- Char Drawoff System Difficulties due to a Low Bed Level and Inherent Design Geometry Inadequacies Requiring Correction
- Intermittent Blockage in Downcomer with Char due to Low Temperatures Resulting from Heater Failure (last day of the test run)

Particle size distributions of feed coal, bed char, cyclone char fines product, and blended char and char fines products were examined based on data received from TP-009 and TP-010 for Minnehaha and Renton coals. The distributions were plotted as cumulative weight per unit versus particle diameter and as weight per unit versus particle diameter. Estimates were then made as to the amount of fines one would expect to be elutriated from the bed under the assumption that no attrition and no agglomeration of coal particles were occurring. These data are shown in Tables 3.1-5 and 3.1-6 and on Figures 3.1-4 and 3.1-5.

Conclusions that can be drawn from these analyses are:

1. Both particle growth and reduction take place in the devolatilizer as a result of inter-particle impact, devolatilization, gasification, agglomeration and popcorning.

2. Fines and oversize fractions of the blended product are produced from the mid-range coal size (note the bi-modal char distribution).

3. Net production of zero to 200 micron material is on the order of 10 percent of the coal feed.

4. As expected, elutriation is a function of freeboard velocity and initial coal particle size.

5. The amount and distribution of overhead product is essentially that which would be elutriated from the bed as coal fines except for a fraction in the zero to 200 micron size range. For example, one can essentially predict overhead product based on the particle size of the coal feed and on the operating velocities in the reactor as if no attrition or agglomeration were dynamically occurring.

The average "fines" particle diameter was about 400μ for Renton coal and about 300μ for Minnehaha coal which corresponds to averages of 210μ as used by Bechtel in designing the PDU agglomerating combustor and of 600μ as used by IGT in their agglomerator. The rates of fines and char production for these two coals were:

	Renton (lb/hr)	Minnehaha (lb/hr)
Coal Feed Rate	648	515
Char Withdrawal	234	215
Fines Product	184	100

TABLE 3.1-5 PARTICLE SIZE DISTRIBUTIONS FOR MINNEHAHA COAL AND CHAR PRODUCTS, TP-009

Micron Size (Range)	Coal Feed (lb/hr)	Bed Char (lb/hr)	Overhead Char (lb/hr)	Blended Product (lb/hr)	Predicted Elutriation* (lb/hr)
0- 200	0.0	0.0	58.5	58.5	0.0
200- 400	38.7	7.5	21.0	28.5	17.8
400- 600	59.2	6.7	11.0	17.7	23.0
600- 800	61.7	11.6	6.5	18.1	13.9
800-1000	56.6	16.1	3.0	19.1	5.6
1000-1200	61.7	21.5	0.0	21.5	0.0
1200-1400	59.2	25.8	0.0	25.8	0.0
1400-1600	54.1	31.2	0.0	31.2	0.0
1600-1800	46.4	31.2	0.0	31.2	0.0
1800-2000	38.7	26.9	0.0	26.9	0.0
2000-2200	20.6	19.4	0.0	19.4	0.0
2200-2400	18.1	10.7	0.0	10.7	0.0
2400-2600	0.0	6.4	0.0	6.4	0.0
2600-2800	0.0	0.0	0.0	0.0	0.0
Totals	515.0	215.0	100.0	315.0	60.3

* Based on simple devolatilization of coal feed without attrition or agglomeration and the consideration of velocity, plugging and other fluid dynamic mechanisms.

TABLE 3.1-6 PARTICLE SIZE DISTRIBUTIONS FOR RENTON COAL AND CHAR PRODUCTS, TP-010

Micron Size (Range)	Coal Feed (lb/hr)	Bed Char (lb/hr)	Overhead Char (lb/hr)	Blended Product (lb/hr)	Predicted Elutriation* (lb/hr)
0- 200	0.0	9.4	40.5	49.9	0.0
200- 400	90.7	11.7	46.0	57.7	47.4
400- 600	97.3	11.7	38.6	50.3	49.0
600- 800	97.2	16.4	23.9	40.3	37.8
800-1000	84.2	18.7	13.8	32.5	23.5
1000-1200	64.8	21.1	8.3	29.4	12.0
1200-1400	58.3	25.8	5.5	31.3	6.7
1400-1600	45.4	23.5	3.7	27.2	3.7
1600-1800	35.6	25.8	3.7	29.5	2.7
1800-2000	25.9	23.4	0.0	23.4	0.0
2000-2200	19.4	18.7	0.0	18.7	0.0
2200-2400	16.2	14.0	0.0	14.0	0.0
2400-2600	13.0	8.2	0.0	8.2	0.0
2600-2800	0.0	5.6	0.0	5.6	0.0
Totals	648.0	234.0	184.0	418.0	182.8

* Based on simple devolatilization of coal feed without attrition or agglomeration and the consideration of velocity, plugging and other fluid dynamic mechanisms.

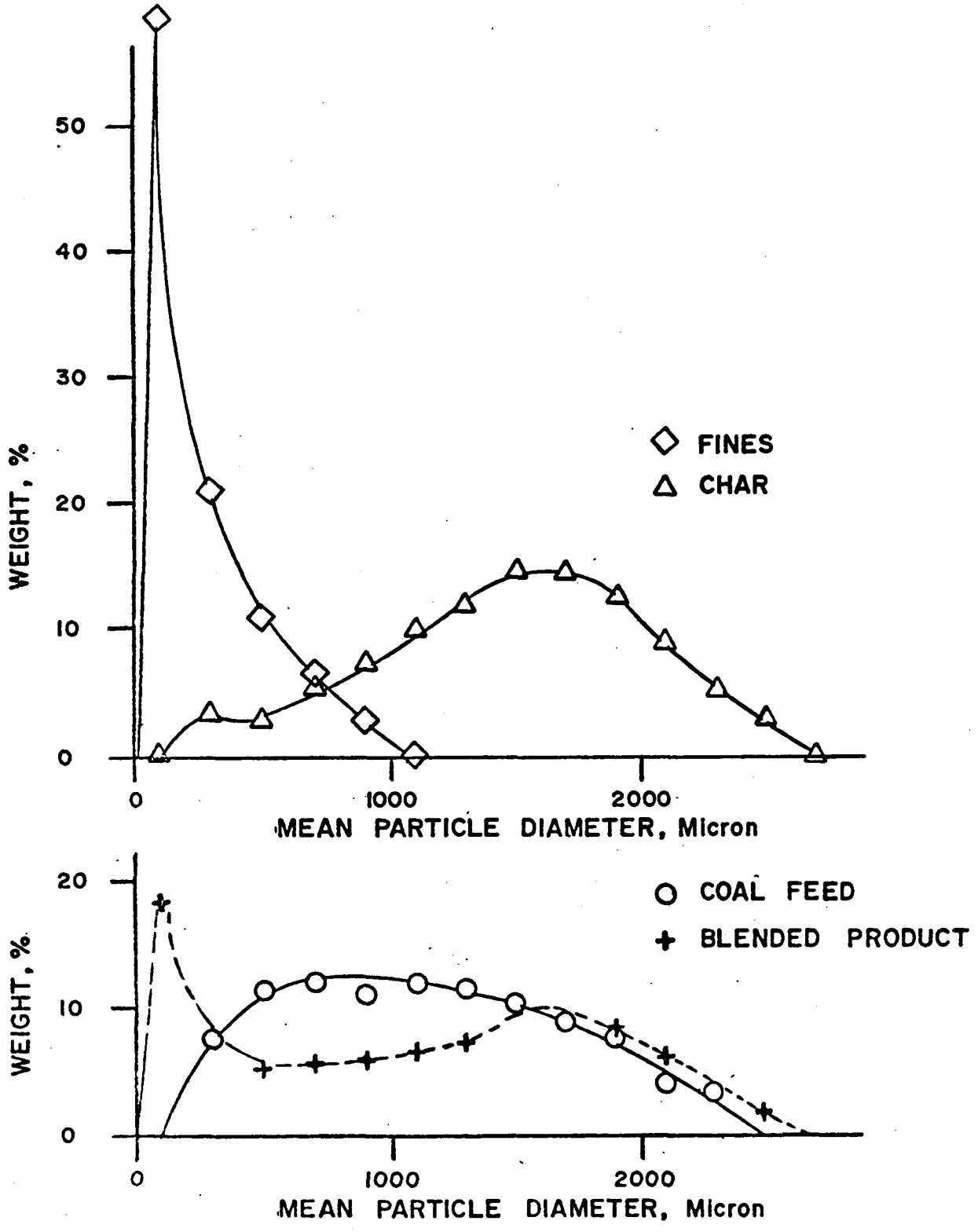

Figure 3.1-4 Particle Size Distributions of Char and Fines Products, TP-009-1 Minnehaha Coal

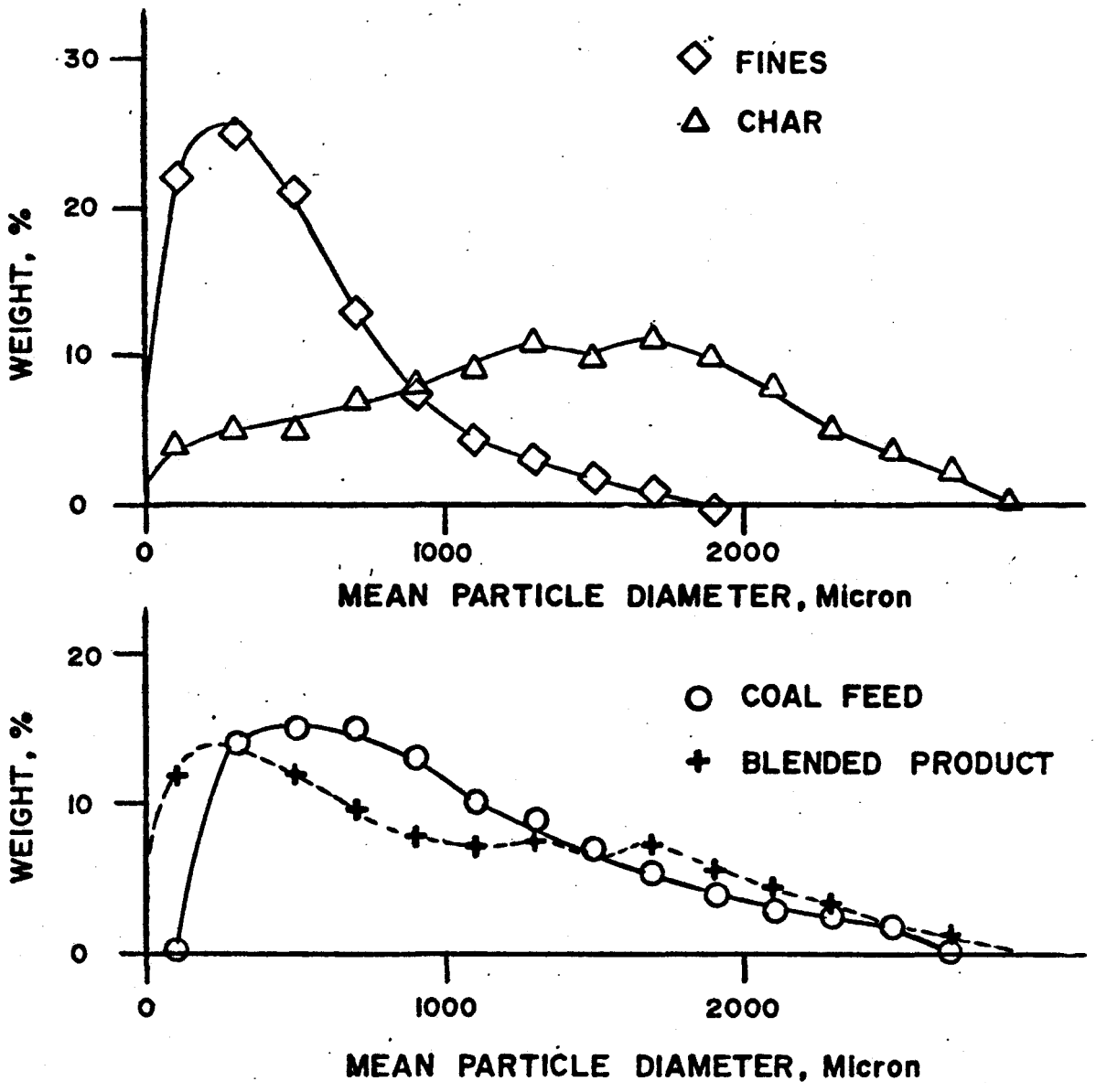

Figure 3.1-5 Particle Size Distributions of Char and Fines Products, TP-010 Renton Coal

Corresponding agglomerating combustor requirements for the PDU at these feed rates of coal would be 180 lb/hr and 140 lb/hr for the two coals based on the original gasifier process design. The fines production rates of the devolatilizer, therefore, were compatible with the requirements of the agglomerator both in terms of particle size and rate. Further work will be performed with the particle size study to include results for Champion coal and to evaluate effects of temperature and other parameters on particle size of product char.

3.1.1.2 Work Forecast For Next Quarter

Complete data analyses for the devolatilizer test series. Recommend revisions to the system for further tests in CY-1977.

3.1.2 Gasifier Tests

3.1.2.1 Work Accomplished

Test planning for gasifier-agglomerator evaluations received major attention following termination of TP-010. The overall gasifier PERT and schedule were updated, startup materials were selected, personnel assignments were made, and drafting of plans and procedures was begun. The basic gasifier plan and tentative schedule are shown below.

		Start	End
• Construction and Checkout of System		7/76	10/76
• Shakedown and Operability Tests:			
TP-001	Subsystem Operability & Checkout	10/76	10/76
TP-006	Solids feed, Discharge, Fluidization, Solids Recirculation, and Ash-Char Interface Studies (cold flow)	10/76	11/76
TP-011	Hot Operability Test of Agglomerating Combustor and Gasifier	12/76	12/76
• Reactor Design Tests, TP-012		1/77	3/77
• Feasibility Demonstration, TP-013		3/77	6/77

Detailed planning of the cold flow tests (TP-001/TP-006) and the first hot test (TP-011) continued. The test plans for TP-001 and TP-006 were drafted along with operating parameter tables and both documents are being reviewed. Switch and alarm settings were specified and work began on specifying an instrumentation signal list.

The work schedule was reviewed with Test Operations personnel, and a task list and schedule were defined. An extensive work list for the gasifier is in progress with work being conducted in the following areas:

1. Mechanical Completion of the System
   - Field inspection and drawing update.
   - Install startup burner and controls.
   - Modify C-119 cyclone.
   - Modify C-102, C-103, C-105 lockhoppers.
   - Install new instrumentation.
   - Modify air tube and instruments on C-115.
2. Precommission Plant Subsystems
3. Test Planning
   - Write operating manual.
   - Write test plans.
   - Coordinate construction activities.
4. Safety and Reliability
   - Failure mode analysis.
   - Hazards analysis.
   - Safety Committee reviews.
5. Technical Support
   - Data acquisition system revisions.
   - Modelling and theoretical analysis.
   - Alternate design concept analysis.
6. Test Operations
   - Write operating procedures.
   - Train Operations personnel.
   - Conduct tests.

Personnel from WESO, Waltz Mill, and Fluidization Research, Churchill, met at the Westinghouse R&D Center to formulate an approach for constructing analytical models for the gasifier. Operating conditions were specified. Thermodynamic data were compiled and a general agreement was reached on kinetic and equilibrium models for the combustor and gasifier. Work was also started on developing the model for heat transfer between the combustor and gasifier.

Various vendors were contacted concerning material availability for conducting the gasifier test program. Conversations were held with Mr. Bair (IGT) and Mr. Tewkesberry (Battelle) to evaluate various candidate materials. These consultations resulted in procurement of four materials

for startup and for initial test phases in the combustor and gasifier:

1. Startup Ash Material - 20 tons of dead-burned dolomite will be procured from J. E. Baker Company of York, PA, in a size range of 12x30 mesh. This material will be employed for simulating an ash bed and for experiments to determine heat transfer between the gasifier and combustor.

2. Agglomerating Seed Material - 20 tons of MULCOA 60 refractory will be procured for use as a seed material with the char to initiate ash agglomeration. This material may also be used in place of the dead-burned dolomite to simulate the ash phase on startup. It contains 60% aluminum oxide, 25% silicon dioxide and 1% iron oxide, and it will be obtained in an 8x20 mesh size.

3. Combustor Feed - Because product char from the devolatilizer tests is limited, 25 tons of coke breeze will be procured from McCormick Company of Pittsburgh with a size distribution to simulate the devolatilizer cyclone product ($\sim$ 40 mesh). This material is available in any size range and is composed of devolatilized coal from various coking operations in the Pittsburgh area.

4. Gasifier Feed - 25 tons of coke breeze in the size range of 4x40 mesh will be procured from the McCormick Company to simulate the devolatilizer char product material.

A meeting was held with representatives from IGT to discuss their work with the agglomerating combustor and to compare the analytical and bench-scale modelling work being performed at IGT and Westinghouse. IGT is planning to build a semi-circular model of their agglomerator which will be four feet in diameter. This meeting was highly successful with an interchange of information on reactor design, modelling, and test operation.

3.1.2.2 Work Forecast For Next Quarter

The change-over of the PDU to the gasifier mode of operation will be completed. Construction and precommissioning will be accomplished, and both cold flow (TP-001, TP-006) and hot flow tests (TP-011) will be conducted.

3.1.3 PDU Engineering and Design

3.1.3.1 Work Accomplished

Waste material dump valves from the cooling water system were redesigned based on experience gained in the two long-duration tests. New valves were procured to incorporate stellite balls and seats to prevent erosion of the seats during the dump cycle. This work is only a portion of a larger task which will involve complete redesign and upgrading of the cooling water and waste handling systems for the PDU.

A review of piping used in the waste handling and cooling water systems is underway to determine safety problems that may exist due to the use of Schedule 40 pipe in low-pressure applications. This study resulted from two TP-010 test piping failures which resulted from excessive corrosion coupled with the use of threaded connections on pipe in an environment including vibrations and mechanical stresses. Pipe will be modified to include only Schedule 80 pipe in such applications. ANSI and NFPA Code requirements were incorporated into specifications for air and propane piping prior to their release.

A report was issued reviewing thermocouple performance during all tests run to this time. Performance of tungsten/tungsten-rhenium thermocouples in silicon carbide thermocouple wells has been excellent. Several instruments have over 1000 hours at high-temperature conditions of 1400°F and above.

Engineering effort is now directed to getting the gasifier system completed and on-line. Major design tasks accomplished were:

1. Raw materials handling requirements were defined. A vacuum conveying system will be used to transport fines from trucks to the D105 bin. The Aerodyne transport line from K106 compressor will be used for the filling operation.

2. Lockhopper expansion joint modifications were specified to eliminate load cell inaccuracies.

3. Starwheel feeder modifications were specified for handling char and fines.

4. Startup burner design was completed, including the flow loop, controls and flame management system.

5. A new 5 curie nuclear densitometer was ordered for measuring the ash-to-char interface in the combustor section of the gasifier. Application for a radiation permit was made through the Advanced Reactors Division Safety Department.

6. A mounting assembly for the pyrometer and flame scanner was completed.

7. Design of a removable air tube was completed which will permit changing the diameter and length of the air injection tube to achieve optimum geometry during gasifier testing. This unit is being fabricated. An evaluation of several alternate designs was completed. A welded transition joint will be used between the existing 4-inch line and the 2-inch extension.

8. A study of saltation velocity of dolomite was made to determine the feasibility of feeding dolomite as a bed startup material through the char transport line.

Redesign work for the water system and preparation packages for integrated operation were also initiated.

3.1.3.2 Work Forecast For Next Quarter

Continue work on integrated operation mode; revise drawings and bid packages. Complete gasifier redesign work.

3.1.4 PDU Maintenance and Operation

3.1.4.1 Work Accomplished

Following the last test with caking coals, activities were directed to PDU cleanup and inspection and performance of maintenance and repair tasks. All main vessels were opened for inspection and thorough cleaning. A major effort was directed toward cleaning the water and waste handling systems including: circulating water pumps, cooling towers, quench scrubber, waste tanks and thermal oxidizer.

Changeover of the PDU system from the devolatilizer mode to the gasifier mode was begun and involved: (1) changing certain lockhoppers from a coal mode to a char mode to feed the gasifier and (2) relocation of refractory-lined pipe from the devolatilizer cyclone to the gasifier cyclone. This work will increase in importance and quantity in the next quarter in order to complete gasifier system completion and checkout and precommission of that equipment.

The following is a work status summary for each major task:

1. Startup Burner - Piping installation was about half completed. Control panel wiring in the Control Room was completed. Fabrication of the flame management scanner mount is in progress.

2. Cyclone - The refractory-lined pipe from C119 to C111 quench scrubber was installed. A spool piece was installed from the cyclone to the C108 lockhopper. Modifications to the J-leg were begun. Flow meters for purges were installed.

3. Lockhoppers - Spool pieces were installed to change all lockhopper service from the devolatilizer mode to the gasifier mode. Installation of the new F117 char fines heater was begun.

4. Instrumentation - The Ircon infrared pyrometer was calibrated by the Standards Laboratory at Westinghouse R&D Churchill. Thermocouples were inventoried, and a sufficient quantity is available for several months of gasifier testing.

5. Gasifier Reactor - This unit was opened and inspected, and the refractory is in excellent condition. Installation of new pressure instruments was initiated.

In addition to the gasifier task list, the following normal maintenance and repair functions are in progress, based on the last year's operation of the devolatilizer:

1. Movement, storage and disposal of raw material and product solids.
2. Heat tracing repair and new installations.
3. Rework and repair of water and waste handling system.
4. Overhaul recycle gas, instrument air and process air compressors.
5. Repair of CO_2 vaporizer.
6. Replace leaking ball valves on lockhoppers.
7. Valve and instrument cleaning, repair and calibration.
8. Pump repair and assembly.
9. Plant winterization.

Operating procedures for the startup burner were completed. Procedures for all plant subsystems are being revised and are ready for issue to Test Operations personnel.

3.1.4.2 Work Forecast For Next Quarter

Complete gasifier installations, precommissioning and checkout. Complete major repair and maintenance tasks. Conduct TP-001, TP-006 and TP-011.

3.1.5 PDU Support Activities

Failure reports on PDU component failures were prepared and submitted to ERDA, Materials and Power Generation Division, as a result of implementation of ERDA's failure report system at WESO, Waltz Mill.

Two summer students were hired to assist in updating Government property inventory listings. Items are in the process of being located on the PDU structure and tagged with the process and property tags.

An analysis of thermal oxidizer stack gas emissions from test TP-010 was completed. Results of this analysis show that the measurement of SO_2 stack gas emissions of 5 to 20 ppm is well within the level of 144 ppm as defined in the original Operating Permit issued by the Pennsylvania Department of Environmental Resources.

A chemical analysis of char, liquid and gaseous samples is being performed at Westinghouse, Waltz Mill and Churchill, and at outside laboratories. This work will be complete for tests TP-009 and TP-010 within the next quarter.

3.2 PHASE I, TASK 3 - LABORATORY SUPPORT STUDIES

3.2.1 Fluidization and Fluid Particle Systems

3.2.1.1 Work Accomplished

The primary effort is directed toward support of the PDU operation test program and evaluation of data. The work reported includes: (1) experimental results and analysis of simulated devolatilizer performance using the semi-circular model, (2) modification of the semi-circular model to simulate combustor-gasifier operation, (3) experimental results on simulation of particle separation in the combustor-gasifier in a 10 cm fluidized bed unit, and (4) experimental data on the electrical resistivity of char-ash mixtures for the purpose of designing a conductivity probe to measure the char-ash interface.

1. Devolatilizer Model Studies: The semi-circular model (Interim Report No. 2, 1974; FE-1514-T-4) was effectively used to support the development and to investigate startup and shutdown procedures for the PDU.

   The semi-circular model was used to investigate the effect of the draft tube diameter prior to converting the unit to simulate the PDU combustor-gasifier design. A series of 15 experimental runs were performed in the semi-circular model with a 5 cm I.D. draft tube. Visual measurement of the particle velocity at the wall, using a stop-watch, indicated a much smaller particle velocity (less than 0.5 in/sec) as compared to the case with a 9.55 cm I.D. draft tube (3 to 6 in/sec particle velocity). This is in accord with earlier projections (see Interim Report No. 3, 1975; FE-1514-T-9). Gas bypassing was also studied by injecting CO_2 gas tracer into the downcomer gas supply and by taking gas samples from both the draft tube side and the downcomer side. Negative gas bypassing (gas bypassing from the draft tube side to the downcomer side) was observed in most of the cases except where high solid transporting gas existed. The results indicate the diameter ratio of the draft tube and the draft tube gas supply nozzle and the distance between them are also important variables to consider in design. The data are now under analysis to compare the performance between the two different sizes of draft tube. The initial results are presented here.

1. Devolatilizer Model Studies: (continued)

There are three gas inlets, as shown in Figure 3.2-1, in the present gas bypassing study. Besides the regular downcomer and draft tube gas supplies, a concentric solid transport tube was added to simulate the concentric coal feeding nozzle in the PDU. Based on the analysis of the turbulent jets of incompressible fluid in a coflowing external stream, the gas bypassing data for the case with a 9.55 cm I.D. draft tube are plotted as shown in Figure 3.2-2. The coordinates in Figure 3.2-2 are defined as

Percent gas bypassing (1)

= (Total gas in draft tube determined experimentally - total gas supplied through the draft tube supply - total gas supplied through the transport tube)/Total gas supplied through the downcomer supply.

M_2 = 2 x Gas velocity in the downcomer side/(Gas velocity in the draft tube supply nozzle + Gas velocity in the solid transport tube) (2)

The gas velocities in Eq. (2) are evaluated as follows:

Gas velocity in the downcomer side (3)

$$= \frac{\text{Total Gas Supplied through downcomer gas supply}}{\text{Total Column Cross-sectional Area - Cross-sectional Area of draft tube gas supply and solid transport tube}}$$

Gas velocity in the draft tube supply nozzle (4)

$$= \frac{\text{Total Gas Supplied through the draft tube gas supply}}{\text{Cross-sectional Area of draft tube gas supply}}$$

Gas velocity in the solid transport tube (5)

$$= \frac{\text{Total Gas Supplied through the solid transport tube}}{\text{Cross-sectional Area of solid transport tube}}$$

In defining Eq. (3), the assumption was made that the bed itself served as an effective gas distributor plate and that the gas, though jetted out horizontally through the nozzles, soon dissipated into a uniform plug flow vertically. The mathematical model developed here seems to describe the gas bypassing phenomena adequately as shown in Figure 3.2-2. The detailed model will be presented after additional refinement.

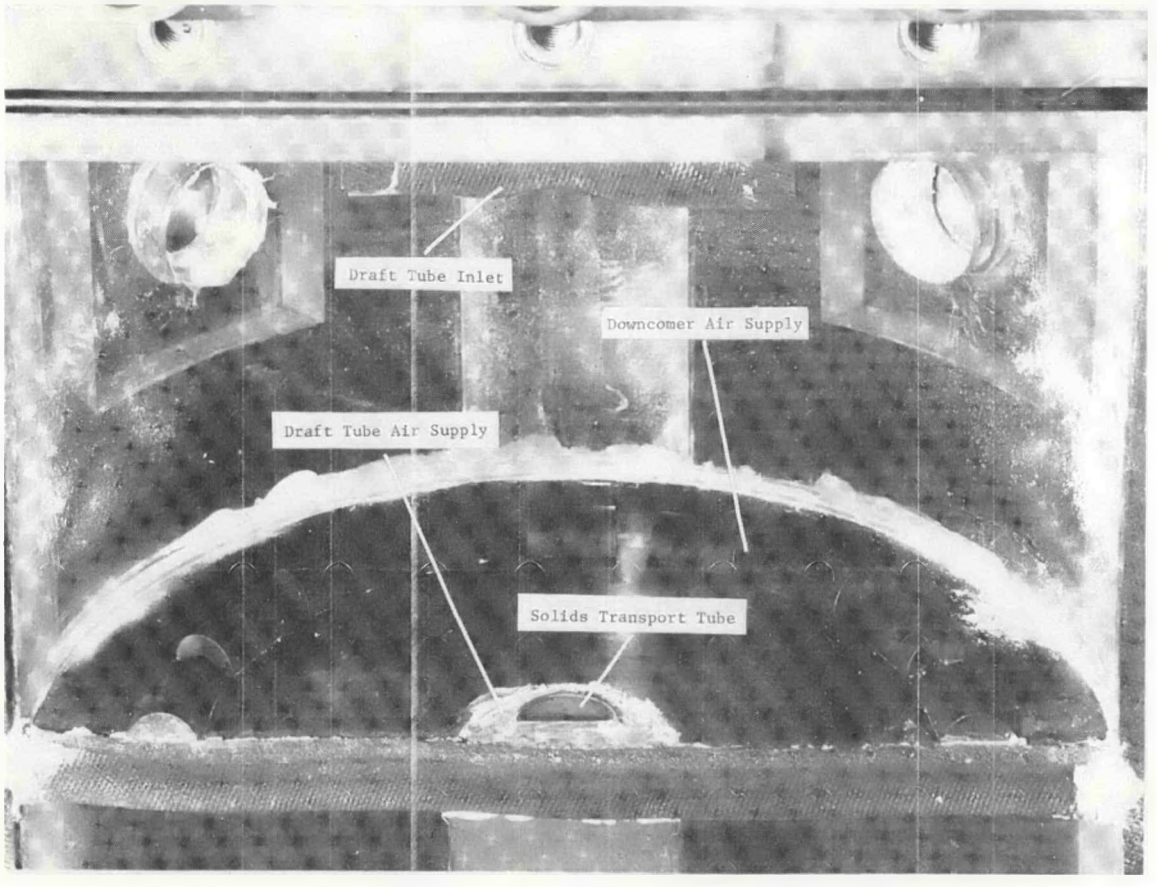

Figure 3.2-1 Design of Grid Plate Region

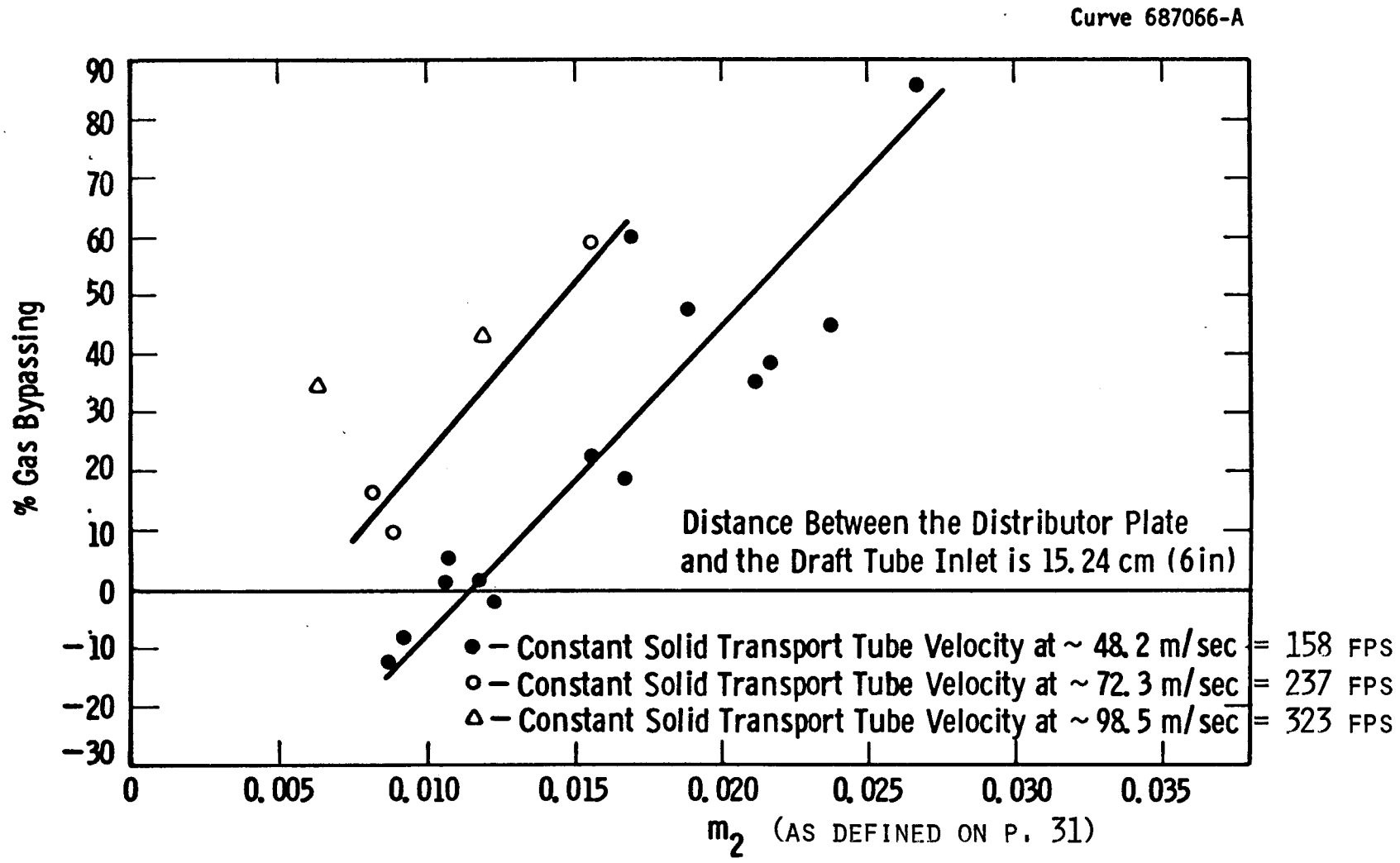

Figure 3.2-2 Gas Bypassing Data with A 9.55 cm I.D. Draft Tube

1. Devolatilizer Model Studies: (continued)

Increasing the velocity ratio between the downcomer side and the draft tube side tends to increase the percentage of gas bypassing from the downcomer to the draft tube. Increase in the velocity to the solid transport tube has the same effect as well. This confirms the earlier gas bypassing projection (presented in Interim Report No. 3, 1975; FE-1514-T-9) based on calculations by applying the modified Ergun equation to the downcomer side substituting gas-solid slip velocities for gas velocities. The flow ratio defined as the flow-to-the-draft-tube/flow-to-the-downcomer was used as the horizontal coordinate in the earlier projection. The flow ratio can be easily converted to the velocity ratio used in Figure 3.2-2. The velocity ratio is preferred because it is derived from the basic consideration of coflowing turbulent jets.

However, the present model does not provide good correlation for the data with a smaller 5 cm I.D. draft tube. Further analysis is being conducted.

Considerable difficulty was encountered in starting the recirculating bed with the smaller 5 cm I.D. draft tube. The draft tube gas supply tended to bypass into the downcomer and slug the downcomer. To circumvent this difficulty, the draft tube gas supply was turned off during startup. The draft tube gas was supplied via the concentric smaller solid transporting tube. This is another indication of the importance of the diameter ratio between the draft tube and the draft tube gas supply nozzle and the distance between them.

Several radio pills were dropped into the column for measuring the solid particle velocity; however, no results were obtained. The radio pills were not recirculating with the bulk solids, and the low solid circulation rate might be the reason why they were inactive. Or, the radio pill might be partially buried inside the stagnant region above the grid plate. As a result, the solid circulation rate was measured visually with a stop watch during the experimental series with the 5 cm I.D. draft tube. The solid circulation rate data are also under analysis. Results from these tests are important for considering scaleup of the devolatilizer concept.

The semi-circular unit was modified for combustor-gasifier simulation. Two expanded sections have been installed in the freeboard and the structural modification to accommodate the new sections has been completed (see Figure 3.2-3). This unit is ready for initial test runs. Discussions with PDU personnel have identified the priority tests in the support program for gasifier-combustor commissioning.

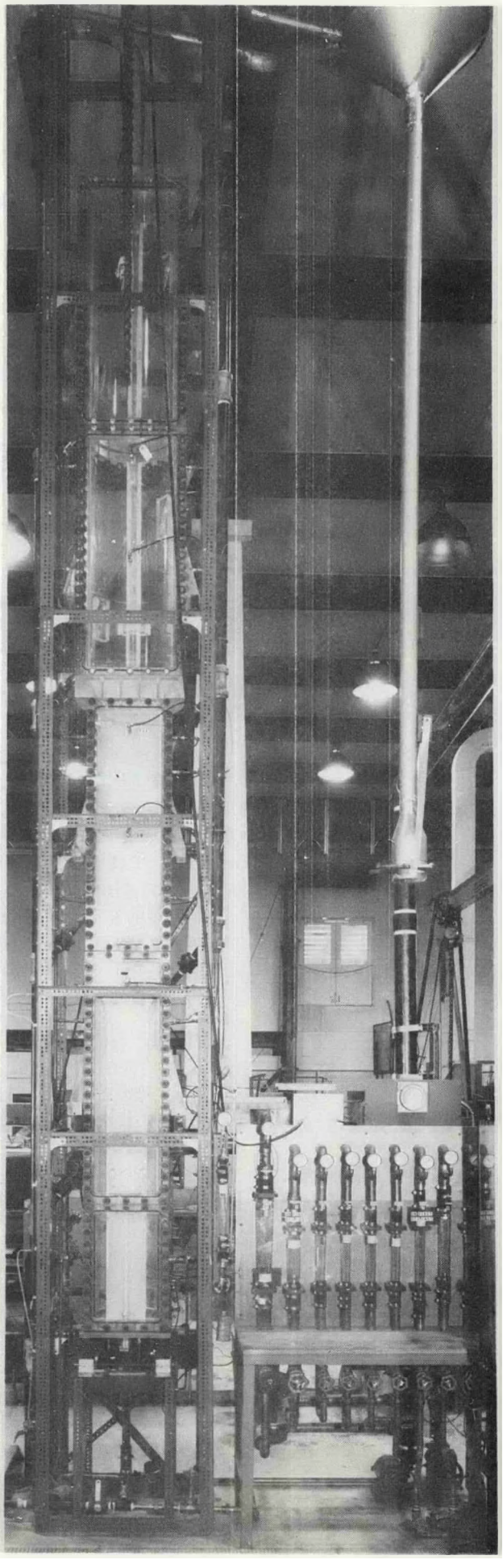

Figure 3.2-3

Modified Semi-Circular Unit for Combustor-Gasifier Simulation

1. Devolatilizer Model Studies: (continued)

Important parameters in operating the gasifier-combustor were identified and each individual parameter is being separately evaluated. The important parameters, beside char gasification rate and the energy and material balances are illustrated:

- Location of jet nozzle supplying air and steam to combustor.
- Location of char fines feed point relative to the air nozzle.
- Solid circulation rate between the gasifier and combustor.
- Startup and shutdown procedures.
- Degree and rate of char-ash separation.
- Detection and control of char-ash interface.
- Ash agglomeration rate.
- Particle size of char fines and their combustion time.

The majority of these parameters will be studied in the semi-circular cold model.

2. Particle Separation: Particle separation tests were previously conducted in a 10.2 cm pressurized model and a 11.4 cm low-pressure model to simulate separation of ash in the agglomerating combustor unit. Particle separation operating at a low gas velocity near the minimum fluidization velocity of the mixture and at a high gas velocity near the terminal velocity of the mixture was investigated. The models were used to investigate alternative agglomerating combustor concepts and to identify critical design and operating parameters. The PDU design utilizes the concept of separating the agglomerated ash at a low gas velocity. The data indicate that >95% separation of the agglomerated ash from char at a rate of $\sim$400 kg/min-m^2 of the separator cross-sectional area can be achieved. This is based on an operating velocity of 1 to 1.5 times the minimum fluidizing velocity of the agglomerated ash. A report on this investigation is presented in Appendix A.

The semi-circular model will be used to check the projections from the 10 cm units and to extend the investigation.

3. Measurement of Char-Ash Interface: The char and ash concentrations in the combustor-gasifier are projected to range from a high char concentration (>75%) in the gasifier to a high ash concentration (>90%) in the char-ash separator. Measurement of the char-ash concentration in the PDU combustor-gasifier will assist in achieving maximum efficiency in reactor performance and control. The primary method to be used to measure char-ash concentrations will be pressure drop measurements. Since it is important to obtain data on the char-ash concentrations in order to understand reactor behavior, alternative measurement techniques are being investigated. An electrical conductivity probe represents one of these alternatives.

   The electrical resistivity difference between char and ash can be utilized to develop an instrument for distinguishing a char-rich mixture from an ash-rich mixture. Development of design data for an electrical conductivity probe to measure and control the char-ash interface has been conducted. The experimental results show that resistivities of mixtures of less than 50 wt percent of ash are similar. A higher ash concentration rapidly increases the resistivity. Criteria for a conductivity probe are developed based on the data and a semi-empirical model for predicting resistivity. Details of the investigation are presented in Appendix B. The performance of such a probe at the operating temperature and pressure has not been demonstrated. Tests are planned in one of the laboratory units and a probe design has been conceived for the PDU.

3.2.1.2 Work Forecast For Next Quarter

Data obtained from the semi-circular unit simulating the devolatilizer configuration will be analyzed to develop a consistent theory for design and scale-up. The semi-circular unit has been modified into the gasifier-combustor configuration. Future tests will be on performing simulation experiments to support the PDU operation of the combustor-gasifier.

Particle separation tests will be incorporated in the semi-circular model test program. Measurement techniques to monitor char and ash concentrations will continue to be developed using the PDU, the semi-circular model and existing coal and ash behavior test facilities.

3.2.2 Coal Behavior

3.2.2.1 Work Accomplished

1. Devolatilization: A paper entitled "Coal Devolatilization Studies in Support of the Westinghouse Fluidized Bed Coal Gasification Process" was written which summarized the previous devolatilization test program and is attached as Appendix C. The contents of this paper were presented at the Symposium on Coal Processing and Conversion, sponsored by West Virginia Geological and Economic Survey, June 2-3, 1976, and the paper will be published in their Proceedings.

   The enhancement of hydrocarbon gas formation by hydrogasification during the devolatilization of Montour coal was studied in two experiments by using a fuel gas to fluidize the bed rather than nitrogen. In these tests, the production of methane increased 65% and the formation of ethylene increased 23%. One-fourth of the methane increase was due to reaction of the hydrogen in the fuel gas with the bed char. A comparable reaction forming ethylene was not observed.

2. Char Gasification: The modeling study to predict the char gasification rates has been completed based on assumed rate expressions. Since the reported variation of reaction rates of different types of chars is large, the prediction should be based on the experimental results for the particular char under consideration. The experimental program to obtain the rate expressions is underway. Predictions on gasification rates will be made upon completion of the experimental program.

   Experiments are being conducted in the same fluidized bed test unit that was used in the devolatilization study. A weighed quantity of char is placed in the reactor and heated to the desired temperature in nitrogen. The system is then pressurized to 10 atm and the bed is fluidized with a steam-nitrogen or a

carbon dioxide-nitrogen mixture of known composition. After stabilizing the gas flow rate and temperature, two samples of the off-gas are taken in evacuated bottles at a one-minute interval. The experimental conditions are then changed, and a second pair of gas samples are collected. Although each test period is of short duration, the number of sets of conditions that can be studied in a single run is limited by the extent of carbon loss from the bed. After the gas samples have been analyzed, a carbon balance is calculated for each period, based on the analytical results, the gas flow rate, and the time at conditions.

The reaction rate of Minnehaha char with steam at a temperature of 1800°F and a pressure of 10 atm has been obtained for different inlet concentrations of steam in nitrogen. The results are given in Table 3.2-1 below.

TABLE 3.2-1 REACTION RATE OF MINNEHAHA CHAR WITH STEAM

Partial Pressure of Steam (atm)	Reaction Rate (g of C/min/g of C)
2.83	0.030
1.65	0.044
1.16	0.049
0.90	0.043

These results do not follow the trend that can be expected with a change in the concentration of steam. This behavior may be due to the increase in the activity of char with reaction time.

The reaction rate of the char with CO_2 at a temperature of 1600°F and 1800°F, and a pressure of 10 atm, has also been obtained for different inlet concentrations of CO_2 in a mixture of CO_2 and N_2. The results are shown in Figure 3.2-4. It can be seen that the reaction rate increases by a factor of about 10 with an increase in the temperature from 1600°F to 1800°F. The order of the reaction also changes from 0.5 to about 0.8 indicating that the order is dependent on the temperature. Comparing the rates of the $C - CO_2$ reaction and the $C - H_2O$ reaction at 1600°F, the former is slower by a factor of about 10 at a partial pressure of 1 atm of the gaseous reactant.

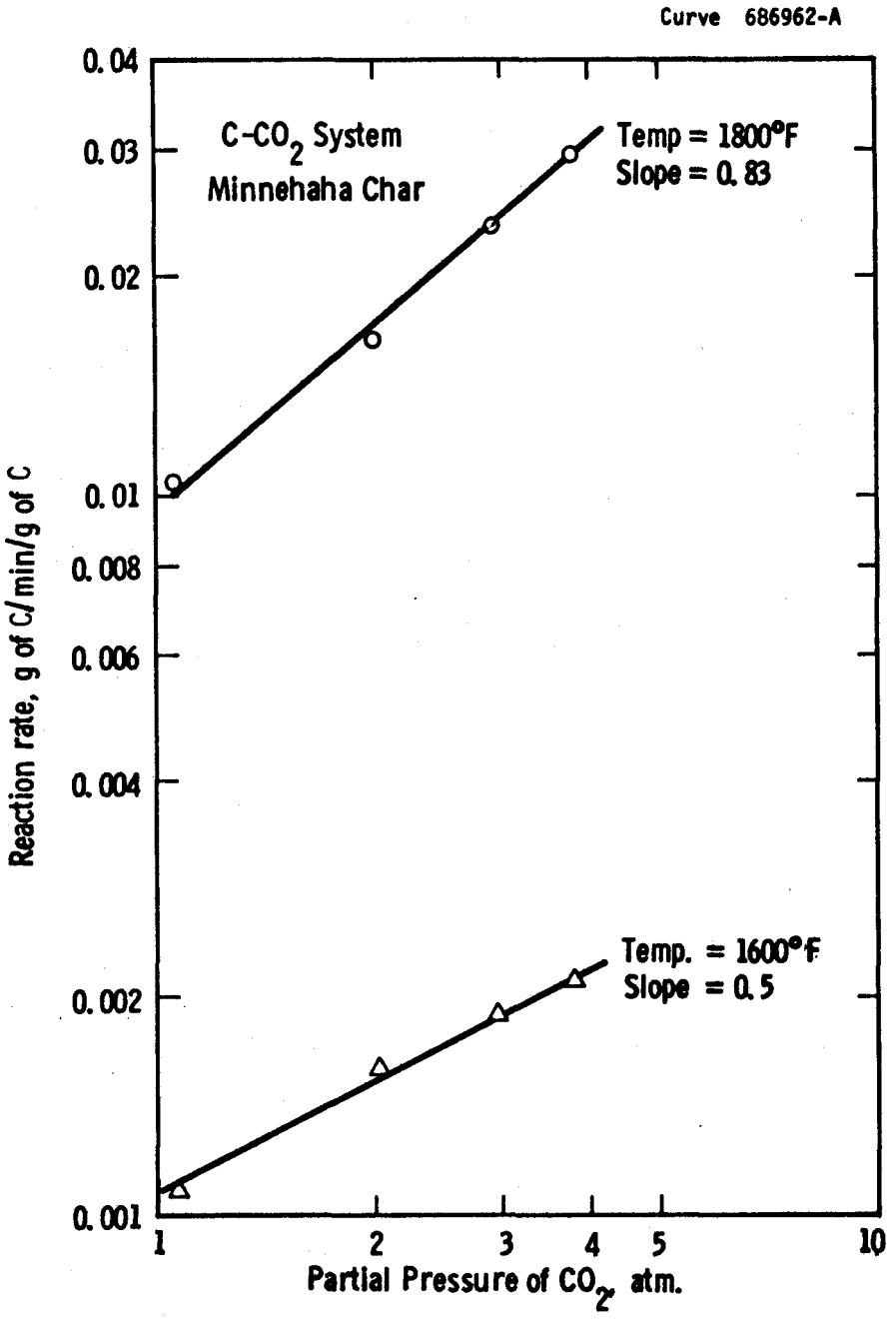

Figure 3.2-4 Reaction Rate of C - CO_2 Reaction

3.2.2.2 Work Forecast For Next Quarter

Coal behavior studies will continue the investigation of the effect of char dust on coal agglomeration in a fluidized bed. Gasification experiments with char from the PDU will also be continued, and the results will be applied to the development of a predictive gasification model.

3.2.3 Ash Behavior

3.2.3.1 Work Accomplished

A schematic diagram of the ash agglomeration combustor is shown in Figure 3.2-5. The reactor shell is made of Inconel 600, and the lining is composed of stabilized zirconia. The gasification capacity is 3.6 lb/hr of char, of which 1.5 lb/hr will be fed into the combustion zone with the air. The estimated requirements of air and steam are 3.5 ft^3/min and 0.062 lb/min, respectively.

Agglomerated ash for use as seed material in the bed at the start of a run has been obtained from IGT. On the basis of experience by IGT, who have successfully operated an ash agglomerator on coke breeze[1], coke breeze has been selected as the startup material for the present system.

Due to the loss of technician support during part of the report period, the ash agglomeration combustor was not completed as planned. Assembly of the equipment is now well underway and will be completed during the next quarter.

3.2.3.2 Work Forecast For Next Quarter

Complete assembly of the ash agglomeration combustor and conduct initial agglomeration tests with coke breeze. After completion of tests using coke breeze, the combustor will then be operated on PDU char.

3.2.4 Sorbent Behavior

3.2.4.1 Work Accomplished

A review of the high-temperature sulfur removal system development work was presented at the session on purification of low-Btu gas during the ACS meeting in San Francisco that was held August 29 through September 3, 1976. This paper is contained in Appendix D.

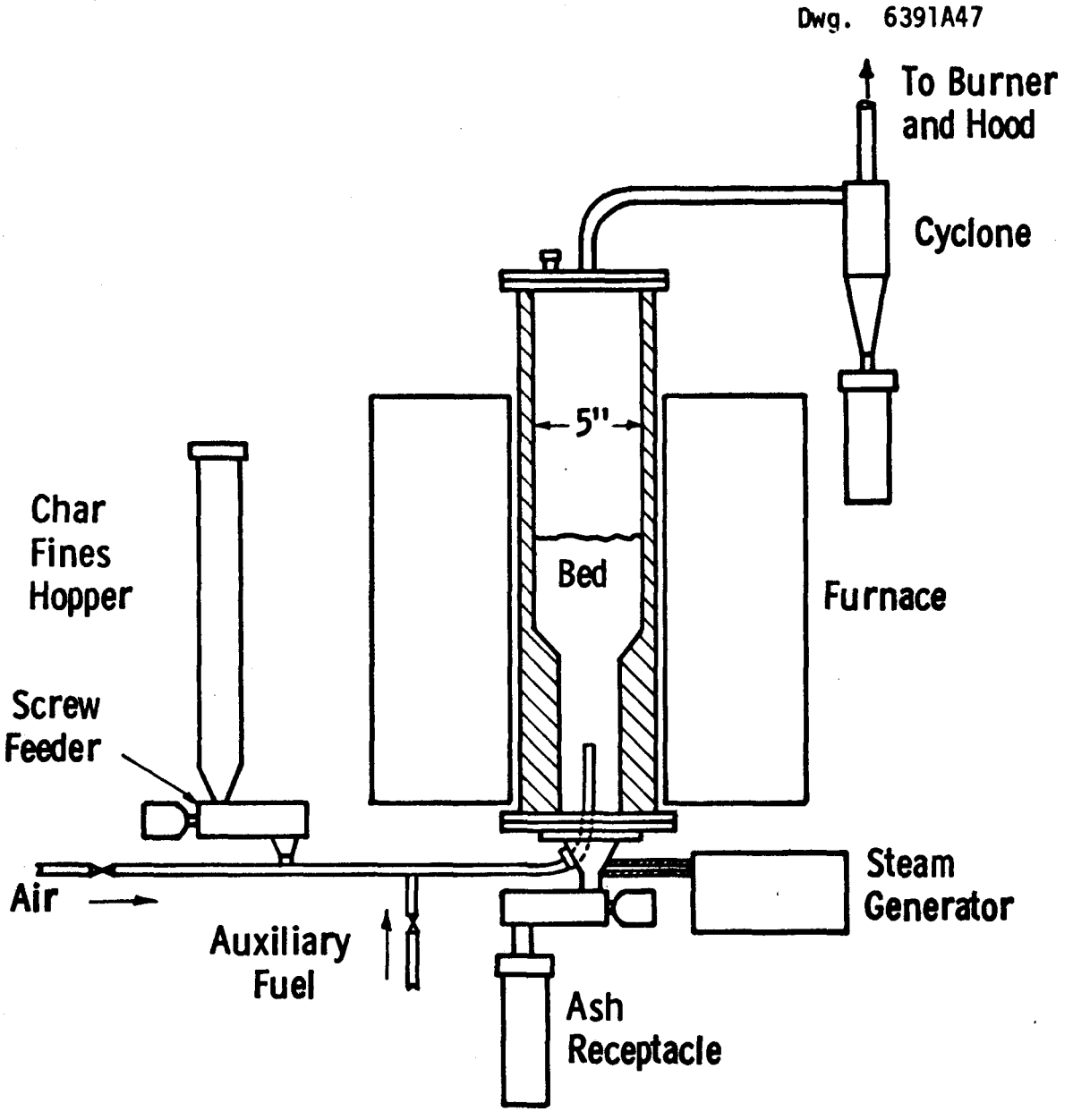

Figure 3.2-5 Ash Agglomeration Combustor

The primary effort during this quarter was in support of the PDU operation. Char-dolomite samples withdrawn from the PDU during TP-009-2 were examined in the TG apparatus. Using small portions of the samples and synthetic mixtures of known char-dolomite composition, it proved possible to determine the char-dolomite ratio in the samples by ignition of the sample to 600°C, followed by a second stage of heating at 900°C to calcine the calcium carbonate in dolomite. Representative portions of the PDU samples were taken by riffling and the char-dolomite ratios determined. Excellent agreement was obtained with direct analysis of the HCl soluble fraction of the mixture for Ca and Mg, assuming the dolomite had converted to $MgO \cdot CaCO_3$ (half-calcined dolomite). The dolomite in the samples was half-calcined, as expected. Conditions during the test were unfavorable for detecting the desulfurizing action of the dolomite due to the large excess of dolomite over sulfur in the input coal, and the high CO_2 gas content and low temperature which give a very low thermodynamic potential for reaction with hydrogen sulfide.

Examination of the samples, before and after ignition in the TG showed that some of the dolomite is embedded in the char particles. Further work is in progress to determine the reactivity of the dolomite recovered from the mixtures, to hydrogen sulfide, in comparison with fresh dolomite.

3.2.4.2 Work Forecast For Next Quarter

Analysis of the char-dolomite solids from the PDU test will continue. Additional support will be provided as needed.

3.2.5 Reactor Analysis

3.2.5.1 Work Accomplished

Combustor-gasifier material and energy balances are being made on the combustion zone and the gasification zone separately in order to estimate the amount of char to be burned for specified temperatures in each zone. The results of the modeling study on char gasification will be used to carry out these balances so that a map of operating conditions can be generated for use in the operation of the PDU.

3.2.5.2 Work Forecast For Next Quarter

The material and energy balances for the combustor-gasifier of the PDU for various operating conditions will continue.

4.0 REFERENCES

4.1 PHASE I, TASK 3 - LABORATORY SUPPORT STUDIES, SECTION 3.2.3

1. Sandstrom, William A., Amirali G. Rehmat, and Wilford G. Bair, "The Gasification of Coal Chars in a Fluidized Bed Ash-Agglomeration Gasifier," 69th Annual Meeting of the American Institute of Chemical Engineers, Chicago, Illinois, November 1976.

5.0 APPENDICES

5.1 APPENDIX A - Westinghouse Research Report

"Particle Separation from a Fluidized Mixture-Simulation of the Westinghouse Coal Gasification Combustor-Gasifier Operation"

5.2 APPENDIX B - Westinghouse Research Report

"The Electrical Resistivity of Char-Ash Mixtures in a Fluidized Bed"

5.3 APPENDIX C - Paper Presented at Symposium on Coal Processing and Conversion, West Virginia Geological and Economic Survey; June 2-3, 1976.

"Coal Devolatilization Studies in Support of the Westinghouse Fluidized Bed Coal Gasification Process"

5.4 APPENDIX D - Paper Presented at ACS Meeting on Purification of Low-Btu Gas in San Francisco, California August 29 to September 3, 1976.

"High Temperature Sulfur Removal System Development for the Westinghouse Fluidized Bed Coal Gasification Process"

SECTION 5.1

APPENDIX A

APPENDIX A
Research Report 76-8X4-PDULA-R1

PARTICLE SEPARATION FROM A FLUIDIZED MIXTURE - SIMULATION OF THE WESTINGHOUSE COAL GASIFICATION COMBUSTOR/GASIFIER OPERATION

J. L.-P. Chen* and D. L. Keairns
Westinghouse Research Laboratories
Pittsburgh, PA. 15235

ABSTRACT

Particle separation data from a 101.6 mm pressurized (up to 660 kPa) model operating at low gas velocity, near the U_{mf} of the mixture, and from a 114 mm Plexiglas model operating at high gas velocity, near the U_t of the mixture, with a nozzle located at the center of a conical bottom, are presented. These models were used to simulate the design and operation of alternative fluidized-bed agglomerating combustor/gasifier concepts. Comparison of the data obtained from these two modes of operation is made and a design for the separation of the agglomerated ash at low gas velocity established. The data indicate that >95% separation of the agglomerated ash from char at a rate of about 400 Kg/min-m^2 of the separator cross-sectional area can be achieved if the operating gas velocity is close to the minimum fluidizing velocity, e.g., 1.0 to 1.5 times U_{mf}, of the agglomerated ash.

* J.L.-P. Chen is currently with Hooker Chemical Co, Niagara Falls, NY

INTRODUCTION

Particle separation data were used to provide design and operating criteria for a multi-stage fluidized-bed coal gasification process being developed at Westinghouse[1,7] to produce low Btu gas for combined-cycle power generation. An experimental investigation of the separation of agglomerated ash in a batch fluidized char-ash mixture at low gas velocity has been reported in an earlier paper.[2] Good particle separation was obtained for an operating gas velocity close to the minimum fluidizing velocity of the separated species.

In order to directly simulate the char-ash separation in the combustor/gasifier and to investigate alternative processes for separating agglomerated ash from the mixture, experiments were carried out to investigate continuous particle separation. Two processes were investigated. One is to separate the agglomerated ash from the fluidized-bed by using a low gas velocity near the minimum fluidizing velocity of the ash and the other is to use a high gas velocity near the terminal velocity of the char. Results from these two experiments are compared. The data are used to project operating conditions for achieving the desired particle separation in the fluidized-bed coal gasification combustor/gasifier. A 15 ton per day process development unit (PDU) has been constructed which incorporates char-ash separation based on the use of minimum fluidizing velocity.

CONCLUSIONS

The conclusions that can be drawn from this study are given below:

1. Separation of agglomerated ash (simulated by dolomite) from a fluidized char-ash mixture has been experimentally simulated in both a low gas velocity, i.e., a fluidized bed operating at a velocity close to the U_{mf} of the mean dolomite of up to 660 kPa, and a high gas velocity, i.e., a conical bottom with a venturi nozzle at atmospheric pressure, char-ash separator. Both the degree and the rate of separation are determined.

2. For a low velocity separation, the maximum degree of separation occurs at a gas velocity near 1.5 times the U_{mf} of the mean dolomite at low pressure and near the U_{mf} of the mean dolomite at high pressure. The degree of separation is generally higher for a high pressure operation and the size distribution of char (420 to 1410 μm) and dolomite (595 to 2000 μm) does not appear to affect the degree of separation. The rate of separation is function of the dolomite feed rate (simulating ash agglomeration rate) and these two rates are equal when the rate is low. In order to prevent accumulation of ash particles in the bed, the cross sectional area of the char/ash separator should be large enough that its unit cross sectional area is to remove not more than 400 $Kg/min\text{-}m^2$ of ash agglomerates.

3. The maximum degree of separation for a high velocity conical separator occurs at a gas velocity between the terminal velocity of the mean char and that of the mean dolomite. The rate of separation decreases asymptotically with the gas velocity at the nozzle.

4. The data obtained in this investigation indicates the low velocity separation process is preferred for process design and control of particle separation. This is based on the results which show the high velocity separation process is sensitive to the gas velocity at the nozzle, the nozzle design, the bed composition and the bed height. The data indicate the low velocity separation process can be controlled by the gas velocity in the char-ash separator. Other factors, such as possible ash agglomeration on the walls of the agglomerating combustor in the low velocity process, may alter this conclusion based on additional hydrodynamic data and high temperature operation results.

LITERATURE

Segregation of two different solid particles with appreciable density difference in a low velocity fluidized bed has been reported by the British Gas Council in their recirculating coal gasification process[3] and by the Consolidation Coal Co. in their CO_2 acceptor gasification process.[4] While the British Gas Council has achieved about 80 to 90% purity of ash separated from their agglomerating gasifier which was fluidized at about 4 times the U_{mf} of the ash mixture, Consolidation Coal Co. has achieved a much higher separation efficiency (>95%) for their spent stone (lime or dolomite) in the CO_2 acceptor process. Previous investigations at Westinghouse[1] indicated that a high separation efficiency, e.g., >95%, can be obtained for the agglomerated ash if a gas velocity close to the U_{mf} of the agglomerated ash is used.

Jéquier, et al.[5] experimented with an alternate concept for coal gasification, ash agglomeration and particle separation. The apparatus consisted of a fluidized chamber at the top and a conical duct between the chamber and a venturi. A high gas velocity prevailed at the venturi which allowed particles of agglomerated ash to fall through but not the fine char. For a gas velocity at the venturi in the order of 15 m/sec, they showed that the separated mixture contained about 95% ash. However, separation of agglomerated ash from the char-ash mixture was not smooth and the efficiency decreased rapidly when the gas velocity at the venturi decreased. Their data also show that an increasse of the gas velocity at the venturi was necessary in order to keep coal fines from falling through the nozzle as the bed height was increased.

EXPERIMENTAL APPARATUS AND PROCEDURES

Two fluidization cold models were used. One is for separation of particles at low gas velocity and the other is for separation at high gas velocity. Three mixtures which simulated the char-ash mixtures in the agglomerating combustor/gasifier were used to study the degree and rate of separation. Dolomite which is slightly heavier than the agglomerated ash[6] was used to simulate the agglomerates. The mixtures consist of two-component and wide-size distribution particles of different size and density. Table 1 shows the property of these materials. The actual particle sizes and densities present in the agglomerating combustor/gasifier will be determined in the PDU. The density difference of char and dolomite is projected to be comparable to that of char and agglomerated ash. Previous studies at Westinghouse[1] indicated that the separation process is mainly controlled by the density difference of char and ash (simulated by dolomite), especially when the gas velocity is close to or greater than the minimum fluidizing velocity of the largest ash particles at high pressure. The results obtained from this study are therefore expected to be representative of the process development unit operation.

Low Velocity Separation

Simulation of the separation of agglomerated ash from char at low gas velocity, close to the U_{mf} of ash, has been carried out in a 102 mm pressurized unit at pressures up to 660 kPA. Figure 1 shows the schematic diagram of the apparatus. The model is similar to that used for the batch experiments as described in the previous paper.[1] The fluidized bed column is composed of two 102 mm diameter glass pipes and two 102 mm steel pipes. The unit is about 2.6 m high and can withstand a pressure up to 1130 kPa. Inside the lower glass section,

Table 1

Char-Dolomite Mixtures Used in the Combustor-Gasifier Cold Models to Simulate Char-Ash Separation

Material	Size, μm	Density gm/cc	U_{mf}^{*} m/sec	U_{t}^{*} m/sec
Mixture A				
char[+]	841 x 420	0.8∿1.2	0.06∿0.12	∿1.74
dolomite[++]	1410 x 841	∿2.88	∿0.64	∿6.9
Mixture B				
char	841 x 595	0.8∿1.2	0.07∿0.14	∿1.8
dolomite	1190 x 841	∿2.88	∿0.6	∿6.7
Mixture C				
char	55% 1410 x 841, 45% 595 x 420	0.8∿1.2	0.07∿0.15	∿1.8
dolomite	40% 2000 x 1410, 60% 841 x 595	∿2.88	∿0.43	∿4.8

*at 101 to 170 kPa and 25.6°C

+projected char size for the PDU: - 6000 μm

++dolomite used to simulate ash agglomerates, uniform and coarse (∿ 3000 to 6000 μm) agglomerates have been obtained by IGT[6] in their agglomerating gasifier

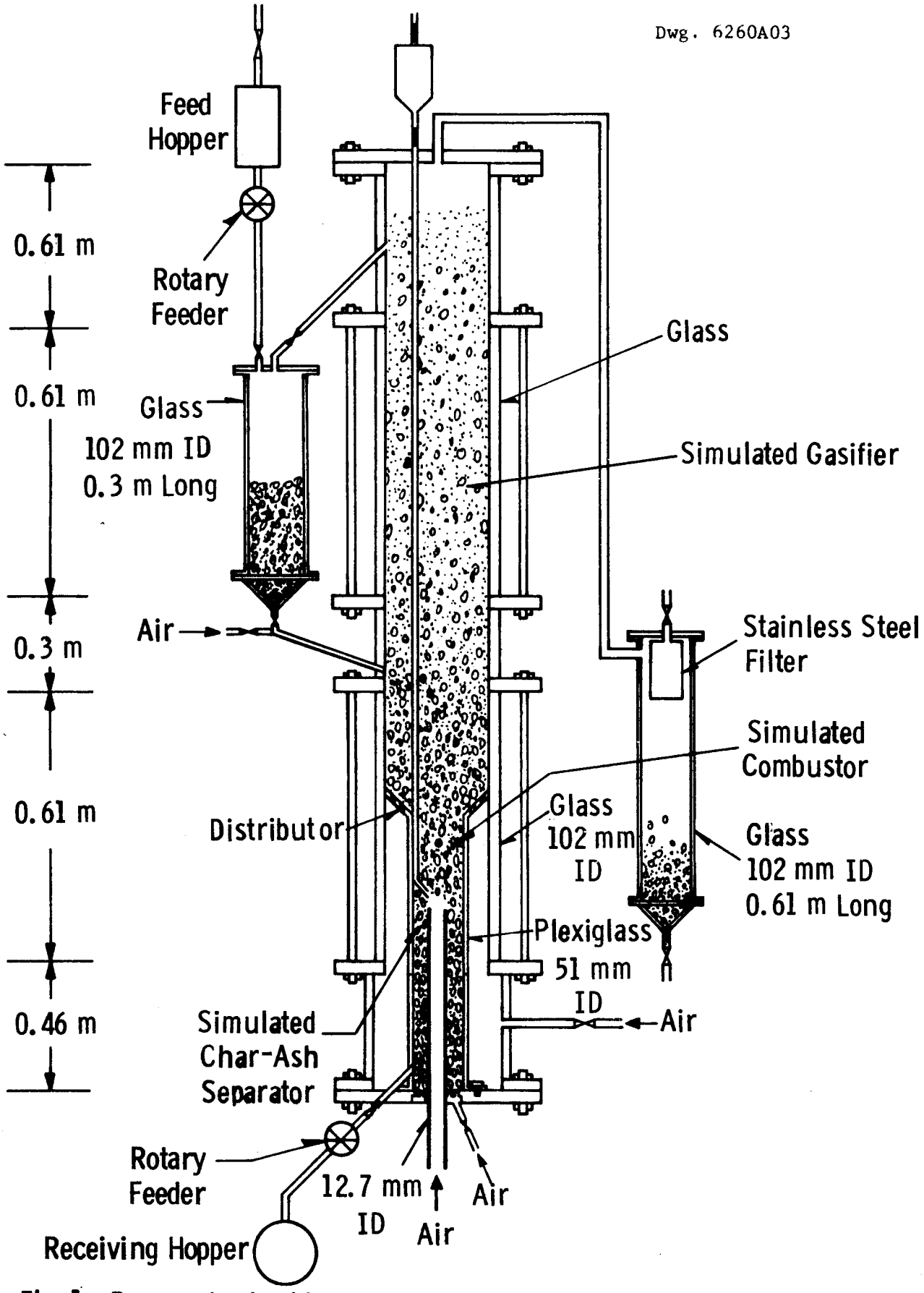

Fig. 1 --Pressurized cold model simulating the combustor-gasifier

a 51 mm I.D. plexiglass tube of 0.762 m length is installed. A conical distributor (60° cone angle with forty-eight 0.8 mm holes arranged in three rings of 6.35 mm apart) connects the 51 mm tube to the 102 mm glass pipe. An O-ring is used to seal the conical distributor from the 102 mm glass pipe. The upper and the lower column simulate the gasifier and the agglomerating combustor, respectively. A 12.7 mm copper tube installed inside the simulated combustor simulates the air inlet and forms the annulus for the char-ash separator. A distributor consisting of thirty-two 0.8 mm holes arranged in two rings of 6.35 mm apart is installed at the bottom of the annulus. All the distributors were covered with 80 μm screen to prevent fine particles from falling through or plugging the orifices.

Independent air supplies are used to fluidize the particles above the conical distributor, the center nozzle and in the char-ash separator. A solid feeding system consisting of feed hoppers and a rotary feeder is used to continuously feed the agglomerated ash (simulated by dolomite) into the fluidized mixture at a controlled rate. A solid withdrawal system comprising a rotary feeder and a receiving hopper is used to remove the separated ash.

The primary measurements consisted of the air flow rates, the pressure of the column and the char concentration of the separated particles. The fluidized bed column was initially filled with the char-ash mixture and fluidized for about 5 min. by controlled gas velocities in the simulated gasifier, agglomerating combustor and the char-ash separator to induce a steady-state segregated particle distribution in the column. Dolomite at a controlled rate was then continuously fed into the gasification section for about 3 minutes, and at the same time, separated mixture was withdrawn from the bed. The solid withdrawal rate was so controlled that the char-rich and dolomite-rich interface was maintained near the top of the char-ash separator. Samples from the removed particles, excluding the quantity initially in the char-ash separator, were screen analyzed to determine their ash (simulated by dolomite) concentration as a function of the gas velocity and the system pressure.

The rate of separation was determined by first fluidizing pure char in the gasifier, the combustor and the char-ash separator. Dolomite was then fed into the gasifier. This dolomite segregated from the mixture and replaced char in the char-ash separator. The rate of char-ash separation was measured by determining the rising rate of the char-ash interface in the char-ash separator.

High Velocity Separation

Separation of ash (simulated by dolomite) from a char-ash mixture by entrainment has been simulated in a 114 mm diameter plexiglass unit as depicted in Fig. 2. The column is similar to that described previously[2] except that a conical bottom of 45° or 60° from the horizontal with a 25.4 mm diameter nozzle was used in this study. The nozzle was initially plugged with a rubber stopper (attached to a 6.35 mm tubing which can be moved up and down) when the bed was filled with the char-ash mixture. Air was introduced into the column as soon as the plug was first slowly and then suddenly removed. A timer was started when the nozzle was completely open. Ash particles which are heavier than char were separated from the mixture by falling through the nozzle counter-current to the high gas velocity. Lighter char particles were entrained back to the fluidized mixture. For a given period of operation, e.g., 1 to 10 minutes, the separated particles were weighed and screen analyzed to determine the rate and the degree of separation. These separated particles were returned to the fluidized bed for the next run. No provision for continuously feeding simulated ash into the bed was made. The rate and degree of separation were determined as a function of the gas velocity at the nozzle, the bed composition, the cone angle and the bed height.

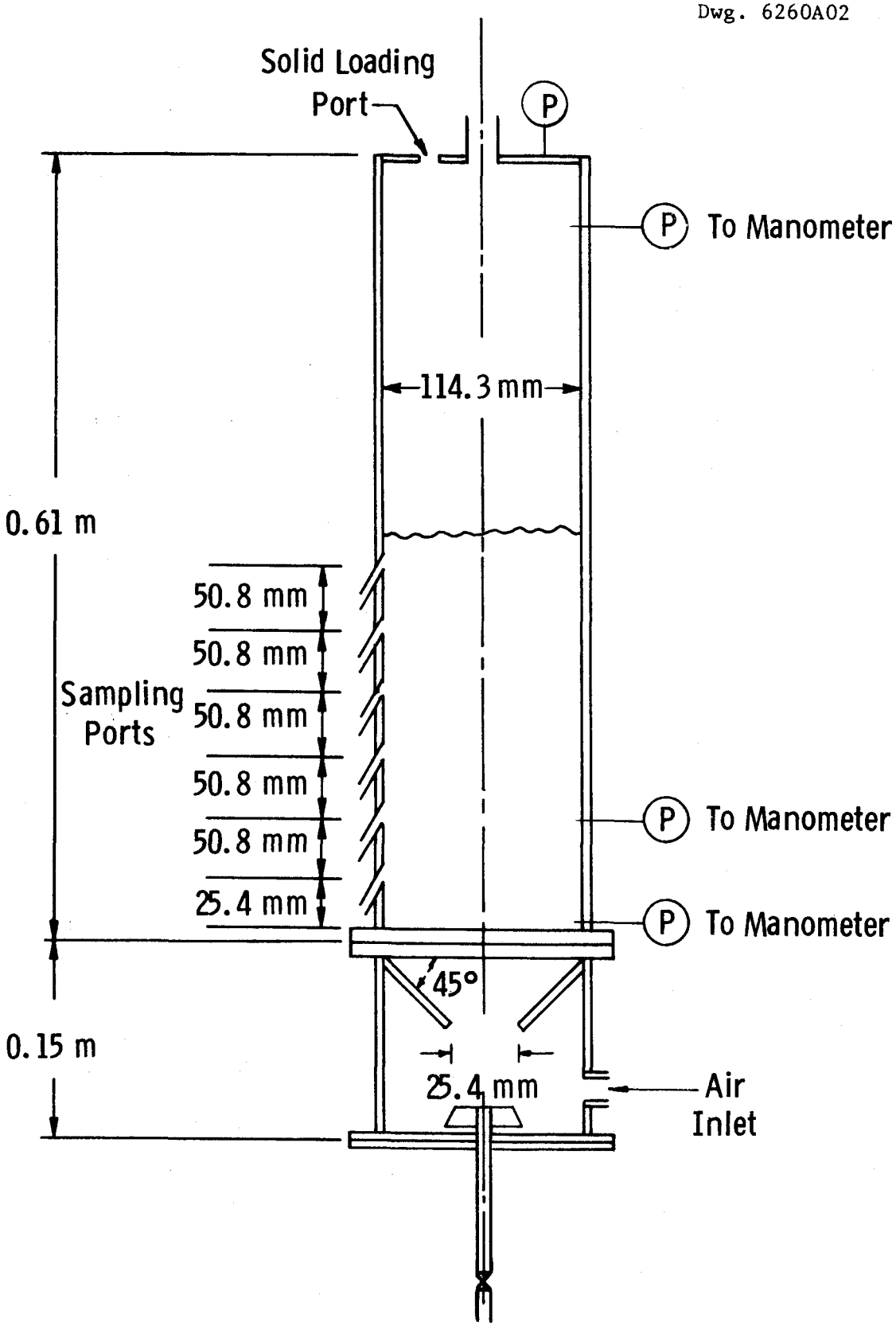

Fig. 2-114.3 mm Plexiglas model with conical bottom

EXPERIMENTAL RESULTS AND DISCUSSION

Low Velocity Separation

Fluidization and Separation Characteristics

A non-uniform air distribution with a high gas velocity at the center nozzle and low gas velocities at the conical annular distributor and the annular char/ash separator was introduced to simulate the particular operating characteristics projected for the Westinghouse gasifier/combustor.[7] Segregation of particles occurs in the bed when a high solid circulation induced by a high velocity jet prevails between the combustor and the gasifier and minimumly fluidized particles prevail in the outer annulus of the gasifier (immediately above the conical distributor) and in the char/ash separator. The jet was stable and confined to the center of the combustor when its velocity was high (> 5.8 m/sec). For lower velocities the jet oscillated and was not stable. Large bubbles were occasionally produced at the jet tip which resulted in slugging bed operation in the agglomerating combustor for velocities < 1 m/s.

In a steady state operation, dolomite from the feed hopper (simulating the generation of agglomerated ash particles) showered through the char bed in the gasifier and descended with the downflow solid into the combustor. Dolomite was then either separated from the mixture by falling into the char/ash separator and was removed from the bottom by a rotary feeder or picked up by the jet to recirculate between the combustor and the gasifier. The gas velocity in the char/ash separator was controlled in the neighborhood of the minimum fluidizing velocity of the mean dolomite size so that heavy dolomite would settle into this region due to insufficient air support of these heavy particles. The lighter char particles which fell into this region, however, were carried upward into the agglomerating combustor by small

gas bubbles in the char/ash separator. At a steady state, a sharp interface between a dolomite-rich and a char-rich mixture was observed. This indicated the feasibility of effectively separating agglomerated ash (simulated by dolomite) from the char bed by this method.

Degree of Separation

The degree of separation of dolomite (simulating agglomerated ash) from the char-dolomite mixture in terms of the wt.% of dolomite in the separated mixture is shown in Fig. 3 for material A (see Table 1) and in Figs. 4, 5 and 6 for material C (Table 1) at operating pressures of 195, 391 and 572 kPa, respectively. The shape of the curves for the degree of separation vs. the gas velocity is similar to that obtained from batch operation.[2] The efficiency of the separation is high when the gas velocity in the char/ash separator is between the U_{mf} and 1.5 times the U_{mf} of the mean dolomite size with the maximum degree of separation occurred near 1.5 times the U_{mf} for low pressure operation and near the U_{mf} for high pressure operation. The maximum degree of separation is generally greater than 97%, but a higher degree of separation, e.g., >99%, may result from high pressure operation. Operation at a velocity away from these optimum values, however, may quickly reduce the degree of separation, presumably due to lack of bubbles in the char/ash separator to remove trapped char fines from the downflow dolomite when the velocity is low or due to violent agitation of the bed particles by the presence of excessive bubbles at high gas velocity. Slugging of the bed mixture in the char/ash separator ($L/D \sim 23$) was observed when the gas velocity is higher than the U_{mf} of the largest dolomite particle for operating pressure < 200 kPa. Slugging was not observed at higher pressures for velocities up to two times the dolomite U_{mf}. A good separation was still achieved even when the bed in the separator slugged. Comparison of the results in Figs. 3, 4, 5 and 6 shows that overlapping char and dolomite particle distribution (char: 420 to 1410 μm, dolomite: 595 to 2000 μm) does not appear to affect the degree of separation. This result indicates that the separation process is practically controlled by the particle density difference and agrees with the results obtained from

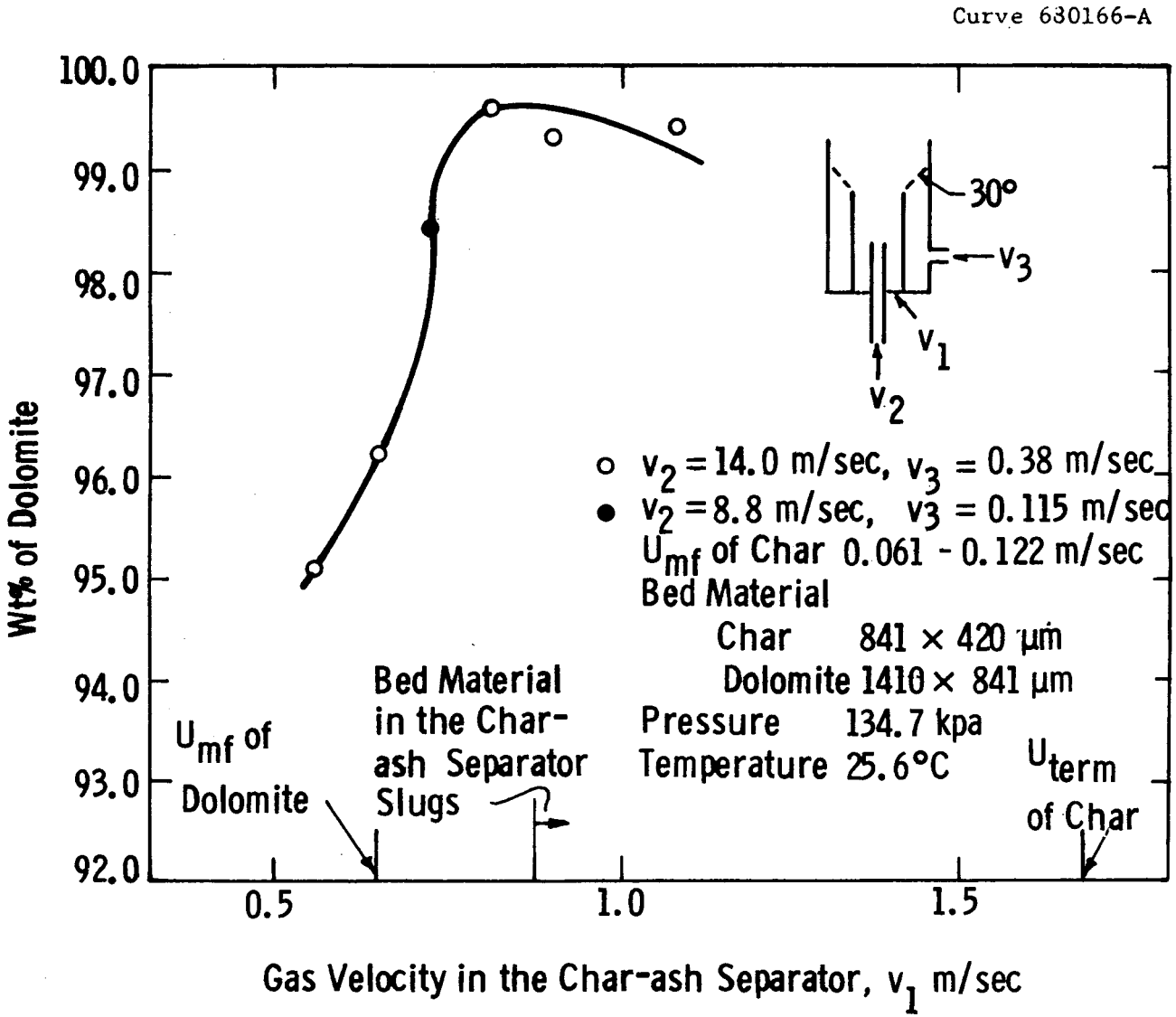

Fig. 3—Concentration of dolomite in the mixture withdrawn from char ash separator

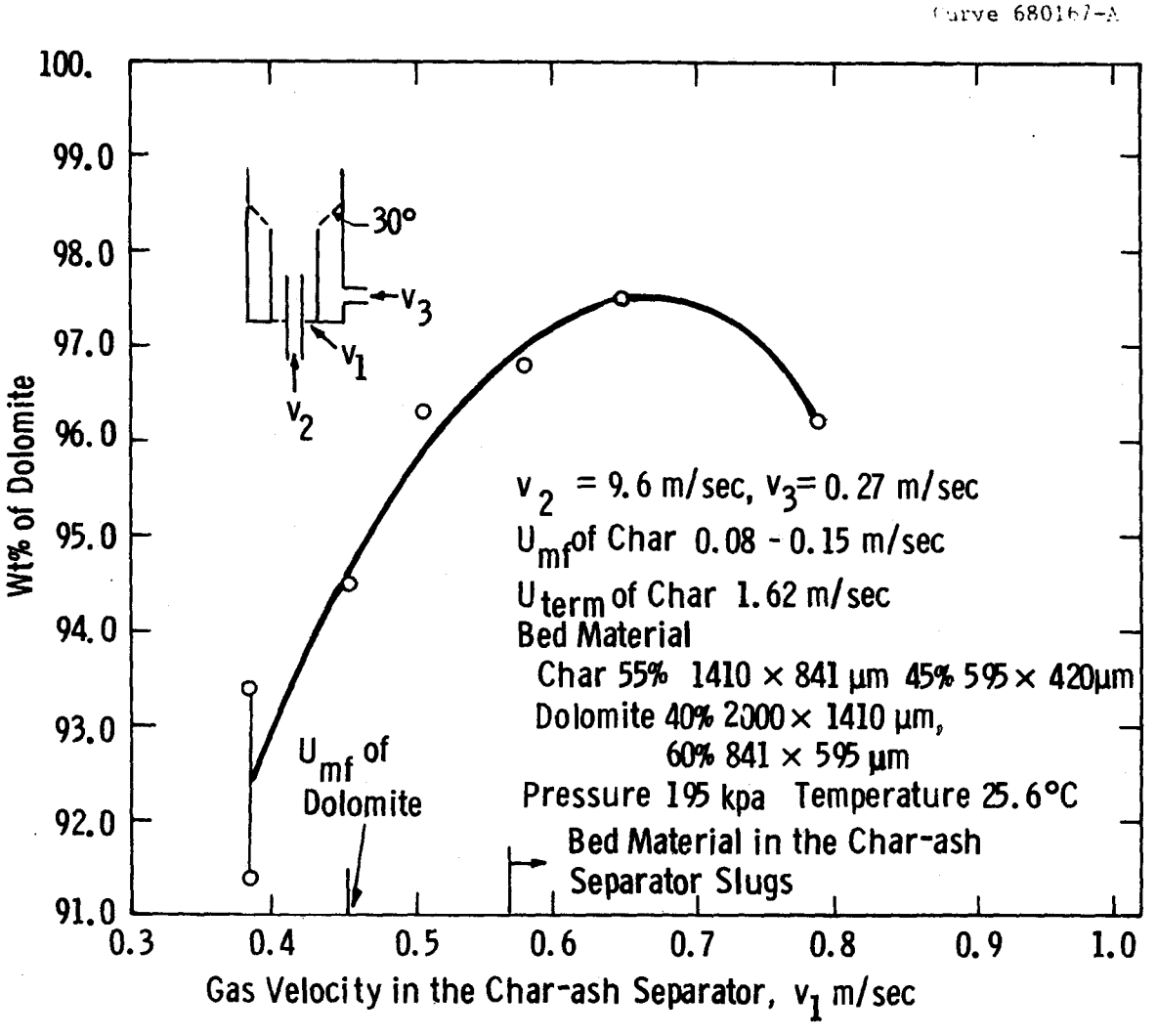

Fig. 4 —Concentration of dolomite in the mixture withdrawn from the char-ash separator

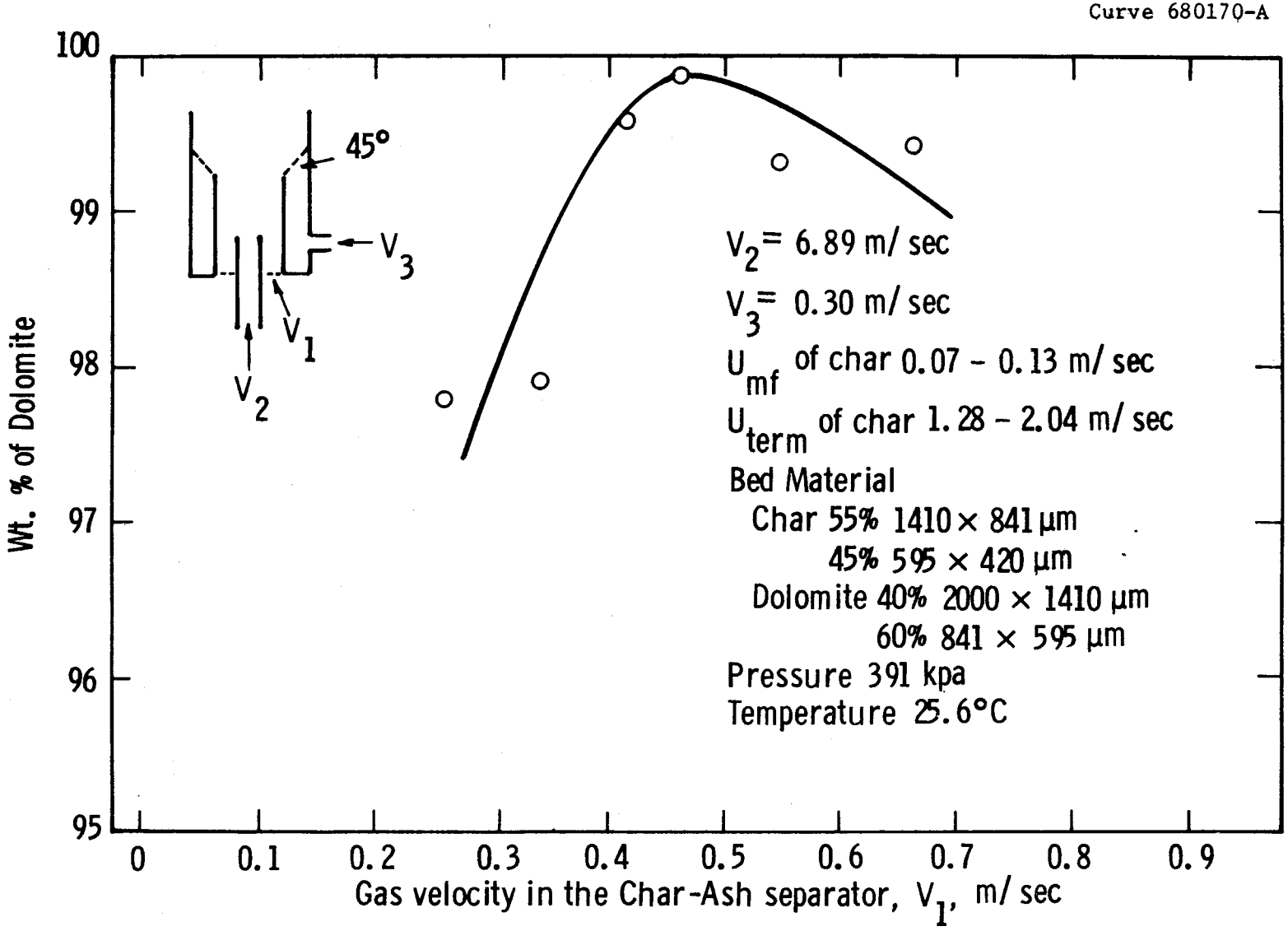

Fig. 5 —Concentration of dolomite in the mixture withdrawn from the char-ash separator

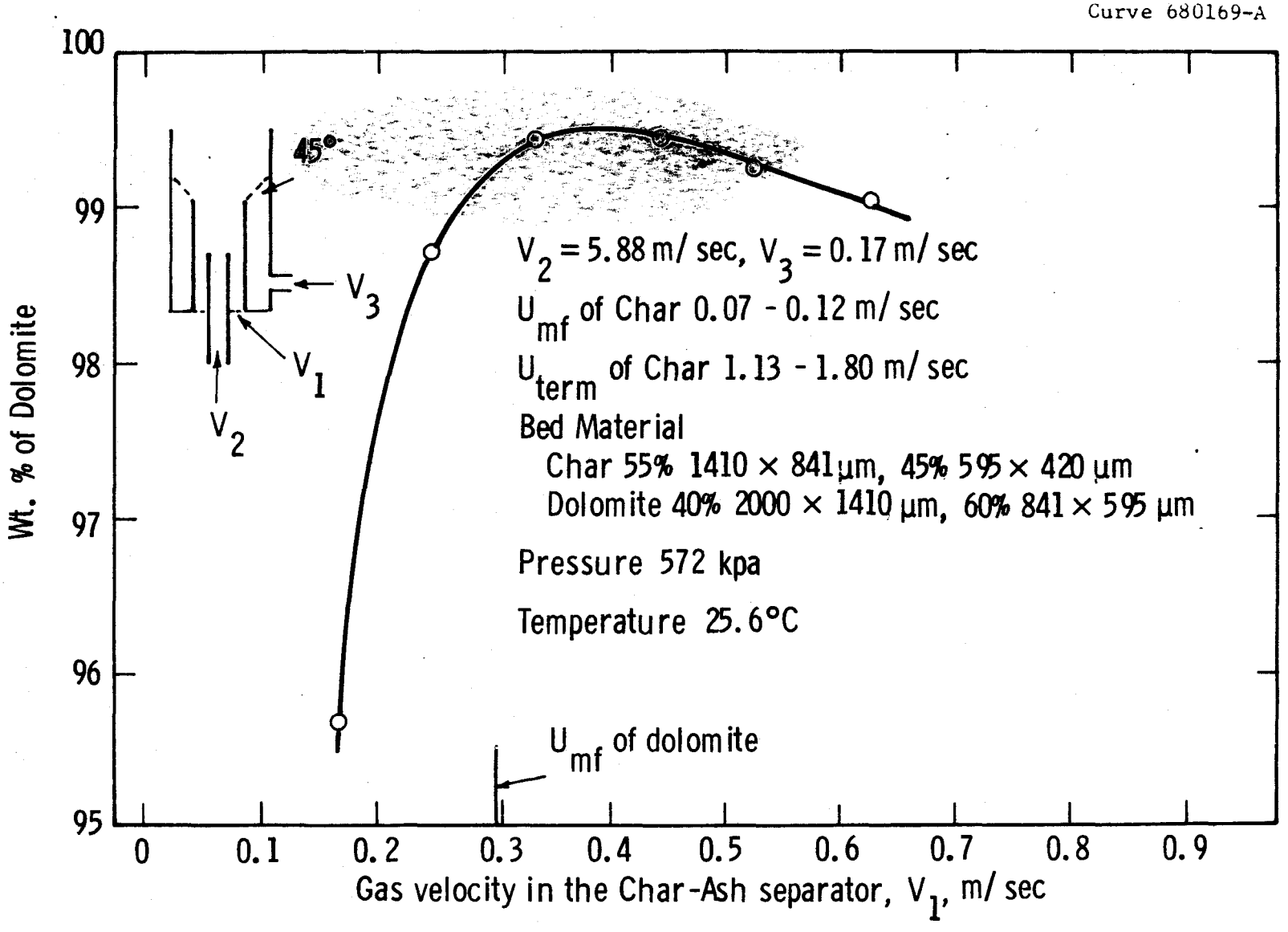

Fig. 6 -Concentration of dolomite in the mixture withdrawn from the Char-Ash separator

the batch operation and the results of other investigators.[6,7,8,9] In the actual plant operation, the char and ash size distribution may differ from the distributions used for study. However, as ash is continuously growing in size through agglomeration, only the portion of large ash agglomerates will be separated from the bed. The fine fraction and the char particles will remain in the agglomerating combustor for further combustion and agglomeration. This condition is similar to what is simulated in this study and, therefore, the data obtained in this experiment would be representative of what may be expected in the actual operation.

Examination of the data reveals that the degree of separation of dolomite from char is affected only by the gas velocity in the char/ash separator. The gas velocities in the jet and at the conical distributor have a minor effect. The degree of separation was also discovered to be independent of the solid removal rate if the removing rate is slower than the dolomite separation rate.

Rate of Separation

The separation rate of dolomite (simulating agglomerated ash) from a dolomite-char mixture (material C) is shown in Fig. 7. When the dolomite feed rate is low, e.g., $\leq$400 Kg/min-m^2 of the separator cross sectional area, the solid separation rate is equal to the dolomite feed rate. However, when the dolomite feed rate is greater than 400 Kg/min-m^2, the separation rate is smaller than the feed rate and an asymptotic value is essentially reached at about 780 Kg/min-m^2. This rate of separation may be affected by the particle size used in the process because the rate is determined by the dolomite descending rate and the char ascending rate. However, the effect may be small when the operating gas velocity is controlled, e.g., near the U_{mf} of the mean dolomite and greater than the U_{mf} of the largest char particles, such that char particles of any size will be carried out of the char/ash separator and the rate of

Curve 680162-A

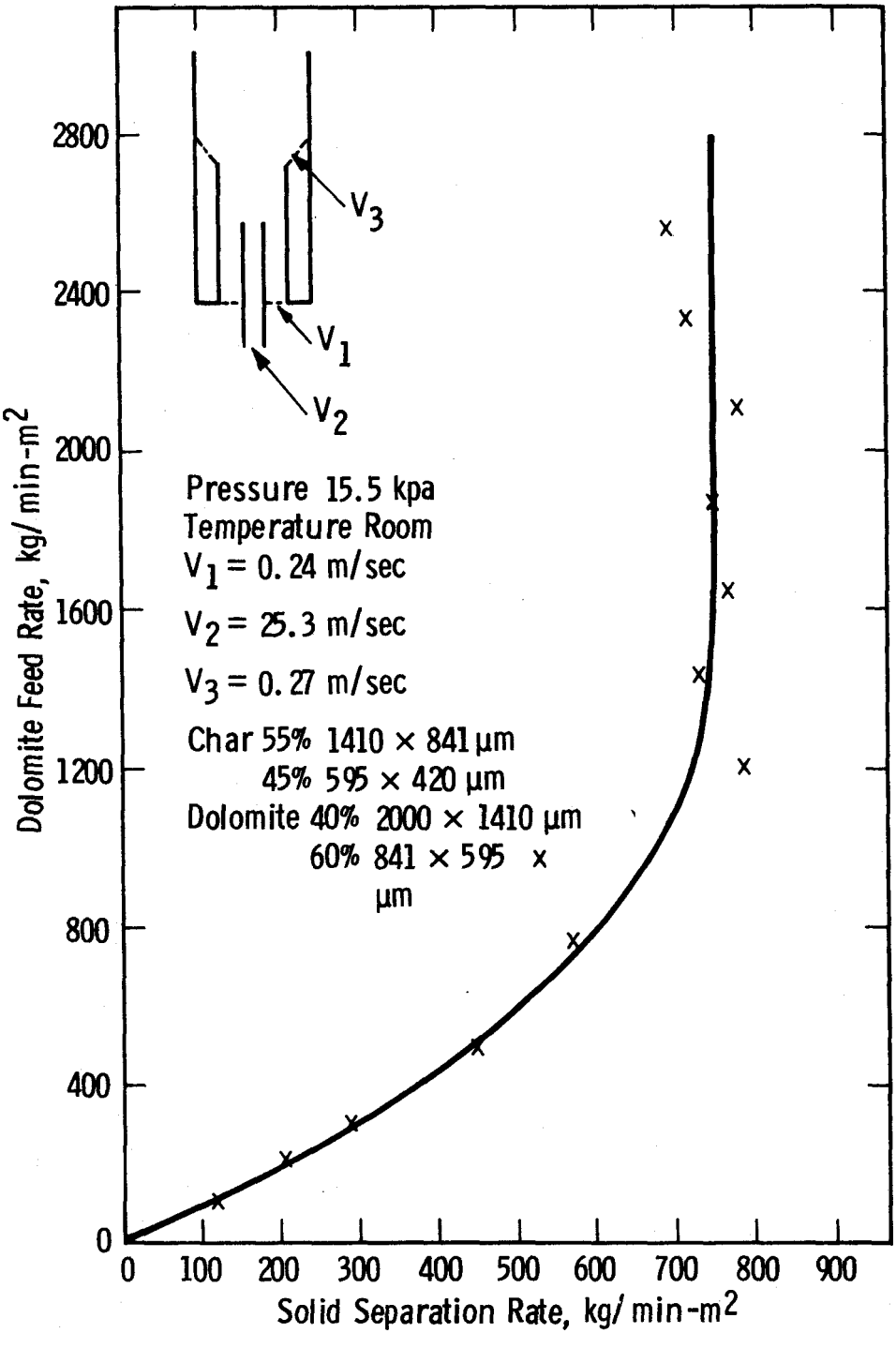

Fig. 7 – Solid separation rate as a function of solid feed rate

separation becomes affected only by the dolomite descending rates which is mainly determined by the density difference between char and dolomite.

The separation rate of dolomite from a batch fluidized mixture of char and dolomite was shown to be about 30 seconds.[2] This is based on tests in a 0.114 m diameter unit with a 2.55 kg bed. This rate of separation is corresponding to a mass rate of about 500 Kg/min-m^2 which agrees reasonably well (about 20% difference) with the results from this study.

In order to avoid accumulation of dolomite (or ash agglomerates) in the combustor/gasifier, the char/ash separator should be so designed that its unit cross-sectional area is to remove not more than 400 Kg/min-m^2 of the separator cross-sectional area. An application of this number to the process development unit design (544 Kg/hr coal feed rate of about 10% ash content) leads to a conclusion that the required char/ash cross-sectional area for complete removal of ash input should not be less than 0.0023 m^2. This is much smaller than that designed for the PDU — the design cross-sectional area is 0.0603 m^2.

A gas velocity lower than but close to the U_{mf} of the mean dolomite and greater than the U_{mf} of the mean char in the char/ash separator was used for this study because the existence of gas bubbles in the separated dolomite mixture can distort the char-dolomite interface and greatly reduce the accuracy of measuring the solid separation rate. The effect of this gas velocity, however, may be minimal because the rate of separation is largely controlled by the descending rate of dolomite particles through the fluidized mixture above the interface. Experiments carried out for particle separation in the batch fluidized bed showed that the rate of separation is insensitive to the gas velocity in the neighborhood of U_{mf}.[2]

High Velocity Separation

Fluidization and Separation Characteristics

When a mixture of char and dolomite (simulating agglomerated ash) is fluidized by a single high velocity gas upflowing through a conical nozzle, circulation of particles occurs in the bed with solid moving upward in the center and downward near the wall. The downflowing particles are either picked up by the gas jet prevailing at the nozzle or fall through the nozzle along the periphery of the nozzle. Depending on the angle of the cone, a static layer of particles may form above the conical wall if the conical angle from the horizon is 45° or smaller. This static layer of particles has an inclination of an angle equivalent to the angle of internal friction, e.g., 60 to 80° from the horizontal for most particles. For a steeper cone angle, e.g., 60° cone, however, no accumulation of particles on the cone wall was observed.

Local segregation of particles occurs in the bed with heavier dolomite (or agglomerated ash) precipitating to the bottom and char floating in the upper part of the bed. When the gas velocity at the nozzle is between 0.7 and 3 m/sec, bridging of particles across the nozzle was observed for this particular system and no particle motion occurs in the bed. This is probably due to the large wall effect resulting from the small nozzle diameter ($\sim$ 25.4 mm) and the interparticle friction forces which prevent particles from falling freely through the nozzle. A high gas velocity, e.g., greater than the terminal velocity of the largest dolomite particle, also keeps particles from falling through the nozzle. There is a limited range of velocity in which the heavier dolomite (or agglomerated ash) can fall through the nozzle and be separated from the mixture.

Degree and Rate of Separation

Figures 8 to 13 show the degree and the rate of separating dolomite (simulating agglomerated ash) from a char-dolomite mixture by entraining char out of the falling char-dolomite mixture through a

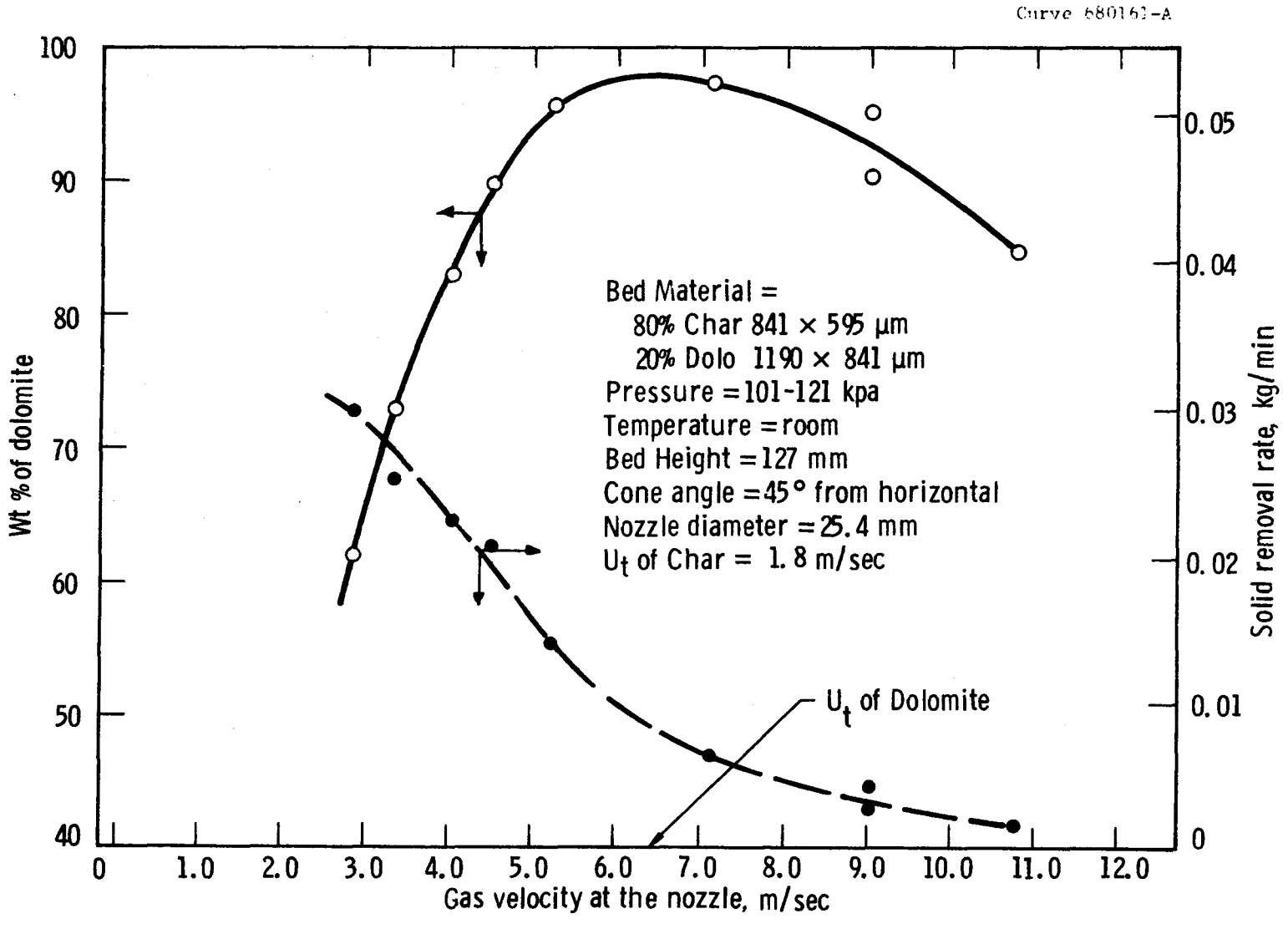

Fig. 8 —Separation of char-dolomite mixture by entrainment

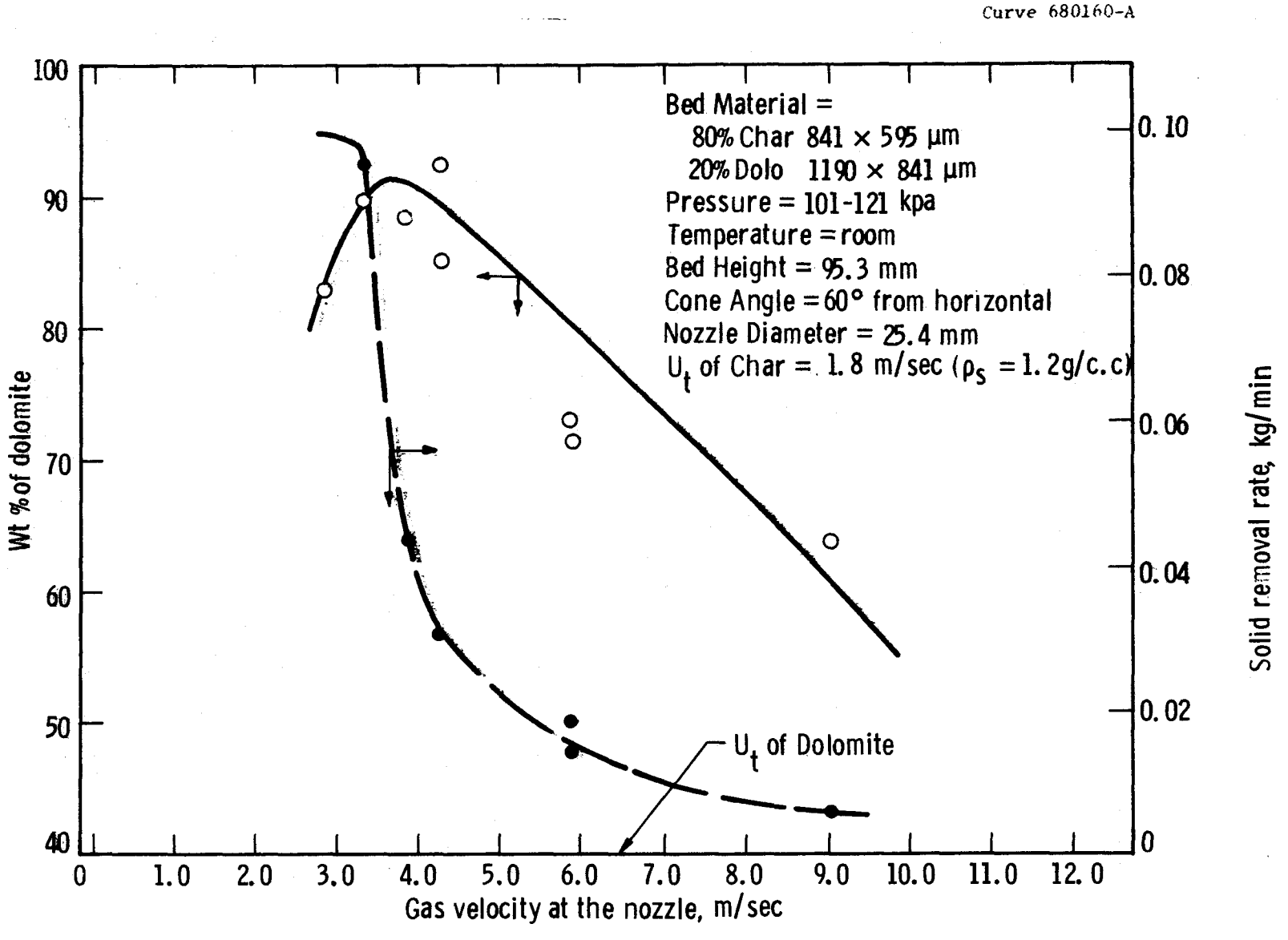

Fig. 9 —Separation of char-dolomite mixture by entrainment

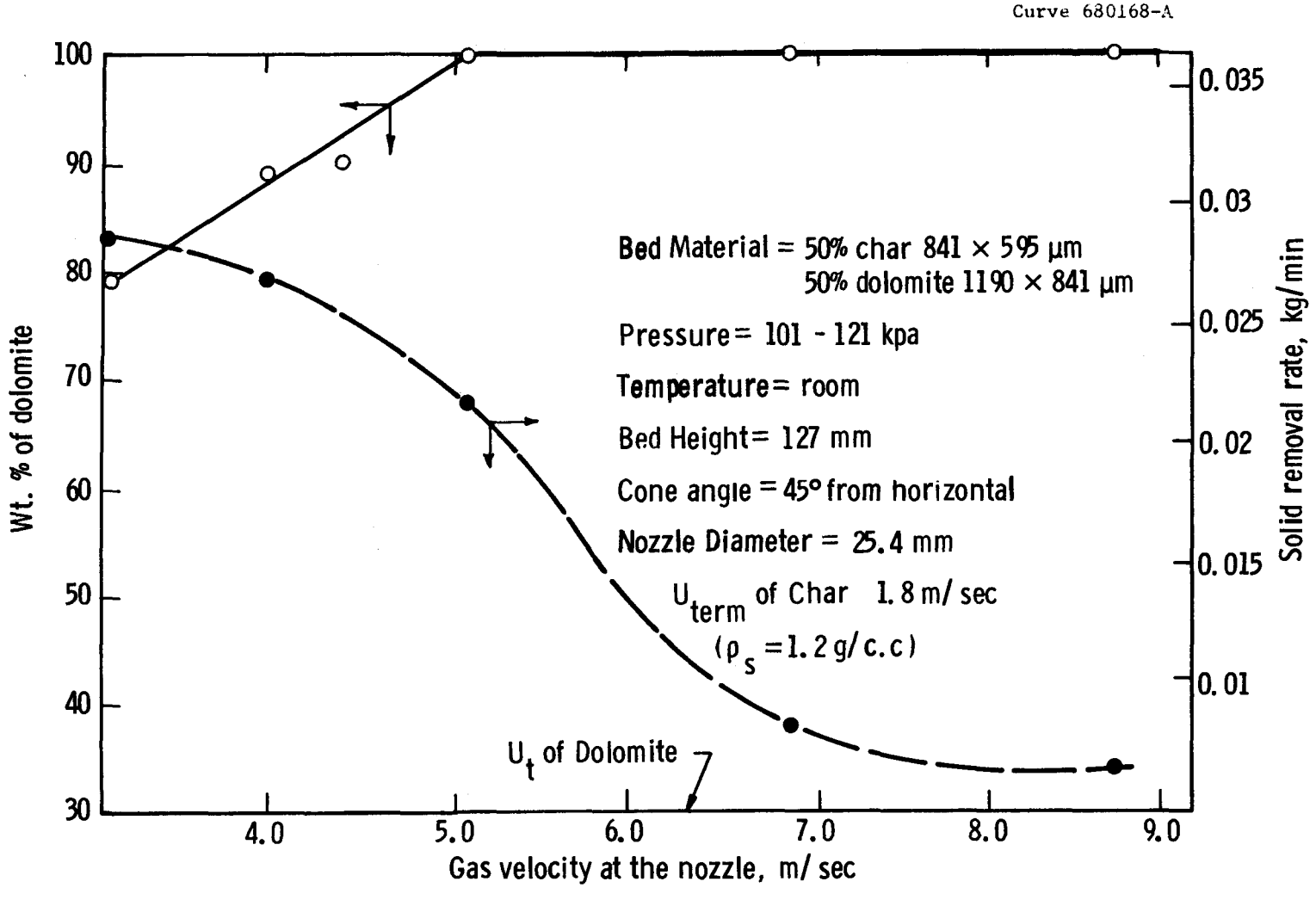

Fig.10—Separation of char-dolomite mixture by entrainment

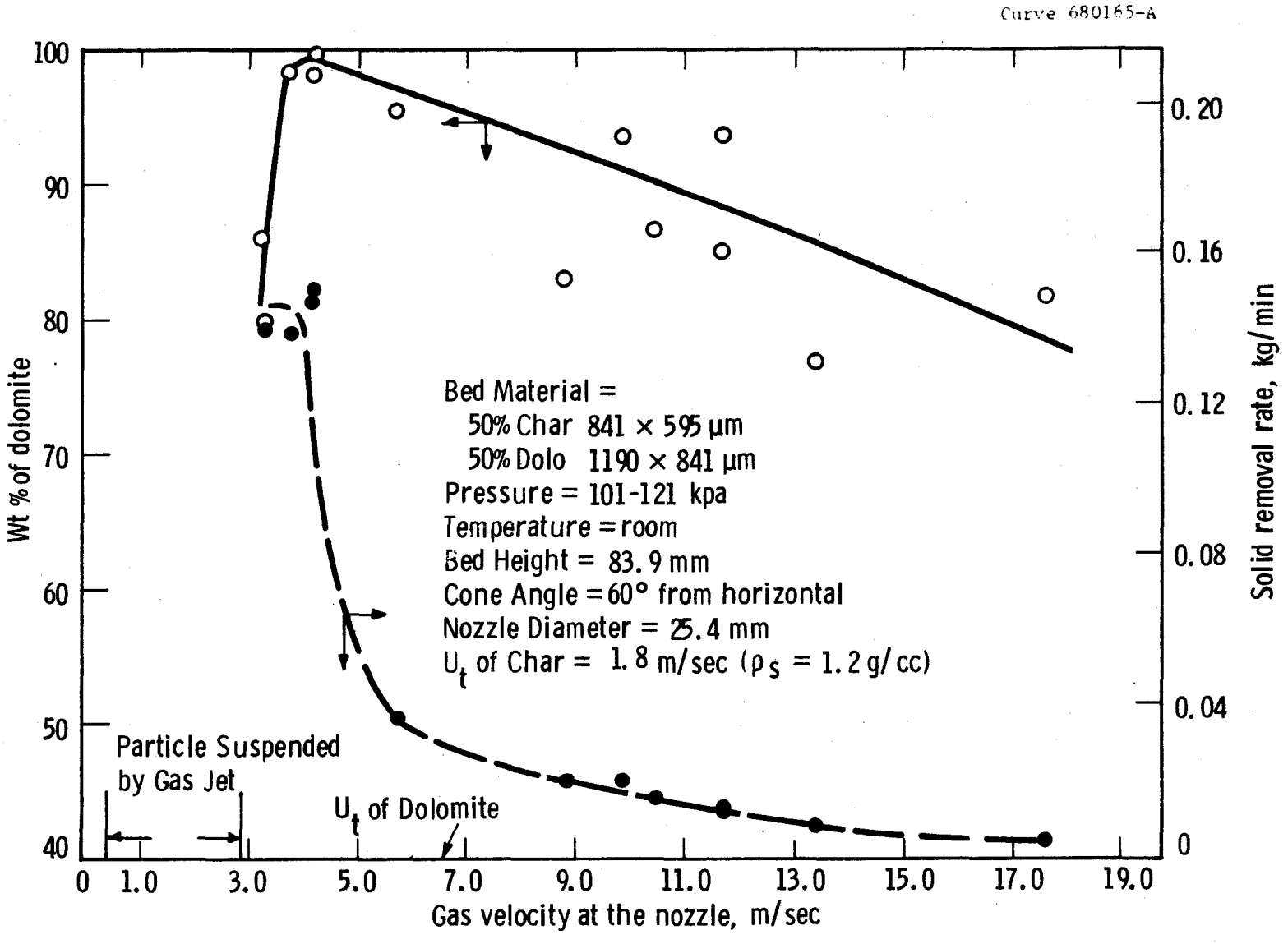

Fig. 11—Separation of char-dolomite mixture by entrainment

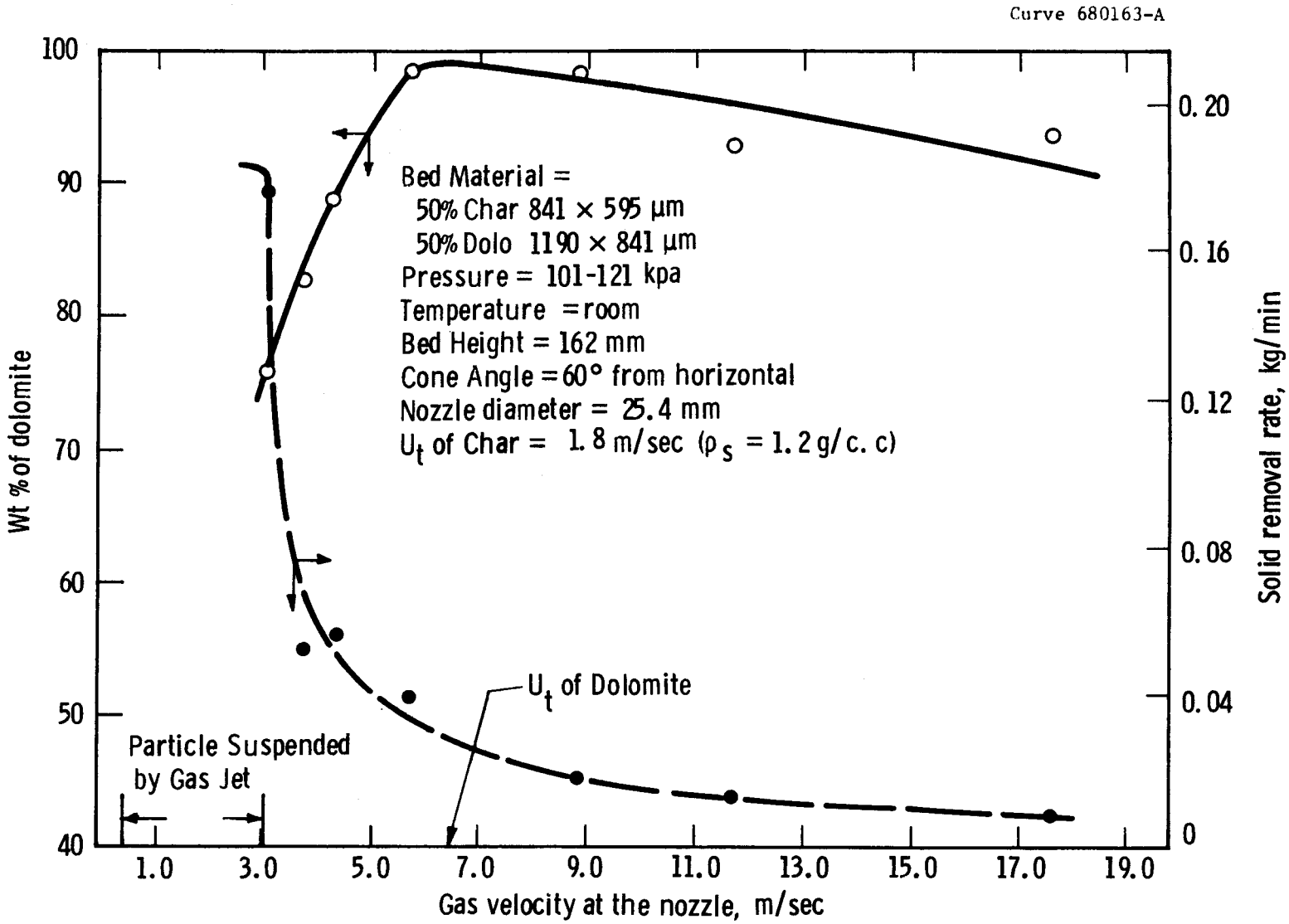

Fig. 12—Separation of char-dolomite mixture by entrainment

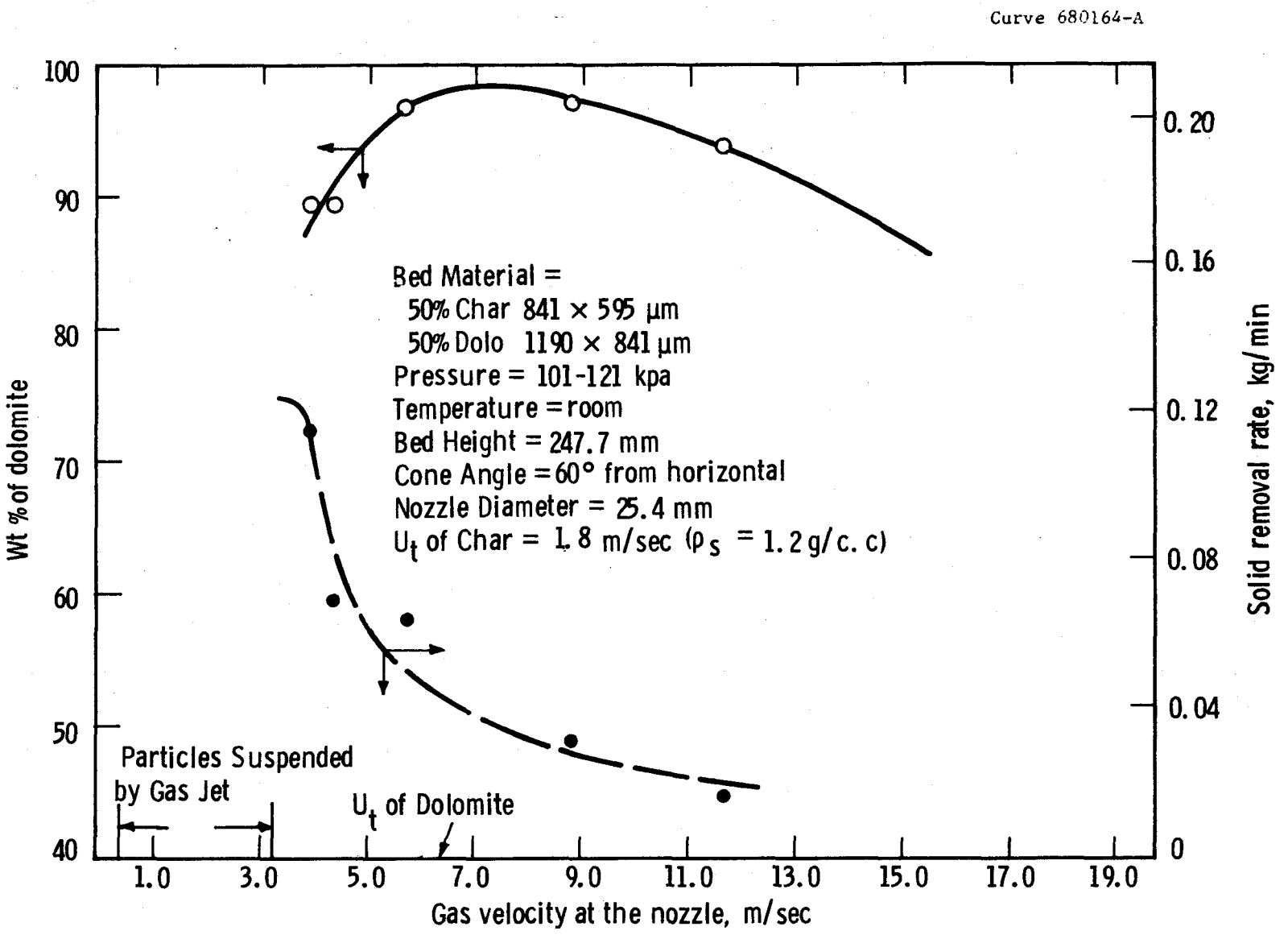

Fig. 13 –Separation of char-dolomite mixture by entrainment

conical nozzle. Figures 8 and 10 are for conical nozzles of 45° from the horizontal and the other figures are for a conical nozzle of 60° from the horizontal. Two narrow sized mixtures of char (841 x 595 μm) and dolomite (1190 x 841 μm) at either 80% char - 20% dolomite (Figs. 8 and 9) or 50% - 50% combination (Figs. 10 to 13) were used for this study. While the degree of separation increases sharply to a maximum (97 to 100% of dolomite in the removed mixture) and then decreases as the gas velocity increases beyond the terminal velocity of char, the rate of separation decreases.

Comparison of Figs. 8 and 10 to Figs. 9 and 11, respectively, indicates that the maximum degree of separation is lower and occurs at a lower gas velocity for a conical bottom of steeper angle. However, the rate of separation at the maximum degree of separation is higher for a steeper cone, e.g., 60° angle from the horizontal. This is probably due to the fact that a steeper cone, with the inclination equal to or greater than the angle of internal friction, provides less friction for particles to fall along the wall. Both dolomite and char are moving downward against the upflowing gas and a large quantity of char and dolomite may roll through the nozzle along the wall where a gas velocity lower than the average velocity prevails. The efficiency of selecting dolomite as against char to fall through the steeper nozzle is therefore lower. The steeper cone may more slowly and smoothly dissipate the gas flow such that less turbulence is created in the cone and an orderly segregation of particles may be achieved with a smaller gas rate compared to that required for a shallower cone.

Comparison of Figs. 8 and 9 to Figs. 10 to 13 shows that both the maximum degree of separation and the separation rate are higher for a bed of greater dolomite concentration.

The effect of bed height can be seen by comparing data shown in Figs. 11, 12 and 13. While the maximum degree of separation does not

seem to be affected by the bed height, the gas velocity required to achieve the maximum degree of separation increases with the bed height, presumably owing to the fact that a higher gas velocity is required to overcome the possible larger particle disturbances due to slugging.

Comparison of Particle Separation by Low and High Gas Velocity

The characteristics of the separation of dolomite from a fluidized char-dolomite mixture by low or high gas velocity can be summarized below:

(1) Low gas velocity separation: the degree of separation appears to be controlled mainly by the fluidizing velocity in the char-ash separator. Density difference between char and dolomite (simulating agglomerated ash) is the major factor for segregation. To achieve maximum degree of separation, the gas velocity in the char-ash separator should be controlled near the U_{mf} of the mean size ash particles to be removed. The rate of separation is rapid and appears to not be sensitive to the process operating conditions, e.g., gas velocity, bed height, etc.

(2) High gas velocity separation: the degree and rate of separating dolomite (simulating agglomerated ash) from the fluidized char-dolomite mixture by allowing dolomite but not char to fall through a conical nozzle where a high gas velocity prevails has been observed to be controlled not only by the gas velocity at the nozzle but also by the cone angle, the bed composition and the bed height. All these variables are interrelated in the laboratory unit to affect the degree and the rate of separation.

Comparison of these two methods of particle separation indicates that the second method, i.e., separation by high gas velocity at the nozzle, appears to be affected by more operating parameters. Thus, controlling such a process may be more difficult. For a single reactor designed to perform three major functions of the combustion process, i.e., char combustion, ash agglomeration and char-ash separation,

it is better to have each function controlled by as simple a variable as possible. Based on the information available, separation of the agglomerated ash at low gas velocity was selected for the Westinghouse coal gasification process. This design is incorporated in the Process Development Unit for pilot scale test.

ACKNOWLEDGMENT

The work was performed as part of the Westinghouse Coal Gasification Program. Discussions with Dr. W. C. Yang contributed to the assessment of the study.

LITERATURE CITED

1. Archer, D. H., Vidt, E. J., Keairns, D. L., Morris, J. P., Chen, J. L.-P., "Coal Gasification for Clean Power Production," Proceedings of the Third International Conference on Fluidized-Bed Combustion, Hueston Woods, Ohio, 1972, issued as EPA 650/2-73-053, December 1973, NTIS No. PD 231977.

2. Chen, J. L.-P. and Keairns, D. L., Can. J. Chem. Eng., Vol. 53, 395, Aug. (1975).

3. Cockerham, R. G., "Process and Apparatus for the Gasification of Ash-Containing Carbonaceous Fuel," British Patent 1047711, 1962.

4. "Bench Scale Research on Continuous Gasification Unit," Consolidation Coal Company R&D Report No. 16 to the Office of Coal Research, Department of the Interior, 1968.

5. Jequier, L., Longchambon, L., and Van de Putte, G., J. Inst. Fuel, 33, 1960, pp. 584-591.

6. Lee, B. S. and Tarman, P. B., "Status of the Hygas Program," paper presented at the Sixth Synthetic Pipeline Gas Symposium, Chicago, Ill., Oct. 28-30, 1974.

7. Merry, J.M.D., Chen, J.L.-P., and Keairns, D. L., "Design Considerations for Development of a Commercial Fluidized-Bed Agglomerating Combustor/Gasifier," Proceedings of the International Fluidization Conference held June 1975, edited by D. L. Keairns, published by Hemisphere Publishing Corporation, 1976.

8. Rowe, P. N., Nienow, S. W., and Aglium, S. J., Trans. Instr. Chem. Engrs., 50, 1972, p. 310.

9. Ibid, 1972, 50, 1972, p. 324.

SECTION 5.2

APPENDIX B

APPENDIX B
Research Report 76-8X4-PDULA-R2 August 31, 1976
Proprietary Class 2

THE ELECTRICAL RESISTIVITY OF CHAR/ASH MIXTURES IN A FLUIDIZED BED

J.L.P. Chen* and D. L. Keairns

ABSTRACT

The electrical resistivity difference between char and ash can be utilized to develop an instrument for distinguishing a char-rich mixture from an ash-rich mixture. Development of design data for an electrical conductivity probe to measure and control the char/ash interfaces in the Westinghouse coal gasification process is described.

The electrical resistivity of char/ash mixtures at ash compositions of 0, 25, 50, 75 and 100 wt.% has been measured for current densities of 3×10^{-9} to 2×10^{-2} amp/cm^2 and fluidizing velocities of 0 to 71.32 cm/sec. A general correlation based on the two-phase theory has been developed for the resistivity of fully-fluidized char/ash mixtures, i.e., $U \geq U_{tf}$ (the total fluidizing velocity), as a function of gas velocity, current density and bed composition. These results provide the basis for a preliminary design of an electrical conductivity probe. A typical design of such a probe is presented.

*J.L.P. Chen is currently with Hooker Chemical Co., Niagara Falls, NY.

SCOPE

An experimental and theoretical investigation of the conductivity properties of char, ash and mixtures was carried out to provide design data required for developing a conductivity probe for measuring and controlling the char/ash interfaces in the agglomerating combustor/gasifier of the Westinghouse coal gasification plant.

Most of the previous studies on the electrical properties of the fluidized system have been confined to the conducting particles of char or graphite[5-9] for the electrothermal fluidized bed reactor application. Only limited data on the electrical resistivity of mixtures of nonconducting and conducting particles were reported[12].

Since char is more conductive than ash or dolomite, a mixture which is rich in char may be distinguished from that rich in ash or dolomite by measuring the resistance of the bed mixture. This concept has been used by Consolidation Coal Company to measure the char-acceptor interface in their CO_2 acceptor process[5]. While their instrument is successful in measuring the char-dolomite interface, no instrument was developed for measuring the char-ash interface.

In this paper, the electrical resistivity of char, ash and their mixtures are examined in light of the current density, the gas velocity and the mixture composition. A semi-empirical model based on the two-phase theory is presented for the electrical resistivity of fully fluidized mixtures. The design criteria for an electrical conductivity probe are established and a typical design of the probe is presented.

CONCLUSIONS AND SIGNIFICANCE

The electrical resistivity of char/ash mixtures as a function of the current density, the gas velocity and the mixture composition is measured experimentally at room temperature and atmospheric pressure. While the mixture resistivity decreases weakly with the current density, it increases with the gas velocity at a slow rate when the gas velocity is either below the U_{bf} or above the U_{tf} of the mixture and at a fast rate when the gas velocity is between these two values. The resistivities of mixtures of less than or equal to 50 wt% of ash are essentially similar. A higher ash concentration, however, increases the resistivity very rapidly. An essentially infinite resistivity is observed for fluidized pure ash particles.

A semi-empirical model for predicting the resistivity of a fully fluidized mixture has been developed,

$$\frac{\zeta}{\zeta_s} = 1 + \frac{(U - U_{tf})^{0.967}}{0.711\sqrt{gC}}$$

and

$$\zeta_s = 1800.0(ID)^{-0.362} \ (1 + 108.7 \ Y^{10.0})$$

where ζ is the mixture resistivity; ζ_s is the resistivity at the total fluidizing velocity, U_{tf}; C is a function of bed diameter and bed height; ID is the current density and Y is the fraction of ash particles in the mixture.

Based on the data and the correlation presented in this paper, an electrical conductivity probe for measuring the char/ash interfaces in the agglomerating combustor/gasifier of the Westinghouse coal gasification plant is developed. The data and the correlation can also be used

to assist designing an electrothermal fluidized bed of mixtures composed of conducting char and non-conducting ash particles.

INTRODUCTION

Westinghouse is developing a two stage fluidized bed coal gasification process for producing low heating-value gas for combined cycle power generation[1,2]. The process includes a devolatilizer/desulfurizer and an agglomerating combustor/gasifier. Coal is devolatilized in the former reactor and the resulting char is burned and gasified in the latter one. The agglomerating combustor/gasifier consists of three reaction zones, i.e., the gasifier at the upper portion of the bed, the combustor/ash agglomerator in the middle and the char/ash separator at the bottom of the bed. As char is burned in the combustor/ash agglomerator, the residual ash particles agglomerate into large and heavy particles which precipitate into the char/ash separator for removal[2,3]. The velocity at each reaction zone can be independently controlled so that a natural segregation of particles in the reactor occurs.[4] Under nominal operating conditions, the gasifier may consist of high char concentration, e.g., $\geq$ 75% of char, for high efficiency of carbon-gas reaction and a combustor/ash agglomerator of high ash concentration, e.g., $\leq$ 25% of char, for complete carbon combustion and high rate of ash agglomeration. Segregation of ash agglomerates from the mixture in the char/ash separator results in a second interface which separates the high ash mixture in the combustor/ash agglomerator from the almost pure ash particles, e.g., $\leq$10% of char, in the char/ash separator. In order that the interfaces of these segregated fluidized mixtures can be measured and controlled for achieving maximum efficiency of the reactor performance, a method which can distinguish the mixture properties and indicate the location of the interface is required.

Since char is more conductive than ash or dolomite, a mixture which is rich in char may be distinguished from that rich in ash or

dolomite by measuring the resistance of the bed mixture. This concept has been used by Consolidation Coal Company to measure the char-acceptor interface in their CO_2 acceptor process[5]. However, no fundamental investigation of the electrical conductivity property of char and ash has been carried out. Design criteria for such an instrument were not given. This study was, therefore, directed to study the conductivity properties of char, ash, and their mixtures for establishing the design criteria for an electric conductivity probe to detect the char/ash interface. Experiments were carried out to determine the electrical resistivity of the char/ash mixtures as a function of the bed composition, current density and gas velocity. A general correlation based on the two-phase theory was developed to provide design equations for the conductivity probe.

While the fundamental data and the correlation developed in this study were used to design the conductivity probe for measuring the char/ash interface, this information may also be used for designing electrothermally fluidized-bed systems.

PREVIOUS WORK

Investigation of the fluidized bed resistance and other electrical characteristics has attracted many investigators' attention since the electrothermal fluidized bed reactors were introduced[6-9]. Most of the previous work on the measurement of the electrical properties of fluidized systems involved measuring the overall interelectrode resistance of fluidized bed systems of conducting particles. Reed and Goldberger[10], and Chen, et al[11], however, measured the bed resistance as well as the total resistance of the system. They discovered that the contact resistance between the electrode and the fluidized bed could be a major component of the total resistance. This contact resistance, however, depends on the type of electrode and decreases as the electrode material is changed from silicon carbide, stainless steel, brass to graphite. Negligible contact resistance resulted from the graphite electrode.

The electrical resistance of bed particles has been found to be affected by gas velocity, temperature, particle size, column diameter and current density[10-13]. This bed resistance has been reported by Reed and Goldberger[10] to follow the well-known resistance equation,

$$R = \zeta \frac{L}{A_p}.$$

where R is the bed resistance; ζ, the resistivity; L, the distance between the two electrodes and A_p, the cross sectional area for current flow.

While the bed resistivity generally increased slowly with gas velocity when the velocity was either below or above the incipient fluidizing velocity, it increased rapidly near the incipient fluidizing velocity [12,13]. The resistivity, however, decreased with increasing

temperature[10,13], particle size[10-13] and column diameter[12,13]. A low current density was found[10,13] to have little effect on the bed resistivity, but the bed resistivity decreased as the current density was increased from 0.0465 amp/cm^2.

Borodulya, et al[13] have investigated the electrical resistivity of mixtures of nonconducting alumina and conducting graphite of equal minimum fluidizing velocity. They showed that the addition of non-conducting alumina particles greatly increased the resistivity of the bed at all gas velocities with the increase being proportional to the concentration of alumina. The dependence of the mixture resistivity on the gas velocity, however, was similar to that of pure graphite particles, indicating that the addition of the non-conducting alumina may simply interrupt some of the conducting chain of graphite particles but not affect the fluidization characteristics of the mixture.

When a mixture of two different materials, with a substantial difference in density, is fluidized at low gas velocity, near the minimum fluidizing velocity of either material, segregation of particles may occur. Chen and Keairns[3,4] investigated the segregation characteristics of a fluidized bed and reported that U_{tf} (total fluidizing velocity) and U_{bf} (beginning fluidizing velocity) instead of U_{mf} of either material should be used as criteria for identifying the mixture to be in a fully fluidized state or in a fixed bed state. Partial fluidization and segregation of particles may occur in a bed fluidized at a velocity between these two velocities. No measurement of the electrical resistance of such a mixture at any gas velocity, however, has been reported in the literature.

EXPERIMENTAL APPARATUS AND PROCEDURE

The experimental apparatus consists of a fluidized bed system and an electrical resistance measuring system as shown schematically in Fig. 1. Measurements of the resistance were limited to room temperature and atmospheric pressure. Eight mixtures consisting of char and ash particles of either uniform size or wide size distribution at an ash composition of 0, 25, 50, 75 and 100 wt% were used in this study. Table 1 shows the size and composition of these mixtures. The wide size distribution particles were so selected that the U_{mf} of the mixture is equal to that of the uniform size particles.

Fluidized Bed System

The fluidized bed system is composed of an air supply system, a pressure regulator, a flow meter, a fluidized bed column and a filter. Figure 1 shows the flow diagram. The fluidized bed column is a 114 mm diameter Plexiglas column of 610 mm long as shown in Fig. 2. A porous stainless steel distributor (pore size 65 μm, 3.18 mm thick) was installed between the fluidized bed and the plenum for uniformly distributing the fluidized gas across the bed. Three pressure taps, 15.9 mm, 85.5 mm and 428.2 mm along the distributor, were used to measure the pressure drop and hence the fluidization characteristics of the mixture. This system is similar to the apparatus used to study the segregation of particles in a fluidized bed[3].

Electrical Resistance Measuring System

Figure 3 shows schematically the electrical resistance measuring system. It consists of two copper electrical conductivity probes, each 18 mm wide, 250 mm long and 3.175 mm thick. The probes are spaced at 85 mm distance and are partially immersed in the

Dwg. 6366A32

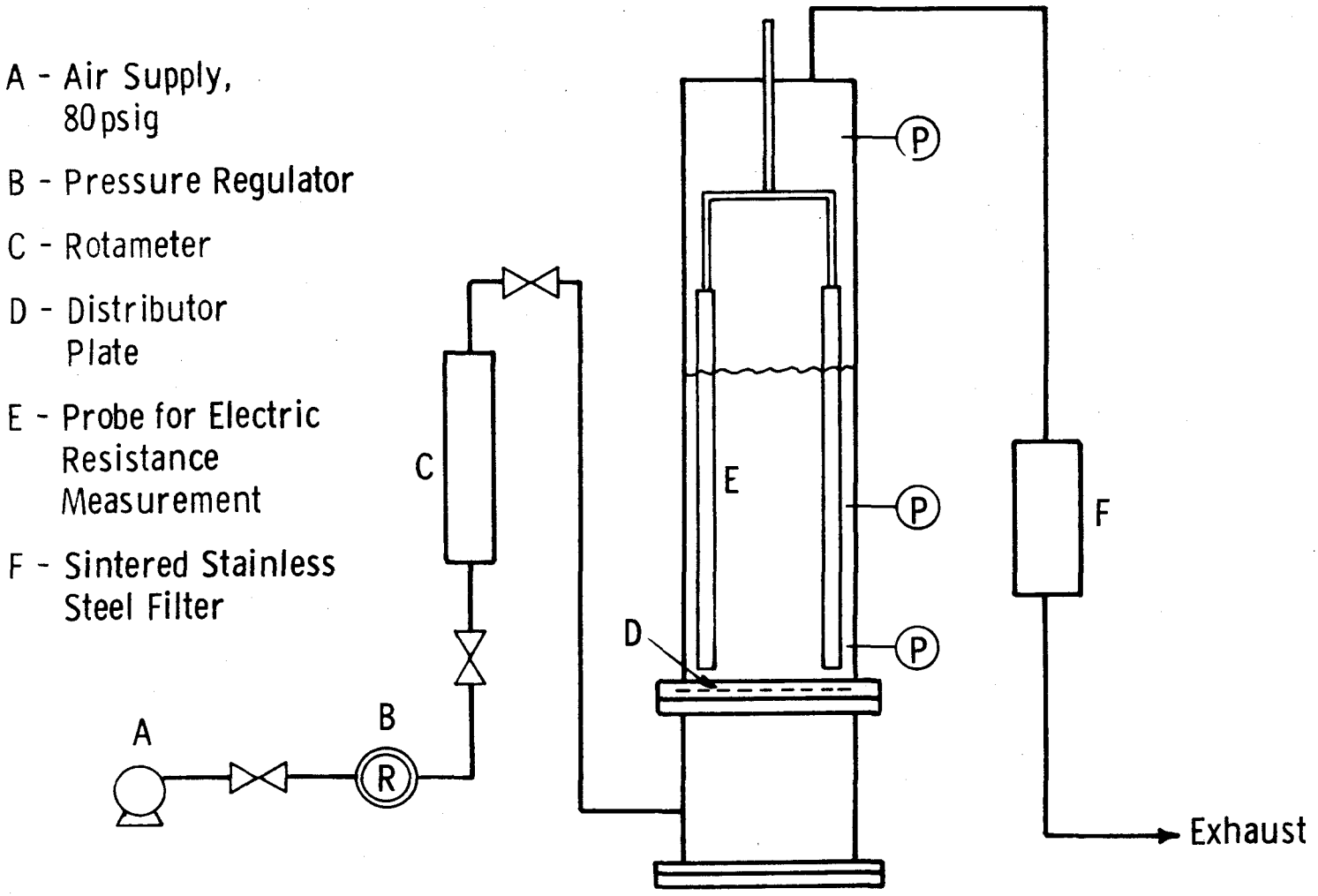

Fig. 1 – Schematic diagram of apparatus

Table 1

Bed Material Used for this Study

Designated Mixture	Material & Size μm		Calculated U_{mf}*** at 101 kPa cm/sec	Composition wt percent
A	Char*	841 x 595	16.5	100
	Ash**	595 x 250	10.5	0
B	Char	841 x 595	16.5	75
	Ash	595 x 250	10.5	25
C	Char	841 x 595	16.5	50
	Ash	595 x 250	10.5	50
D	Char	841 x 595	16.5	25
	Ash	595 x 250	10.5	75
E	Char	841 x 595	16.5	0
	Ash	595 x 250	10.5	100
F	Char	1680 x 1190	16.5	10
		1190 x 841		35
		841 x 595		19
		595 x 420		36
	Ash	595 x 250	10.5	0
G	Char	1680 x 1190	16.5	5
		1190 x 841		17.5
		841 x 595		9.5
		595 x 420		18
	Ash	595 x 250	10.5	50
H	Char	1680 x 1190	16.5	2.5
		1190 x 841		8.75
		841 x 595		4.75
		595 x 420		9
	Ash	595 x 250	10.5	75

*Char: Supplied by FMC, particle density ∿ 0.72 g/c.c.

**Ash: Slag ash from Willow Island Power Station, Monongahela Power Company. Particle density ∿ 2.7 g/c.c.

***U_{mf} calculated based on mean particle size and the equation proposed by Wen and Yu.[13]

$$U_{mf} = \frac{\mu}{D_p \rho_g} \left\{ \left[(33.7)^2 + 0.0408 \frac{D_p^3 \rho_g (\rho_s - \rho_g) g}{\mu^2} \right]^{1/2} - 33.7 \right\}$$

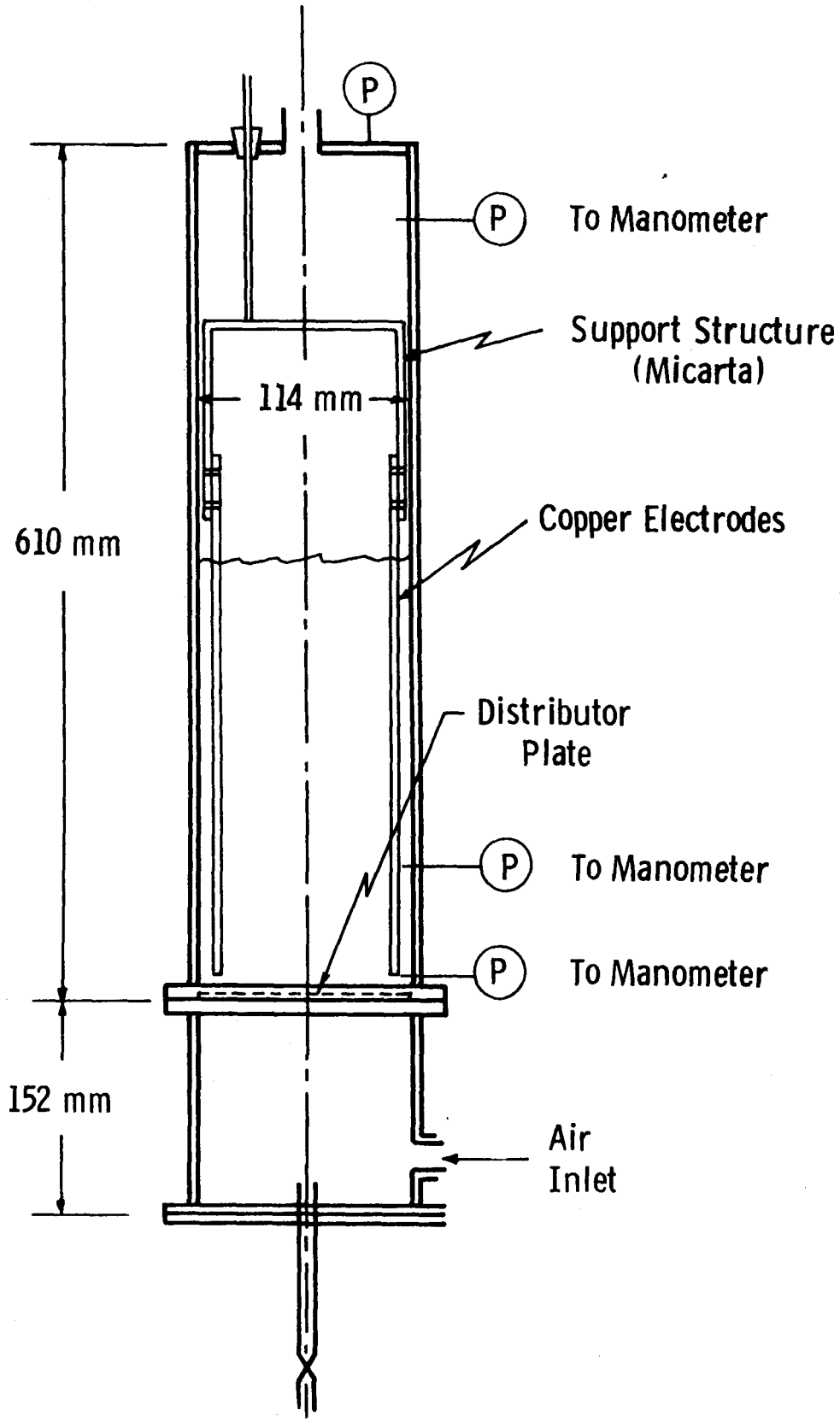

Fig. 2—Plexiglas fluidized bed column

Dwg. 6366A34

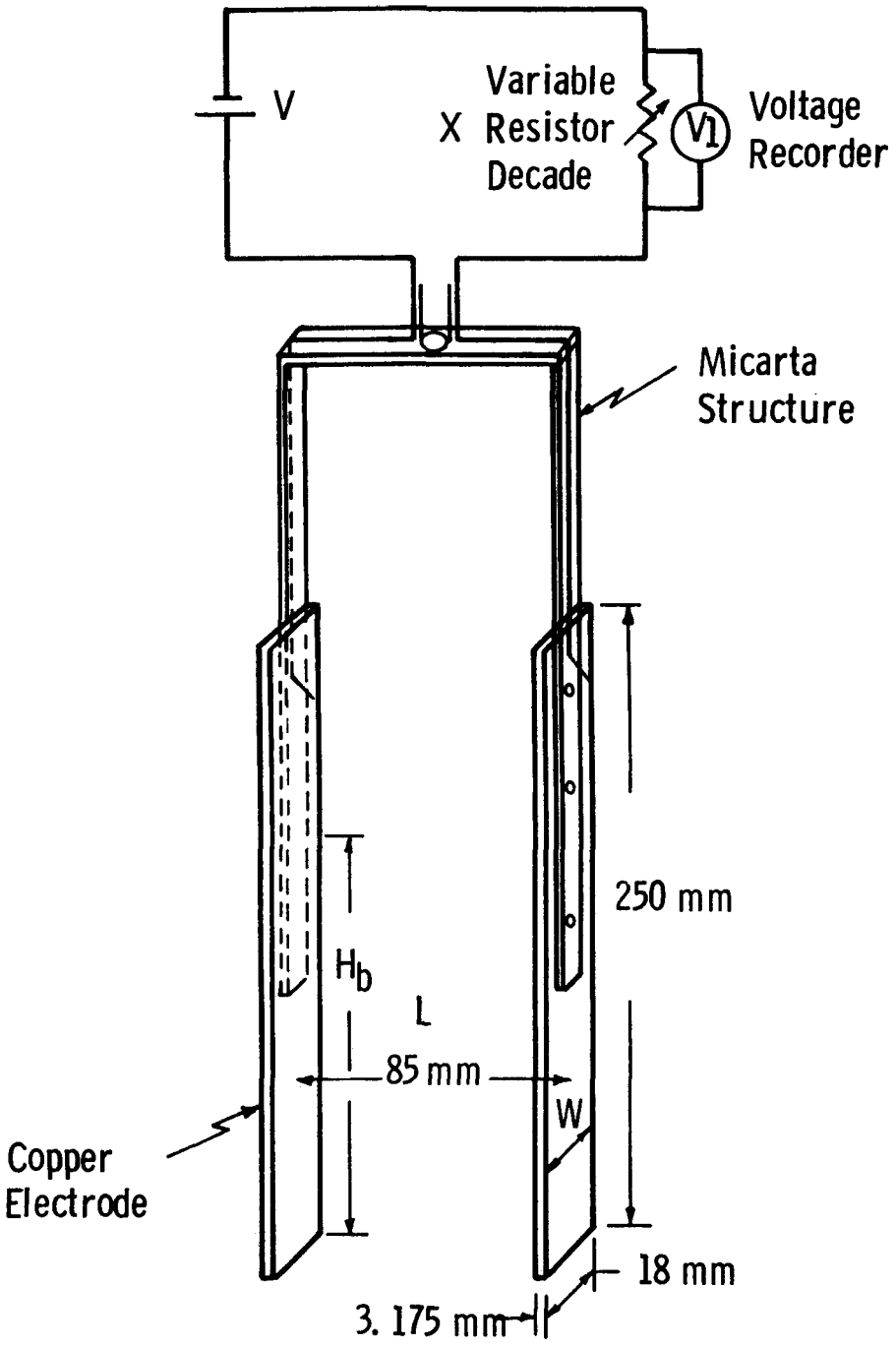

Fig. 3—Schematic diagram of the electrical resistance measuring system

fluidized bed. An electric circuit with a power supply (V), a variable resistance decade (X) and a voltage recorder (V_1) was used to measure the interelectrode resistance of the mixture.

Procedure

For a char/ash mixture of known composition, the interelectrode resistance of the fluidized bed was measured for a sequence of gas velocities, starting from a high value and gradually decreasing to the U_{bf} (the beginning fluidizing velocity), and a sequence of power supplies for different current densities. The bed height of the mixture was maintained below the upper ends of the electrodes so that the current passes through the whole bed height and an average bed resistance can be obtained if there is non-uniform distribution of particles in the fluidized bed. The resistance of the static mixture at velocities below U_{bf} was measured by loading the bed with well-mixed particles and gradually increasing the gas velocity from zero to U_{bf}. Visual observation and pressure drop measurement as described by Chen and Keairns[3] were used to determine the U_{tf} (total fluidizing velocity) and the U_{bf} (beginning fluidizing velocity) of the mixture.

The resistance at the decade (X) is adjusted to give a voltage drop (V_1) within the measurable range of the recorder. The resistance of the bed mixture (R) can be calculated from the decade resistance (X) and the voltage (V_1) across this resistor by the following equation:

$$R = X \left[\frac{V}{V_1} - 1 \right]$$

and the current density can be calculated from

$$ID = \frac{V_1}{X \cdot H_b \cdot W}$$

with H_b being the fluidized bed height and W being the electrode width.

The resistivity of the fluidized mixture is calculated by using the resistance equation

$$\zeta = R \frac{H_b \cdot W}{L}$$

where L is the distance between the two electrodes.

EXPERIMENTAL RESULTS AND DISCUSSION

Fluidization Characteristics of the Mixture

When the char/ash mixtures were fluidized at velocities decreasing from a high value, e.g., 4 to 5 times U_{mf} of ash aprticles, to the U_{bf}, the particles segregated into a partially fluidized bed at velocities between the U_{tf} and the U_{bf} of the mixture. The upper fluidized portion consisted of high char concentration particles whereas the lower static portion consisted of high ash concentration. Velocities above the U_{tf} or below the U_{bf} resulted in a well-mixed fully fluidized bed or a static bed, respectively. These results are consistent with those reported by Chen and Keairns[3]. The measured U_{tf} and U_{bf} of the mixtures used in this study are given in Table 2. The electrical resistivity of a mixture measured at velocities either greater than the U_{tf} or smaller than the U_{bf} of the mixture represents the resistivity of a uniformly distributed mixture. However, measurements carried out at velocities between the U_{tf} and the U_{bf} of the mixture may represent the resistivity of a combined fluidized and static bed of different bed composition.

Effect of Current Density

The resistivity of char/ash mixtures at a composition of 0, 25, 50, 75 and 100 wt% of ash, i.e., material A, B, C, D and E in Table 1, and at various fluidized states,is shown in Figs. 4 thru 8, respectively, as a function of current density in the range of 3×10^{-9} to 2×10^{-2} amp/cm^2. The resistivity decreases with the increase of current density for mixtures fluidized at any velocity. The data plotted on a log-log scale show an approximate linear relationship of constant slope, e.g., -0.362, indicating that the same type of functional

Table 2

Measured U_{bf} and U_{tf} of the Mixtures Used in This Study

Designated Mixture*	U_{bf} cm/sec	U_{tf} cm/sec
A	16.1	16.1
B	13.4	28.3
C	13.4	28.3
D	13.4	28.3
E	10.5	10.5
F	16.1	16.1
G	13.4	28.3
H	13.4	28.3

*See Table 1 for material, size and composition

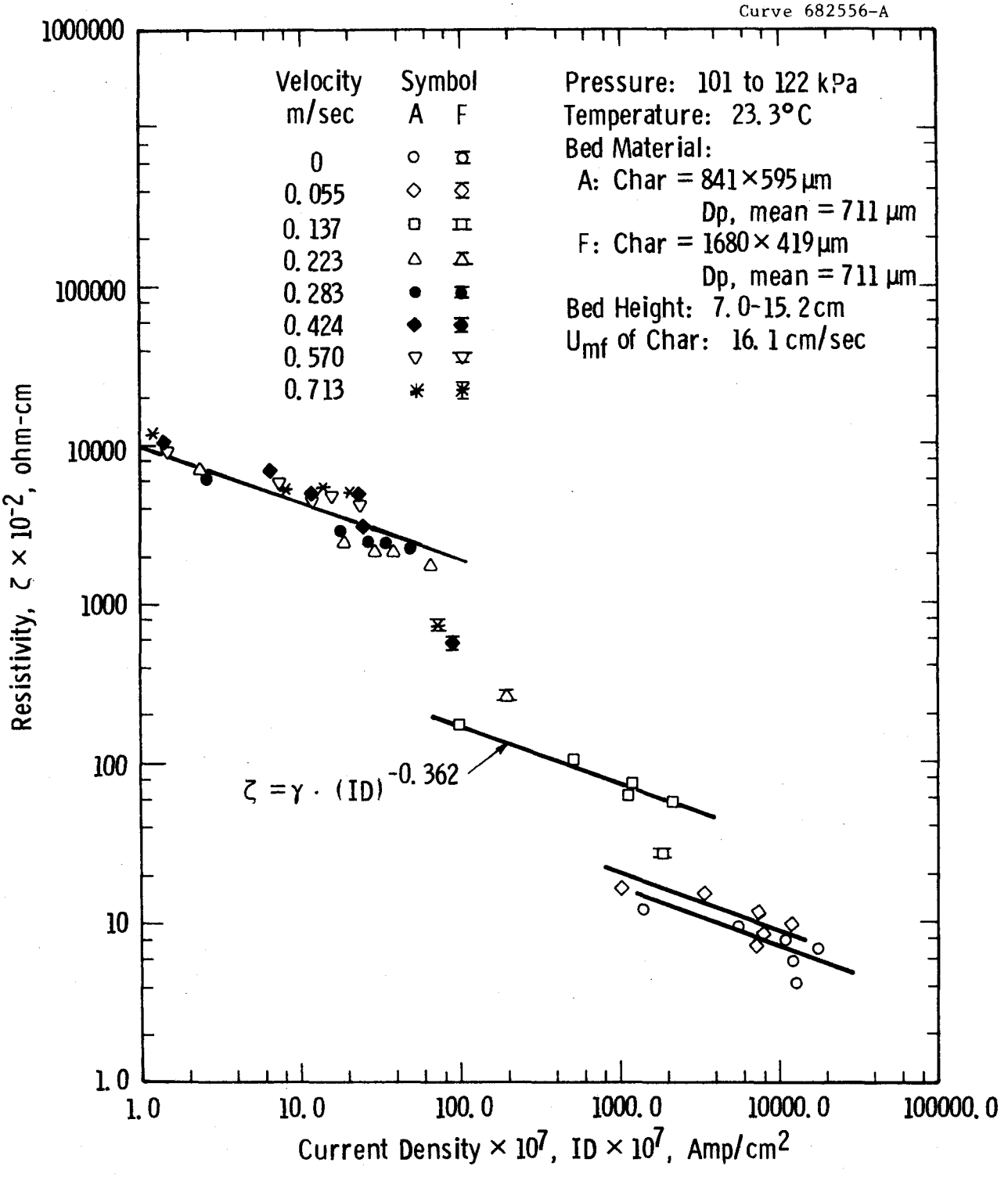

Fig. 4—Resistivity of char/ash mixture as a function of current density

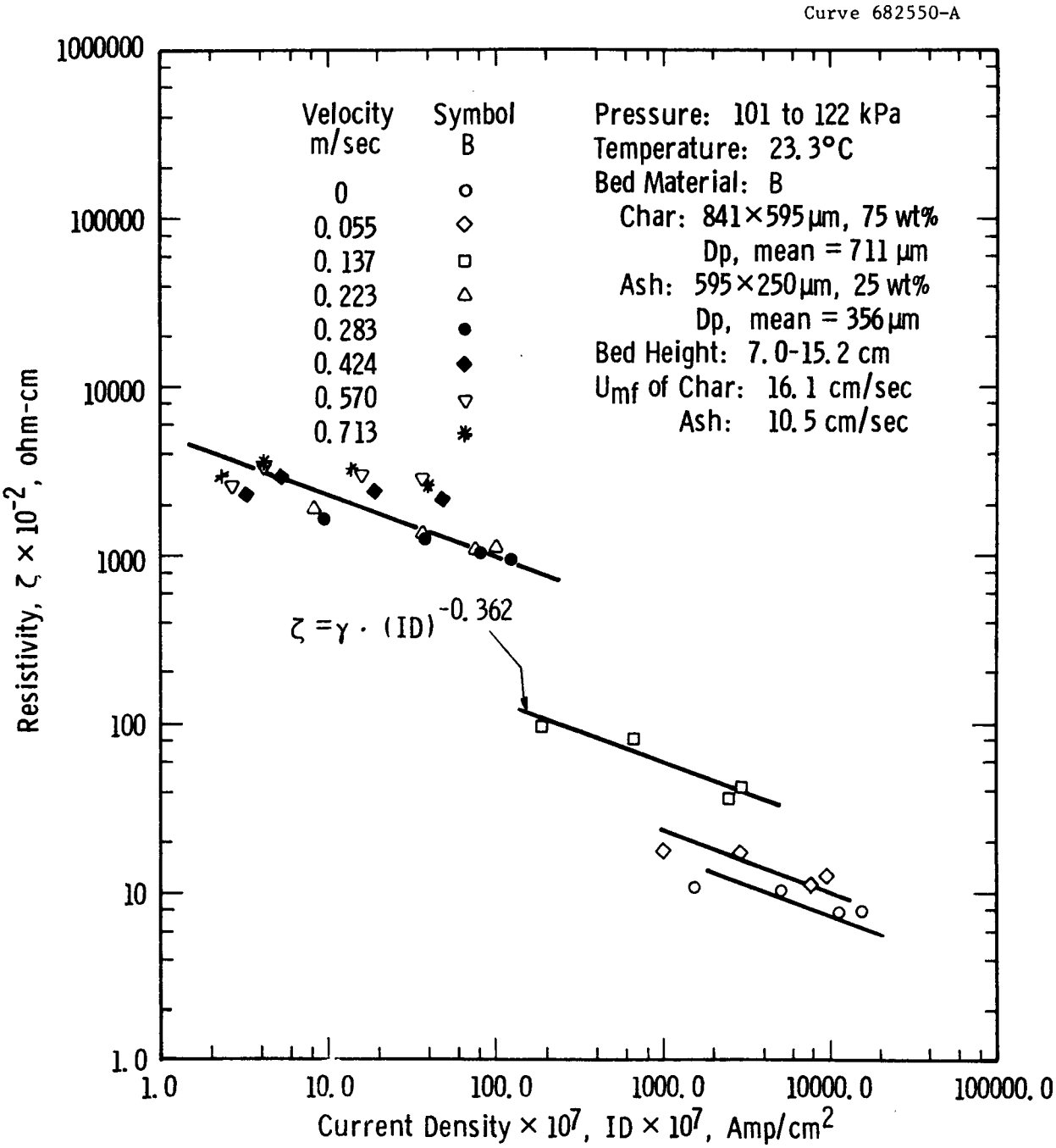

Fig. 5—Resistivity of char/ash mxiture as a function of current density

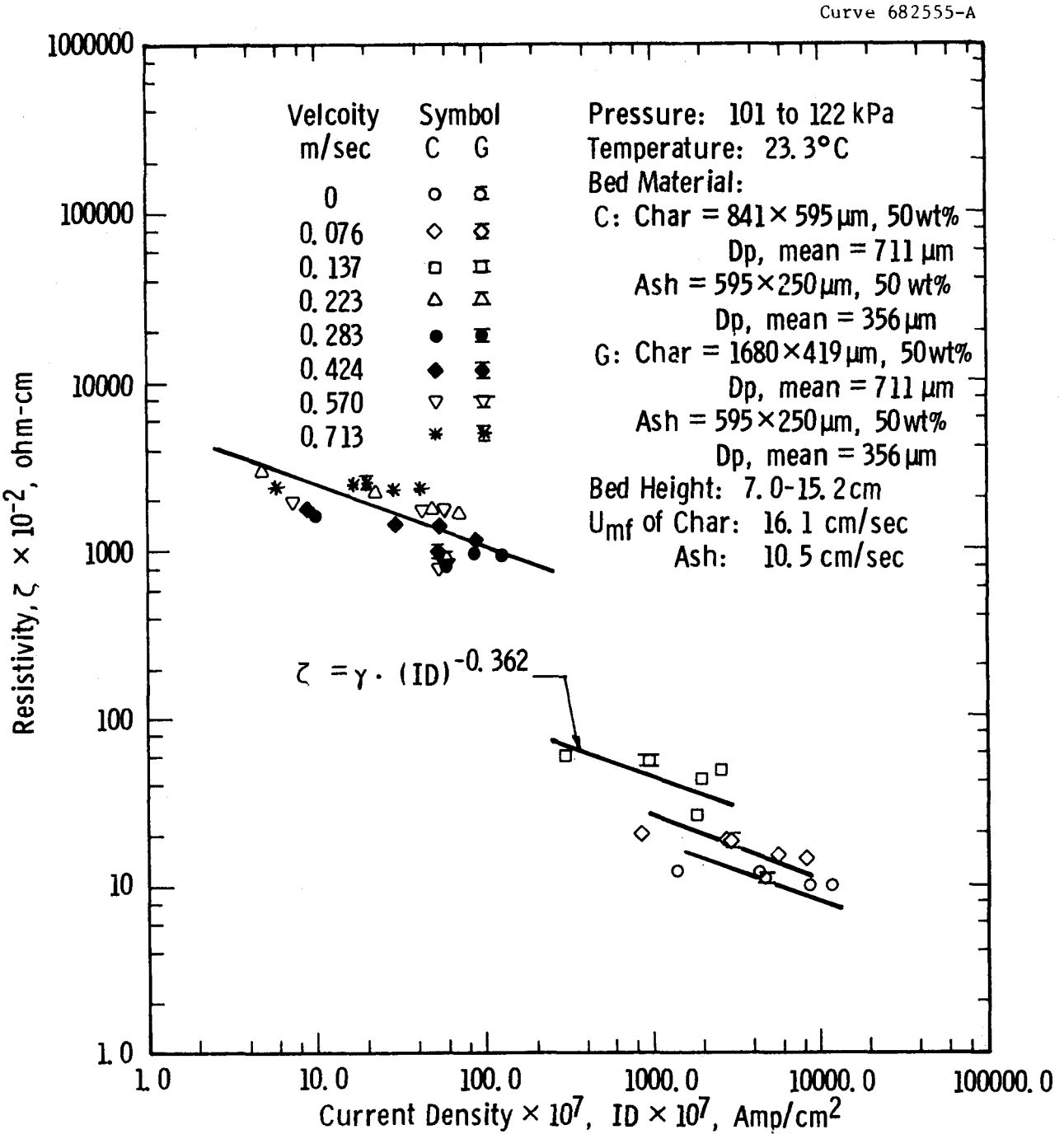

Fig. 6—Resistivity of char/ash mixture as a function of current density

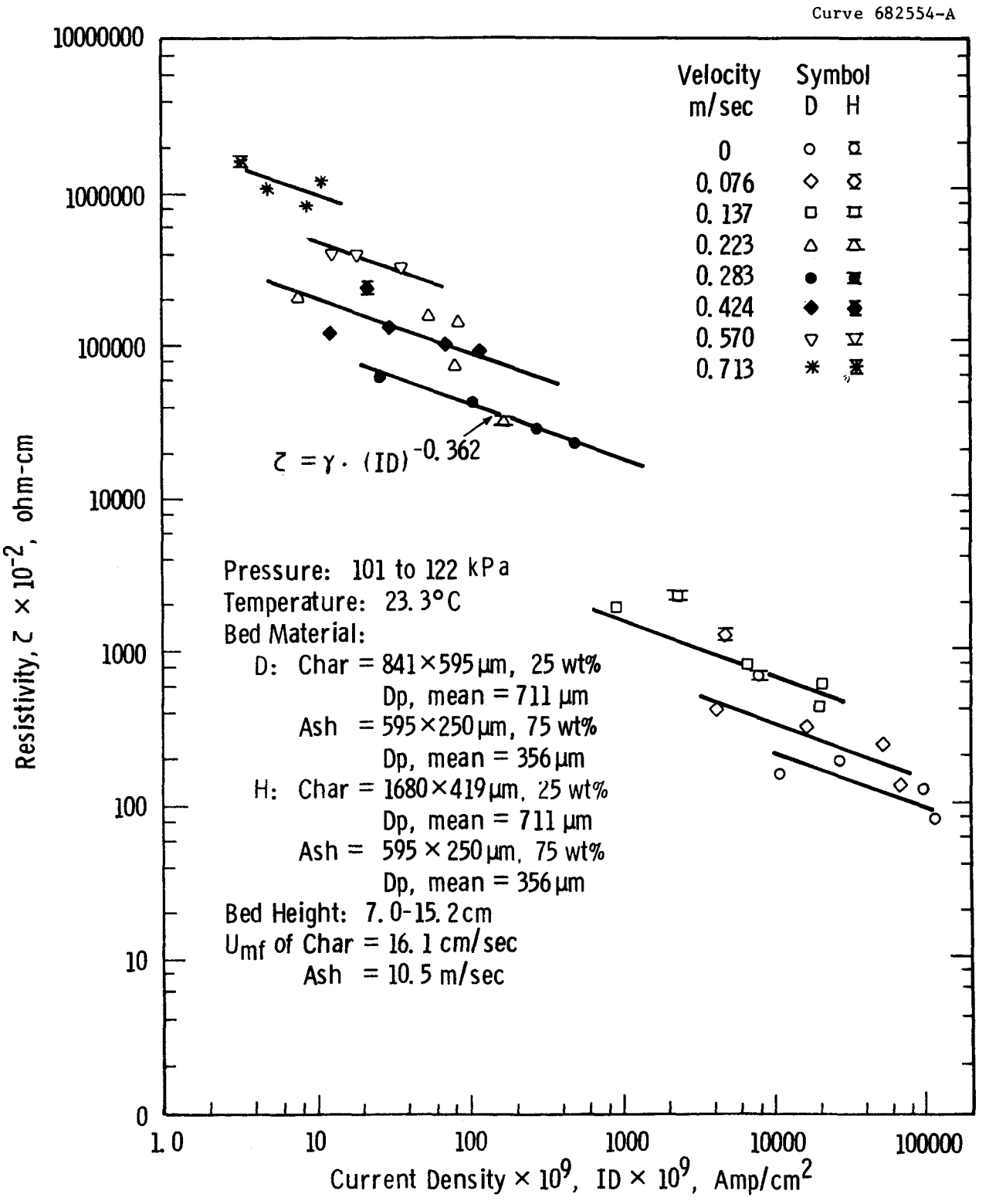

Fig. 7—Resistivity of char/ash mixture as a function of current density

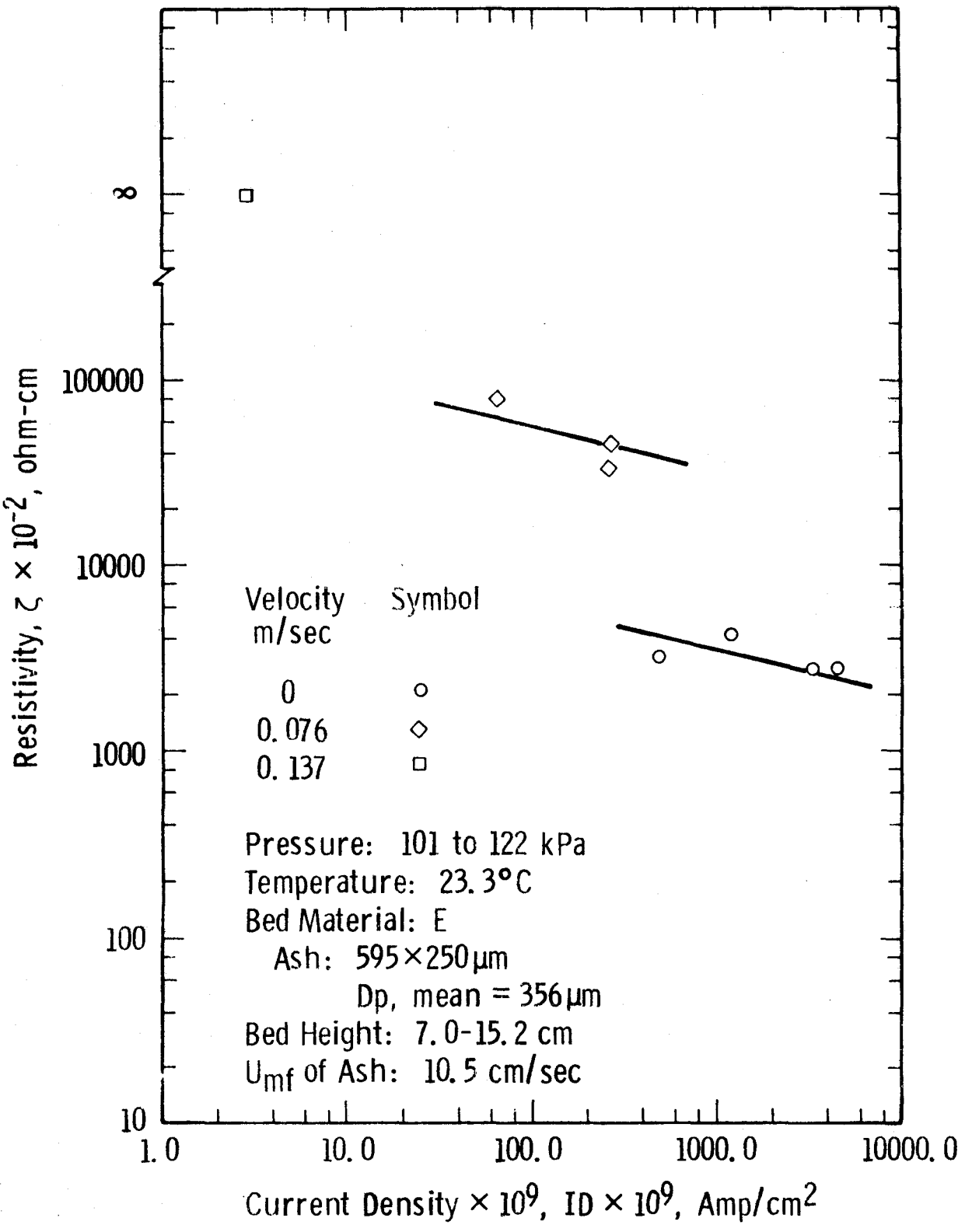

Fig. 8—Resistivity of char/ash mxiture as a function of current density

dependence of the resistivity on the current density may prevail for all mixtures fluidized at any velocity. Segregation of particles at velocities between the U_{tf} and the U_{bf} does not seem to affect this relationship, possibly due to the fact that both the resistivity and the current density are intensive quantities per unit cross sectional area for current flow. The reduction of the cross sectional area for current passage has the same effect on the resistance and the current flow if the resistance of the fluidized and the static portions of a segregated mixture are parallel and a much higher resistance prevails in the static bed. The resistivity and the current density calculated from these two quantities are therefore not affected. The measured resistivity in this velocity range, however, may not actually represent that of the mixture, but rather represents approximately that of the mixture in the fluidized portion of the segregated bed. The functional relationship of the resistivity and the current density may be represented by the following equation

$$\zeta = (ID)^{-0.362} \cdot \gamma$$

where γ is a function of the mixture properties and the gas velocity.

The resistivities of the mixtures were calculated from the overall resistance without subtracting the electrode-to-bed resistance. Undoubtedly, this resistivity may be different from the actual bed resistivity. However, since the contact resistivity of the copper electrode is small,[11] e.g., less than 10% of the interelectrode resistivity for mixtures containing char and ash, and uniform over the velocity range of this investigation, the difference may be compensated by a constant which is eliminated when a relative resistivity instead of an absolute resistivity is used.

Effect of Gas Velocity, Bed Composition and Size Distribution

In order to investigate the effect of the gas velocity and the mixture properties, e.g., the bed composition and the size distribution,

on the mixture resistivity, a modified resistivity, i.e., a resistivity independent of the current density, $\gamma = \zeta \cdot ID^{0.362}$, is plotted against the velocity for mixtures consisting of 0 to 100 wt% of ash.

For mixtures of less than 50% of ash, the modified resistivity increases smoothly with the gas velocity, at a slow rate with velocities either below the U_{bf} or above the U_{tf} and at a fast rate with velocities beyond the U_{bf} but less than the U_{tf} of the mixture. This result is consistent with Borodulya, et al's finding.[12] For mixtures of greater than or equal to 50% of ash, the modified resistivity exhibits a peak at a velocity between the U_{bf} and the U_{tf} of the mixture. This behavior is similar to that reported by Chen, et al[11] and can be explained by noting that segregation of particles prevails in this velocity range and the actual cross sectional area for current passage (assuming most of the current passing through the upper bed) may be largely reduced for these high ash composition mixtures. The resistivity computed by using the cross sectional area of the whole mixture may be larger than that computed by using the reduced cross sectional area for current flow. Further analysis of the resistivity of the segregated mixture in this velocity range is beyond the scope of this report.

The modified resistivities of mixtures of less than or equal to 50% of ash are essentially similar. While the curves drawn through average data points of these mixtures show that the resistivity decreases with increasing ash composition, the data points are actually overlapping and of the same order of magnitude, making it difficult to justify whether these curves may distinguish the difference in their resistivity. A higher ash concentration, however, increases the resistivity very rapidly. An essentially infinite resistivity was observed for fluidized pure ash particles.

Since ash particles are essentially non-conducting, their addition to the char bed may interrupt the carbon chains for current passage. When the ash concentration in the mixture is low, e.g., $\lesssim$ 50%, the frequency and area of contact for the carbon particles are

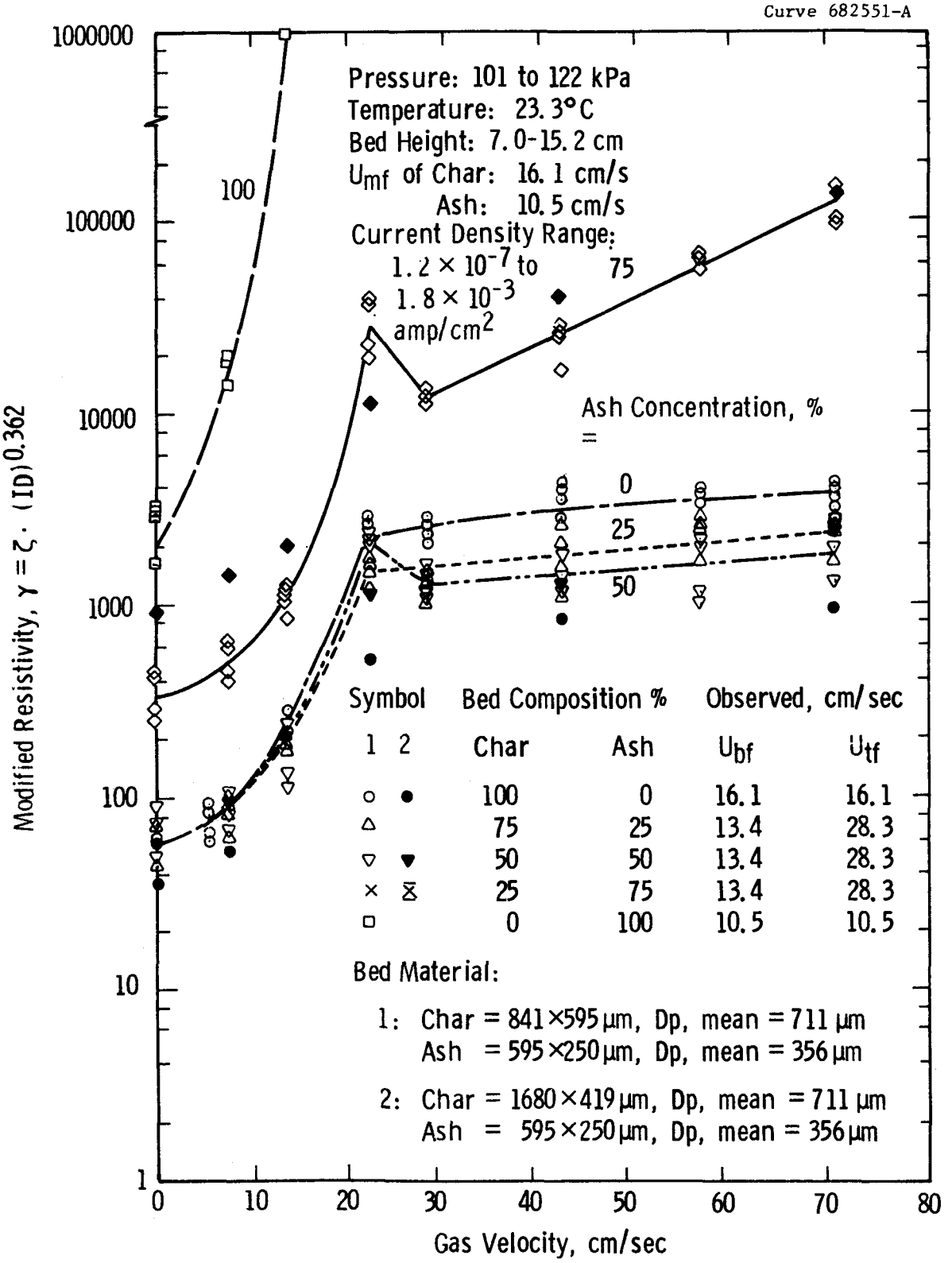

Fig. 9—Resistivity of char/ash mixture as a function of gas velocity

practically not reduced by the presence of ash particles because of rapid movement of particles in the fluidized bed. However, a higher ash concentration, e.g., $\geq$ 75%, may trap each individual char particle in the interstices of ash particles and hence interrupt completely the conducting chains of carbon particles. The whole bed may behave like a fluidized bed of composite particles (carbon particle at the center and ash particles in the surrounding) and a higher bed resistivity may be expected.

The resistivities of mixtures of wide sized char and narrow sized ash, e.g., material F, G, and H in Table 1, are also shown in Fig. 9 for mixtures of 0, 50 and 75% of ash. While the resistivity of a wide sized char-ash mixture is lower for beds containing less than 50% of ash, it is higher for beds containing equal to or greater than 75% of ash. This may be due to the fact that the quality of fluidization is improved by increasing the wideness of the size distribution. The mixing and hence the contact of char particles with wide size distribution of char may be better and the conduction of current through the carbon chain may be higher for mixtures containing less than 50% of ash. However, when the ash concentration is greater than 75%, each individual char particle is completely surrounded by ash particles when the mixture is very uniformly mixed. Improvement of the particle mixing by increasing the size distribution may enforce this effect and hence increase the mixture resistivity by helping to interrupt the conduction chain of carbon.

THEORETICAL CONSIDERATION

When a mixture of two different materials, with a substantial difference in density, is fluidized at a velocity between the U_{bf} and the U_{tf} of the mixture, segregation of particles may occur.[3,4] Experiments carried out for this study have confirmed this fluidization characteristic. The electrical resistivity measured for this mixture may represent the actual resistivity of a uniformly distributed mixture only when the gas velocity is either below the U_{bf} or above the U_{tf} of the mixture. The theoretical development to correlate the data, however, is confined to the region where the velocity is equal to or greater than the U_{tf} of the mixture since the resistivity of mixtures which are well mixed and fluidized is of particular interest.

Development of the Theoretical Model

The following assumptions are made in the theoretical development of the model:

(1) The two-phase theory is applicable to these mixtures with the bubbling phase initiated at a velocity equal to the U_{tf} of the mixture. The particulate phase is in a minimally fluidized state.

(2) The resistances of the bubbling phase and the particulate phase at any vertical plane (see Fig. 10) are in parallel. The total resistance of the mixture between the two electrodes is the series sum of the resistances at each vertical plane.

(3) An average bubble size with respect to the bed height is applicable to this fluidized bed.

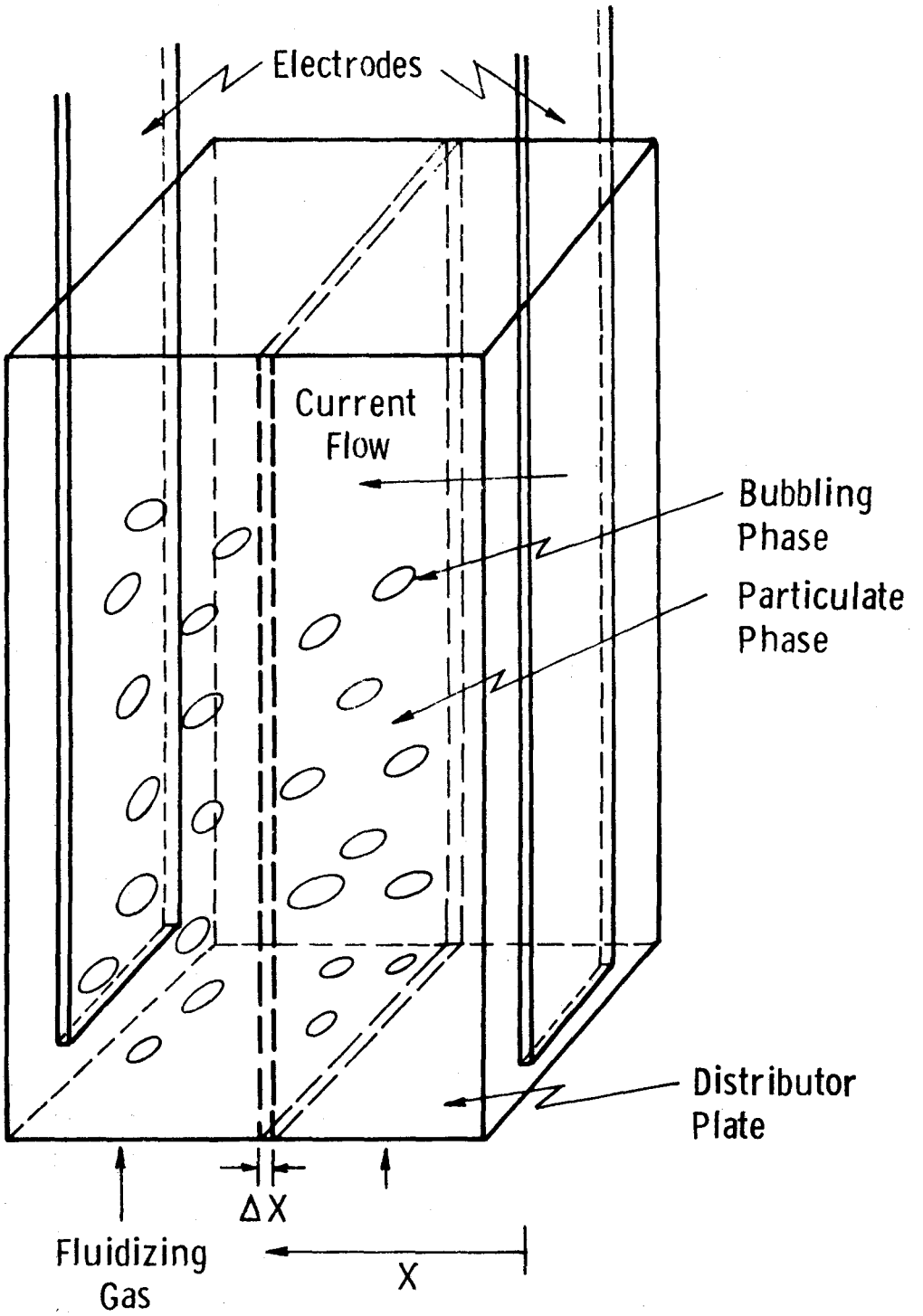

Fig. 10—Schematic diagram of bubbling and particulate phases in a fluidized bed

Based on these assumptions, the resistance of the bed mixture, R_i, at a location X can be calculated from the resistance of the bubbles, R_g, and that of the particulate phase, R_s, from the following equation

$$R_i = \left(\frac{R_g \cdot R_s}{R_g + R_s} \right)_i \tag{1}$$

Since the resistance of the gas bubbles is essentially infinite, Equation (1) can be simplified to

$$R_i \approx (R_s)_i \tag{2}$$

The total resistance of the mixture between the two electrodes is the sum of the individual resistances:

$$R = \Sigma R_i = \Sigma (R_s)_i = R_s \tag{3}$$

Applying the resistance equation for both terms of Eq. (3) leads to

$$\frac{\zeta L}{A_p} = \frac{\zeta_s L}{A_s} \tag{4}$$

where ζ and A_p are the resistivity and the cross sectional area of the fluidized bed for the current flow and ζ_s and A_s are those quantities for the particulate phase of the fluidized bed.

Since the electrodes cover the whole bed height, the total cross sectional area for the current passage is the product of the bed height, H_b, and the width of the electric field, $\bar{W}$. The cross sectional area for the current passage through the particulate phase is equal to the product of the minimum fluidized bed height, H_{mf}, and the width of the electric field, $\bar{W}$. Substituting these quantities into Eq. (4) results in

$$\zeta = \zeta_s \frac{H_b}{H_{mf}} \tag{5}$$

From the two phase theory, the increase in bed height over that at minimum fluidization is due to the presence of bubbles alone, i.e.,

$$N\ V_b\ H_b = H_b - H_{mf} \tag{6}$$

where N is the number of bubbles per unit bed volume and V_b is the bubble volume.

The volumetric gas flow rate can be calculated by considering the continuity of the gas quantity, i.e.,

$$N\ V_b\ U_a = U - U_{mf} \tag{7}$$

where U_a is the bubble velocity and U and U_{mf} are the superficial gas velocities.

The absolute rising velocity of a bubble, U_a, is the sum of the natural rising velocity, U_b, as given by Davis and Taylor[15] and the upward velocity of the particulate phase between the bubbles, i.e.,

$$U_a = (U - U_{mf}) + 0.711 \sqrt{g\ \bar{D}_b} \tag{8}$$

where $\bar{D}_b$ is the effective or mean bubble diameter.

Combining Eqs. (6), (7) and (8) results in

$$\frac{H_b}{H_{mf}} = 1 + \frac{U - U_{mf}}{0.711 \sqrt{g\ \bar{D}_b}} \tag{9}$$

The bubble diameter in a fluidized bed can be calculated by using Mori and Wen's correlation,[16]

$$D_b = D_{bM} - (D_{bM} - D_{bo})e^{-0.3\ h/D_t} \tag{10}$$

where D_{bM} and D_{bo} are the maximum and initial bubble size, respectively and D_t is the fluidized bed diameter. h is the elevation above the distributor.

Integrate Eq. (10) with respect to the elevation above the distributor results in a mean bubble diameter, i.e.,

$$\overline{D}_b = D_{bM} - \frac{D_t}{0.3\ H_b} (D_{bM} - D_{bo})\ (1 - e^{-0.3\ H_b/D_t}) \tag{11}$$

The maximum bubble diameter is[16]

$$D_{bM} = 0.652\ \{\ A_t\ (U - U_{mf})\ \}^{0.4} \tag{12}$$

The initial bubble diameter is, for a porous distributor plate,

$$D_{bo} = 0.00376\ (U - U_{mf})^2 \tag{13}$$

for a perforated distributor plate,

$$D_{bo} = 0.347\ \{\ A_t\ (U - U_{mf})/N_d\ \}^{0.4} \tag{14}$$

where A_t is the cross-sectional area of the fluidized bed and N_d is the number of orifice openings on the distributor.

For a fluidized bed with a perforated distributor plate of large orifice numbers, the D_{bo} is small compared to the D_{bM} and may be neglected.

Substituting Eq. (12) into Eq. (11) leads to

$$\overline{D}_b = 0.652\ A_t^{0.4}\ \{\ 1 - \frac{D_t}{0.3\ H_b} (1 - e^{-0.3\ H_b/D_t})\ \}$$

$$(U - U_{mf})^{0.4} = C \cdot (U - U_{mf})^{0.4} \tag{15}$$

where

$$C = 0.652\ A_t^{0.4}\ \{\ 1 - \frac{D_t}{0.3\ H_b}\ (1 - e^{-0.3\ H_b/D_t})\ \} \qquad (16)$$

is a strong function of the fluidized bed cross sectional area and a weak function of the H_b/D_t ratio.

Substituting Eqs. (15) and (9) into Eq. (5) results in the resistivity equation

$$0.711\ (\frac{\zeta}{\zeta_s} - 1)\ \cdot\ g^{1/2}\ \cdot\ C^{1/2} = (U - U_{mf})^{0.8} \qquad (17)$$

Since the dependence of the resistivity on the current density at any gas velocity has been found experimentally to follow the functional relation,

$$\zeta = (ID)^{-0.362}\ \cdot\ \gamma \qquad (18)$$

and the U_{mf} of the mixture should be replaced by U_{tf} for mixtures possessing particle segregation tendency, Eq. (17) can be modified to

$$0.711\ (\frac{\gamma}{\gamma_s} - 1)\ \cdot\ g^{1/2}\ \cdot\ C^{1/2} = (U - U_{tf})^n \qquad (19)$$

The constant n will be determined from the experimental data.

Determination of the Constant and the Correlation

Equation (19) suggests that plotting the logarithm of the quantities on both sides of the equation should yield a straight line passing through the origin and having a slope equal to the constant n. The data presented in Fig. 9 were used to compute these quantities and those values with gas velocities greater than the U_{tf} were plotted in Fig. 11. The current density for these data was within 1.2×10^{-7} and 1.8×10^{-3} amp/cm^2. An examination of these data points reveals that

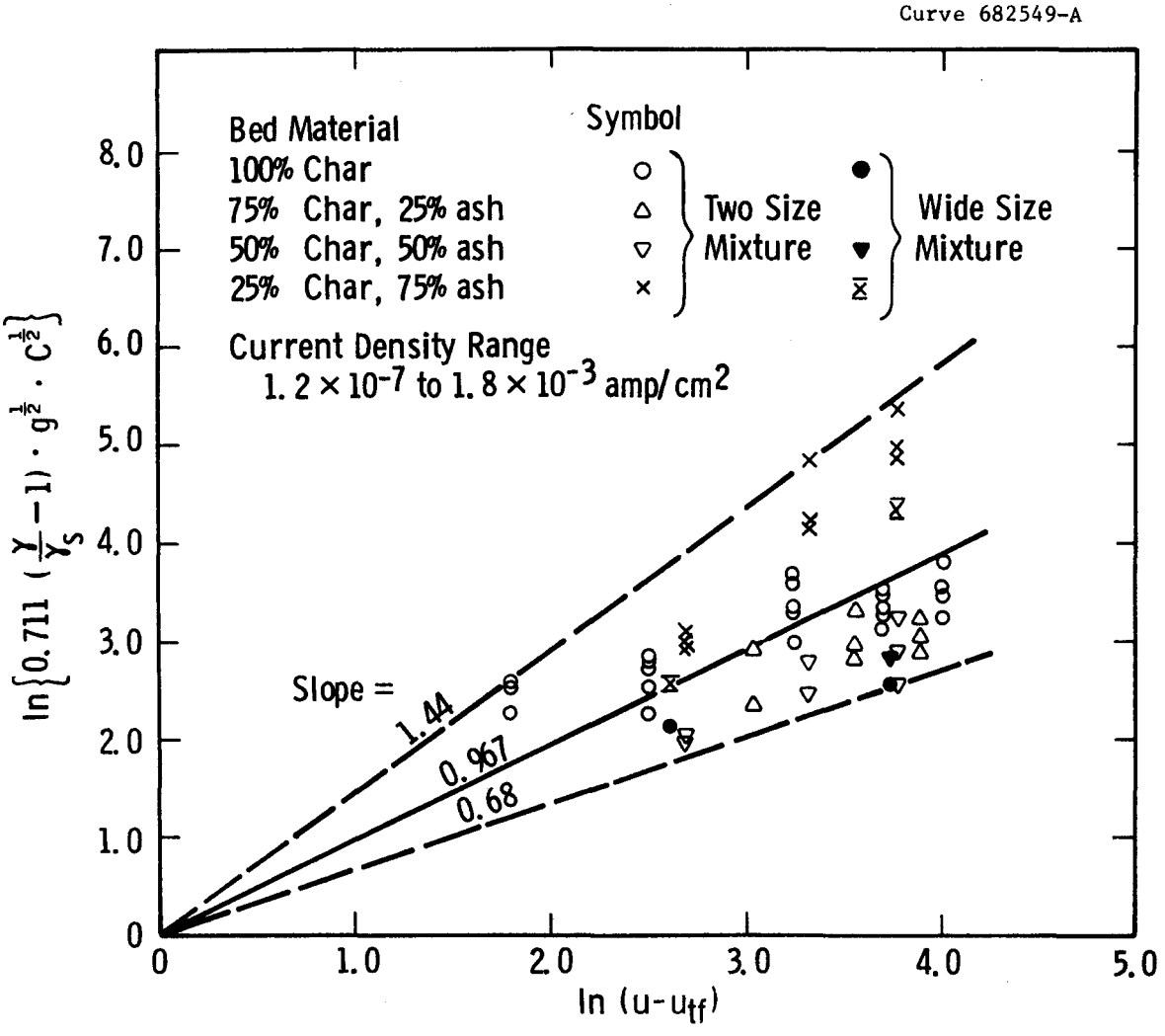

Fig. 11—Correlation of experimental data

they are bounded by two straight lines which pass through the origin and have slopes of 1.44 and 0.68, respectively. Least square straight line fitting of the data with the constraint of zero intercept shows that the slope of the straight line is 0.967. This slope is slightly higher than the theoretical value, 0.8, as given in Eq. (17) presumably due to the fact that the U_{mf} of the mixture is replaced with the U_{tf}. The span of the data, i.e., +48.9% and -29.7% of the slope 0.967, however, covers the theoretical slope, 0.8, indicating the good agreement between the model and the experimental results.

By combining Eqs. (19) and (18), the resistivity of fully fluidized char/ash mixtures at gas velocities up to 2.5 times the U_{tf} of the mixture and at a composition of 0 to 75% ash can be predicted by the following equation

$$\frac{\zeta}{\zeta_s} = 1 + \frac{(U - U_{tf})^{0.967}}{0.711 \sqrt{g \cdot C}} \qquad (20)$$

The resistivity of the char/ash mixture at U_{tf}, ζ_s, is a function of the current density and the bed composition. From the data shown in Fig. 9, an empirical correlation which fits the data of mixtures consisting of 0 to 75% ash can be formulated. This is given below

$$\zeta_s = 1800.0 \cdot ID^{-0.362} (1 + 108.7\ Y^{10.0}) \qquad (21)$$

where Y is the weight fraction of ash in the mixture and ζ_s is the interelectrode bed resistivity at U_{tf}. This resistivity is close to the mixture resistivity when the contact resistance between the electrode and the bed is small, e.g., graphite or copper electrode.

The resistivity of fluidized ash particles, as measured by experiment is larger than that predicted by Eq. (21). Extrapolation of the resistivity data to mixtures of > 75% ash by using the correlation, Eq. (21), may project a bed resistivity lower than the actual

value. However, this projection may be conservative when the information is used to design a conductivity probe for distinguishing the concentration difference of the mixture.

DESIGN CONSIDERATION OF A CONDUCTIVITY PROBE FOR MEASURING AND CONTROLLING THE CHAR/ASH INTERFACE

It is expected that the particles in the gasifier (upper portion of the reactor) may contain < 25% of ash and the agglomerating combustor > 75% of ash. The char/ash separator may contain > 90% of ash. Measurement of the interfaces of these mixtures near the intersection of the gasifier and the combustor and near the connection between the combustor and the char/ash separator are of interest to understand reactor performance and develop optimal operating conditions.

Since the electrical resistance of a fluidized char/ash mixture can be calculated from its resistivity by using the resistance equation,

$$R = \zeta \frac{L}{A_p} \tag{22}$$

a mixture of high ash concentration ($\gtrsim$ 75%) will exhibit a high resistance because of its high resistivity. The resistivities of the three aforesaid mixtures can be predicted by utilizing Eqs. (20) and (21) for representative gas velocities of U_{tf}, 2 U_{tf} and 3 U_{tf}. Figure 12 shows the results for a fluidized bed of 30.5 cm diameter (PDU scale) and a height to diameter of about 6.

Assuming the mixtures are fluidized at U_{tf} and at a current density of 0.0001 amp/cm^2, the resistance of the three mixtures as a function of the electrode distance and the cross sectional area for the current flow is shown in Figs. 13, 14 and 15. The resistance of the bed mixture decreases toward asymptotic values as the probe area is increased. A large probe, e.g., $\gtrsim$ 100 cm^2 is therefore selected so that the bed resistance is not sensitive to the probe area. This will reduce the effect of the possible deflection of the probe and hence the reduction

Curve 682553-A

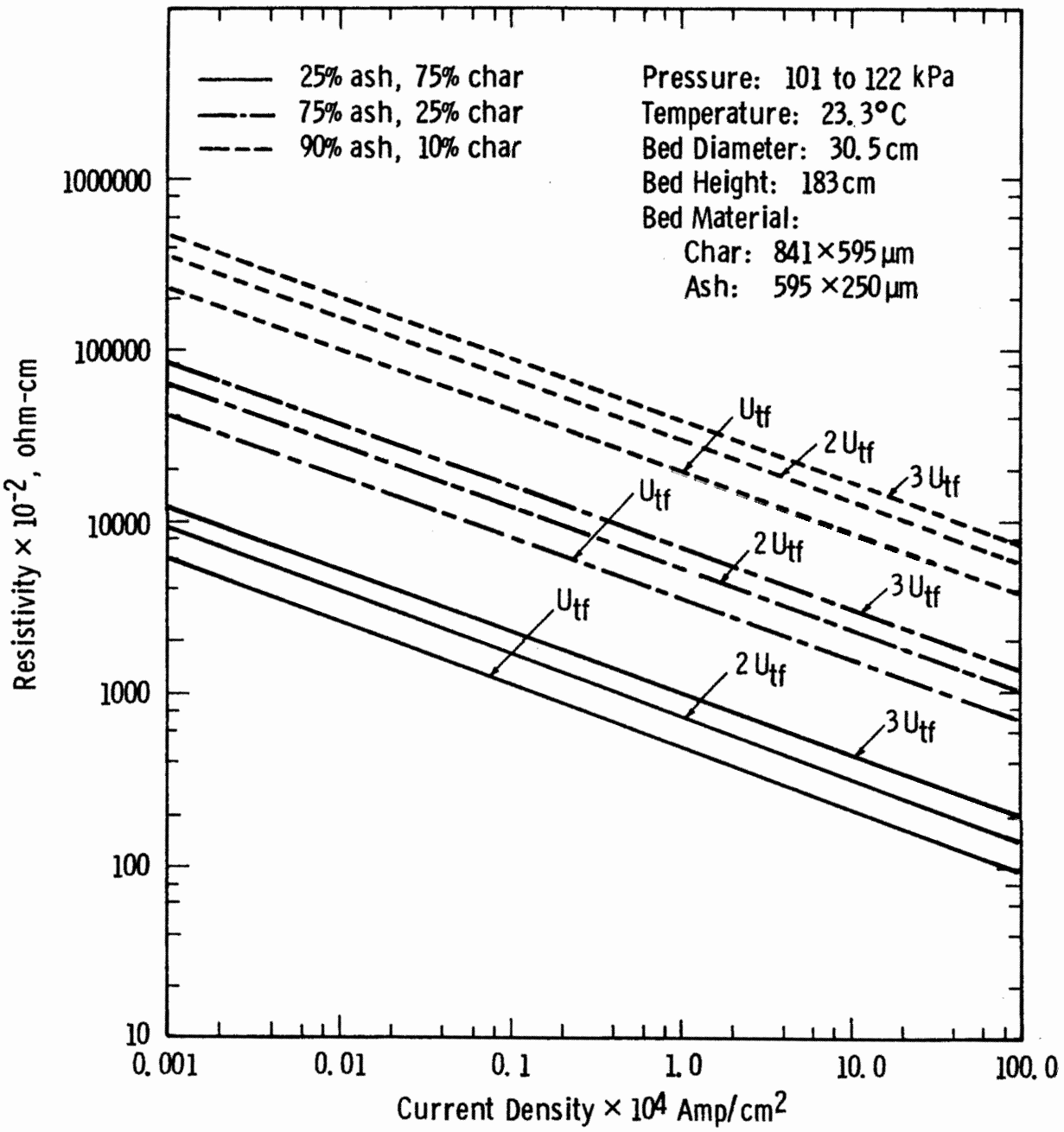

Fig. 12—Computed resistivity as a function of current density, gas velocity and bed composition

Curve 682543-A

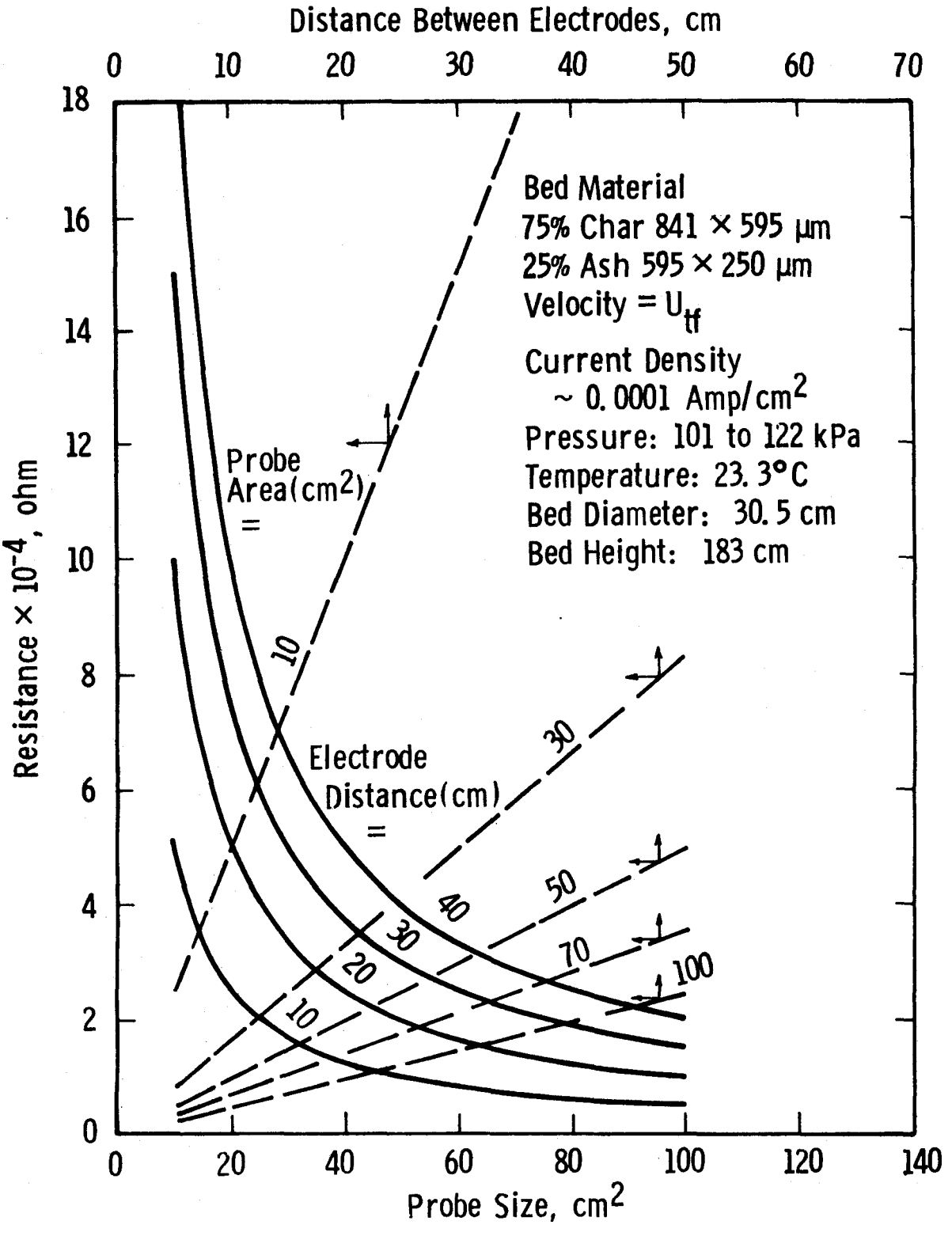

Fig. 13—Mixture resistance as a function of probe size and distance

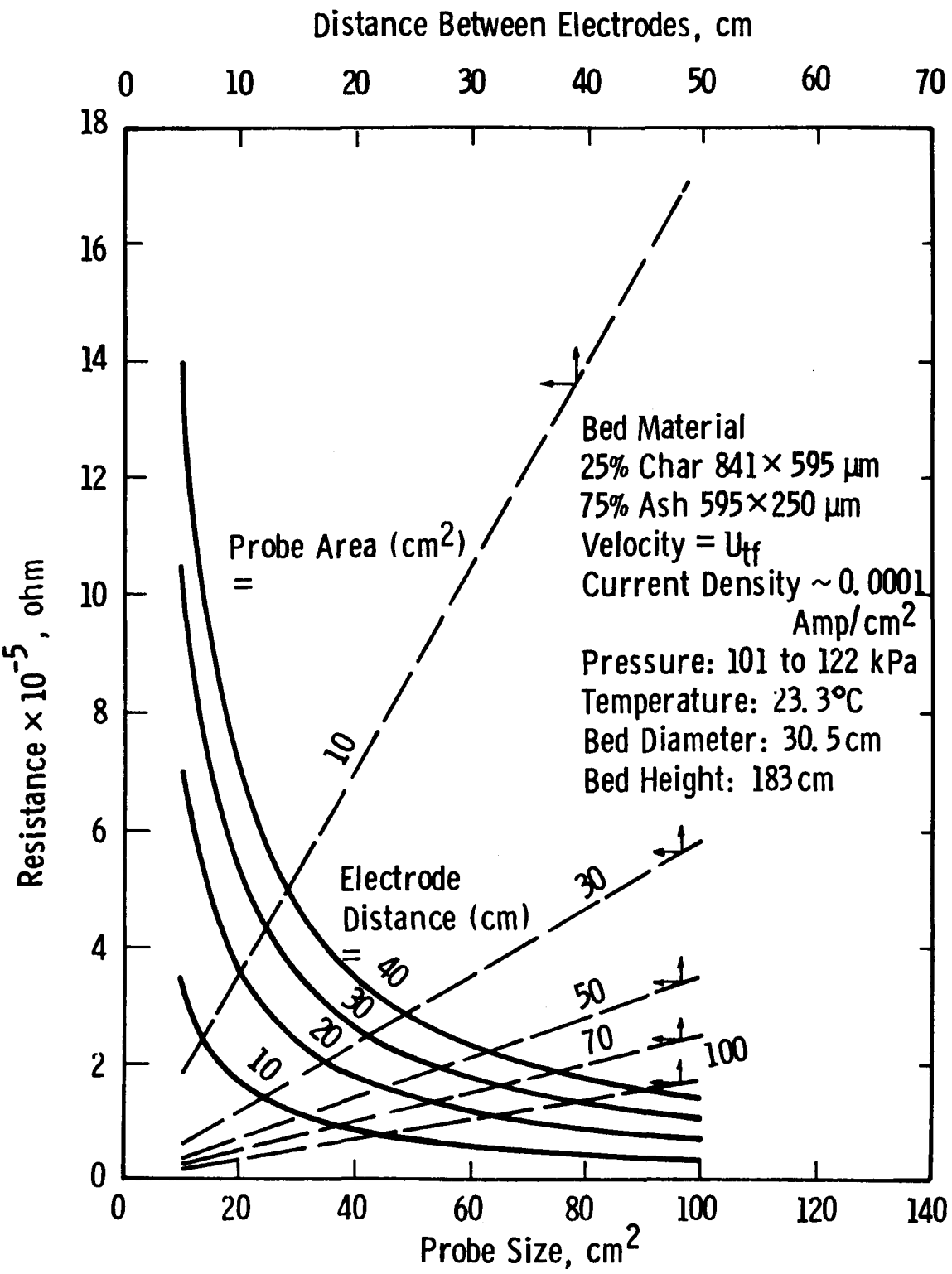

Fig. 14—Mixture resistance as a function of probe size and distance

Curve 682542-A

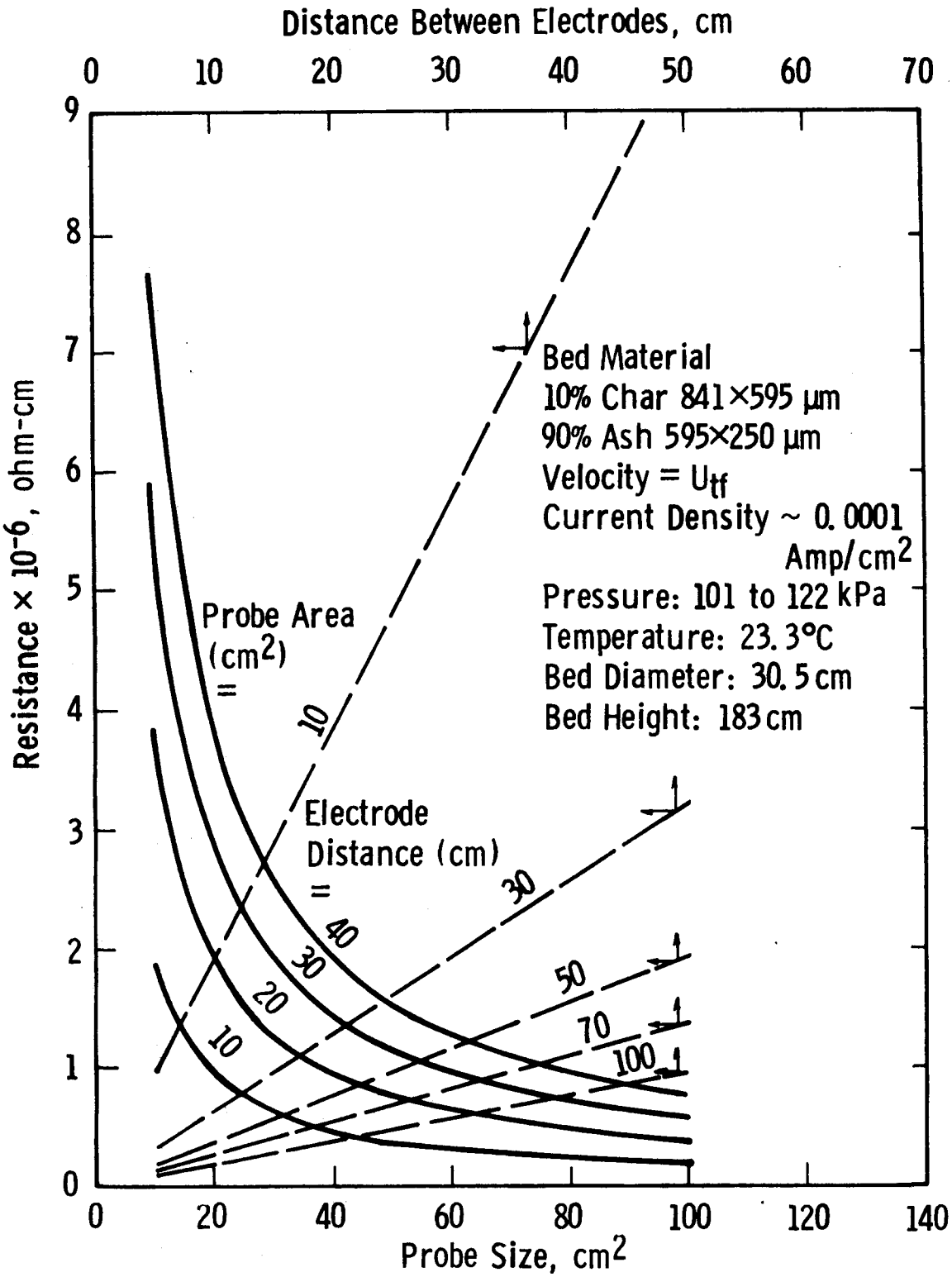

Fig. 15 — Mixture resistance as a function of probe size and distance

of the cross sectional area for current flow by the particle motion in the bed. A reasonable probe distance, e.g., 20 cm is chosen to easily fit the probe into the reactor and at the same time the probe does not interfere with the particle movement. The probe can be made of any temperature resistant metal, e.g., Inconel 600 or 304 stainless steel. However, it should be noted that, with these materials, the electrode-to-bed resistance and the overall interelectrode resistance may be higher[11]. For example, approximately 15 to 25% of the total resistance may be attributed to the contact resistance if the stainless steel electrodes are used.

Although the resistance of a fluidized bed of graphite has been reported[13] to decrease with increasing bed temperature and particle size, whether this same effect may prevail in char/ash mixtures requires further testing. The circuit design for the conductivity probe should therefore be flexible enough that a wide range of current density, e.g., 10^{-8} to 1.0 amp/cm^2 can be supplied and a wide range of bed resistance, e.g., 10 to 10^8 ohm, can be measured.

ACKNOWLEDGMENT

This work is being performed as part of the Westinghouse Coal Gasification Program. The project is being carried out by a six-member industry/government partnership comprising ERDA, Public Service of Indiana, Bechtel, AMAX Coal Co., Peabody Coal Co. and Westinghouse. This work has been funded with federal funds from the Energy Research and Development Administration under contract E(49-18)-1514. The content of this publication does not necessarily reflect the views or policies of the funding agency. Discussions with Dr. W. C. Yang contributed to the development of the model. The authors appreciate helpful discussions with Drs. J. M. D. Merry and W. G. Vaux.

NOMENCLATURE

A_s	cross sectional area of the particulate phase for current passage, cm^2
A_p	size of the conductivity probe or the cross sectional area for current flow, cm^2
A_t	cross sectional area of the fluidized bed, cm^2
C	a parameter, defined by Eq. 16
D_b	bubble diameter, cm
D_{bo}	initial bubble diameter at the distributor, cm
D_{bM}	maximum bubble diameter, cm
D_t	diameter of the fluidized bed, cm
g	gravitational constant, cm/sec^2
h	elevation from the distributor, cm
H_b	fluidized bed height, cm
ID	current density, amp/cm^2
L	distance between the two electrodes, cm
N	number of bubbles per unit bed volume
n_d	number of orifice on the distributor plate
R	mixture electrical resistance, ohm
R_g	electrical resistance for current passing through the bubbling phase, see Fig. 10
R_s	electrical resistance for current passing through the particulate phase, see Fig. 10

U_{mf}	minimum fluidizing velocity, cm/sec
U_a	bubble velocity, cm/sec
U_{bf}	beginning fluidizing velocity, cm/sec
U_{tf}	total fluidizing velocity, cm/sec
U	superficial fluidizing velocity, cm/sec
V_b	volume of a single bubble, cm^3
W	width of the electrode, cm
$\bar{W}$	width of the electric field, cm
Y	fraction of ash particles in the mixture
ζ	mixture resistivity, ohm-cm
ζ_s	resistivity of the particulate phase, ohm-cm
γ	modified mixture resistivity, $= \zeta \cdot (ID)^{0.362}$
γ_s	modified particulate phase resistivity, $= \zeta_s \cdot (ID)^{0.362}$

REFERENCES

1. Archer, D. H., E. J. Vidt, D. L. Keairns, J. P. Morris, and J. L.-P. Chen, "Coal Gasification for Clean Power Production," Proceedings of the Third International Conference on Fluidized Bed Combustion, Hueston Woods, Ohio, (1972).

2. "Advanced Coal Gasification System for Electric Power Generation," Annual Technical Reports, (1973)-(1974) to Office of Coal Research, U. S. Department of the Interior by Westinghouse Electric Corporation, Contract No. E(49-18)-1514.

3. Chen, J. L.-P. and D. L. Keairns, Can. J. Chem. Eng., August (1975). Also, "Particle Segregation in a Fluidized Bed," Chen, J. L.-P. and D. L. Keairns, Westinghouse Report 74-8X1-PDULA-P1.

4. Chen, J. L.-P. and D. L. Keairns, "Separation of Particles from a Fluidized Mixture - A Simulation of Westinghouse Coal Gasification Combustor/Gasifier Operation," Westinghouse Report 76-8X4-PDULA-R1.

5. "Bench-Scale Research on CSG Process," Consolidation Coal Company, R&D Report #16,(1968).

6. Shine, N. B., Chem. Eng. Progr., 67, 52 (1971).

7. Goldberger, W. M., J. E. Hanway, and B. G. Langston, Chem. Eng. Progr., 61(2), 63 (1965).

8. Pulsifer, A. H. and T. D. Wheelock, I.E.C. Process Design Develop., 11, 229 (1972).

9. Lee, B. S., E. J. Pyrcioch, and F. C. Schora, Jr., Chem. Eng. Progr. Symposium Ser. No. 105.66, 152 (1970).

10. Reed, A. K. and W. M. Goldberger, Chem. Eng. Progr. Symposium Ser. No. 67, 62, 71 (1966).

11. Chen, T. P., E. Yuan, and A. L. Pulsifer, "Bed and Contact Resistances in an Electrically Conducting Fluidized Bed," paper presented at the A.I.Ch.E. meeting, Washington, D.C., Dec. 1974.

12. Jones, A. L. and T. D. Wheelock, I. Chem. E. (London), Symposium Series No. 30, 174 (1968).

13. Borodulya, V. A., S. S. Zabrodsky and A. I. Zheltov, Chem. Eng. Progr. Symposium Series, No. 128, 69, 106 (1973).

14. Wen, C. Y. and Y. H. Yu, Chem. Eng. Progr. Symp. Series 62, 62, 100 (1966).

15. Davies, R. M. and Sir G. Taylor, Proc. Roy. Soc. (London), A200, 375 (1950).

16. Mori, S. and Wen, C. Y., A.I.Ch.E. J. 12, 1, 109 (1975).

SECTION 5.3

APPENDIX C

APPENDIX C

Proceedings of Symposium on Coal Processing and Conversion, sponsored by West Virginia Geological and Economic Survey, June 2 and 3, 1976.

COAL DEVOLATILIZATION STUDIES IN SUPPORT OF THE WESTINGHOUSE FLUIDIZED BED COAL GASIFICATION PROCESS*

J. P. Morris and D. L. Keairns
Westinghouse Research Laboratories
Pittsburgh, PA 15235

ABSTRACT

Coal devolatilization studies are being carried out with a pressurized laboratory fluidized bed reactor. The tests show the behavior of caking and noncaking coals during rapid heating in a fluidized bed. Small samples of coal are injected into a hot bed of char; the off-gas is sampled and analyzed; and the char and agglomerates produced are examined and characterized. Data obtained on the variation of gas evolution rates with time are used to predict the duration of the plastic or sticky phase during transition of the coal to char. All tests were conducted at 10 atm pressure; bed temperature and coal particle size were varied.

*This work is being performed as part of the Westinghouse Coal Gasification Program. The project is being carried out by a six-member industry/government partnership comprising ERDA, Public Service of Indiana, Bechtel, AMAX Coal Co., Peabody Coal Co. and Westinghouse. This work has been funded with federal funds from the Energy Research and Development Administration under contract E(49-18)-1514. The content of this publication does not necessarily reflect the views or policies of the funding agency.

COAL DEVOLATILIZATION STUDIES IN SUPPORT OF THE WESTINGHOUSE FLUIDIZED BED COAL GASIFICATION PROCESS*

J. P. Morris and D. L. Keairns
Westinghouse Research Laboratories
Pittsburgh, PA 15235

INTRODUCTION

Westinghouse is developing a two-stage fluidized bed coal gasification process to produce low Btu gas for combined cycle power generation.[1,2] The process is designed to operate with caking, high-sulfur coals. Laboratory experiments and theoretical studies have been in progress for several years at Westinghouse Research Laboratories and a process development unit (PDU) has been constructed and is currently operating at Waltz Mill, Pa. The capacity of the PDU is 15 tons of coal per day.

The process utilizes two fluidized bed reactors. One devolatilizes the coal and produces char; the other reacts the char with air and steam to produce fuel gas. Sulfur can be removed at high temperature from the fuel gas by absorption on dolomite, either in the devolatilizer or in a separate vessel.[3] Ash is agglomerated and separated in the gasifier. A flow diagram of the process is shown in Fig. 1.

The key feature of the devolatilizer is the draft tube. Its use makes possible the treatment of caking coals. Hot fuel gas from the

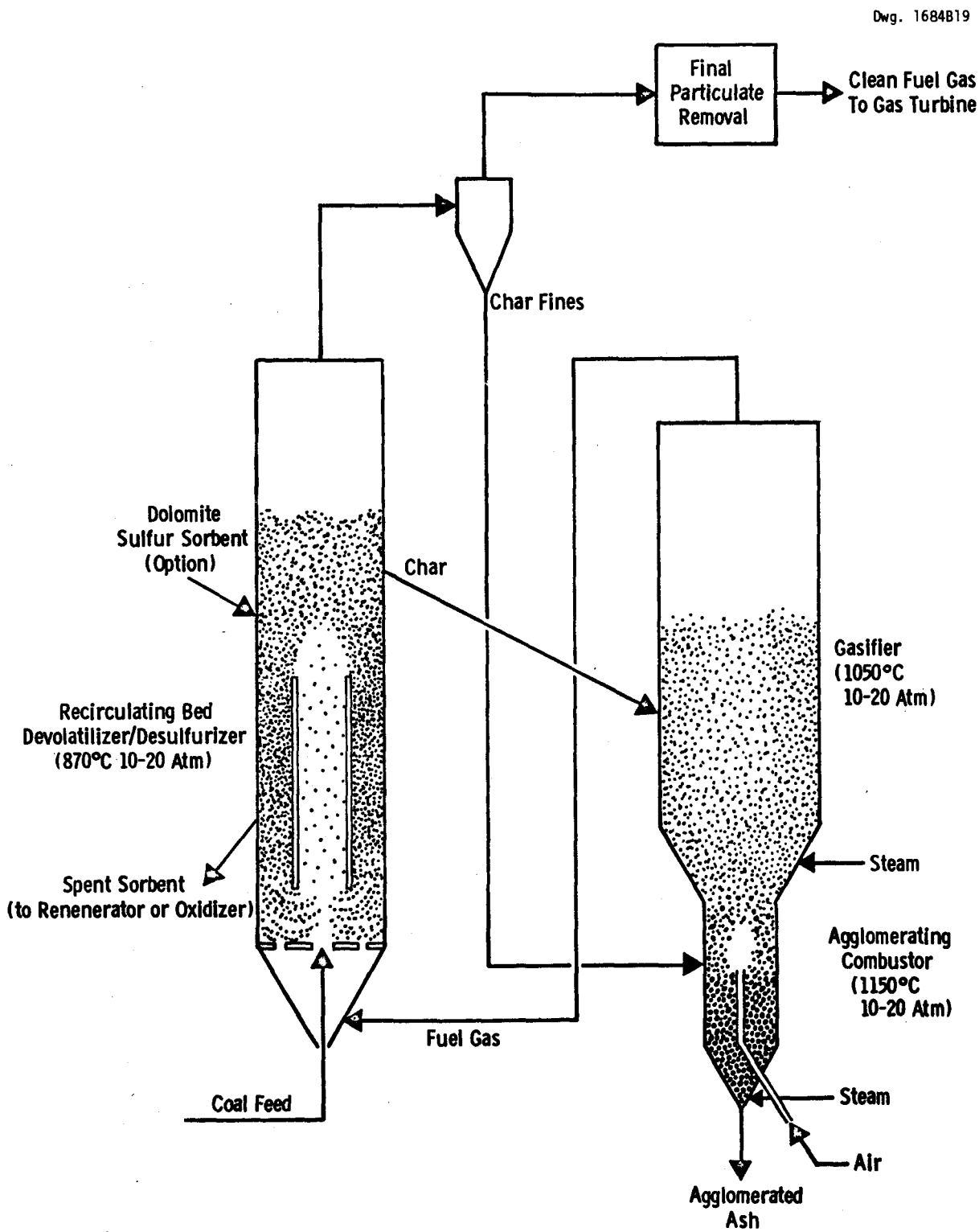

Fig. 1 – Westinghouse fluidized bed coal gasification process

gasifier, flowing upward at high velocity through the draft tube, causes the bed to circulate. Solids move downward through the annulus between the tube and the vessel wall, become entrained in the incoming gas at the bottom of the draft tube, and are then carried upward into the fluidized bed section at the top. Dilution of the coal feed by the circulating solids and the high-velocity, turbulent flow through the draft tube prevent agglomeration as the coal devolatilizes and passes through the sticky phase on initial heating.

The laboratory experiments described in this report were undertaken to provide a better understanding of how the coal behaves when heated under conditions similar to those in the devolatilizer. The immediate objectives were to identify and measure the major volatile products, to determine the time required for a coal particle to devolatilize and pass through its sticky phase, and to characterize the char and agglomerates that are produced.

A noncirculating bed was used in conducting the experiments. Coal was added batchwise and the natural stirring of the fluidized bed was utilized to disperse the coal before the particles became sticky. Rapid dispersion was promoted by adding very small samples.

APPARATUS

A diagram of the fluidized bed reactor and auxiliary equipment is shown in Fig. 2. The reactor was made of Inconel 600 and was 3.5 cm I.D. by 33 cm high. A 6-m long tube coiled around the reactor was used to preheat the fluidizing gas, and the hot gas passed into the bed through a perforated distributor plate. The coal sample was contained in a horizontal side tube. A solenoid valve and small pressurized bottle of nitrogen were used to inject the coal into the reactor. The temperature of the bed was measured with an immersed thermocouple.

The reactor was contained inside a larger vessel which was maintained at the same pressure as the reactor. The outer vessel also contained the furnace heaters and insulation. Gas samples were taken with evacuated bottles operated by solenoid valves. A programmable timer controlled the injection of the coal sample and the operation of the sample bottles.

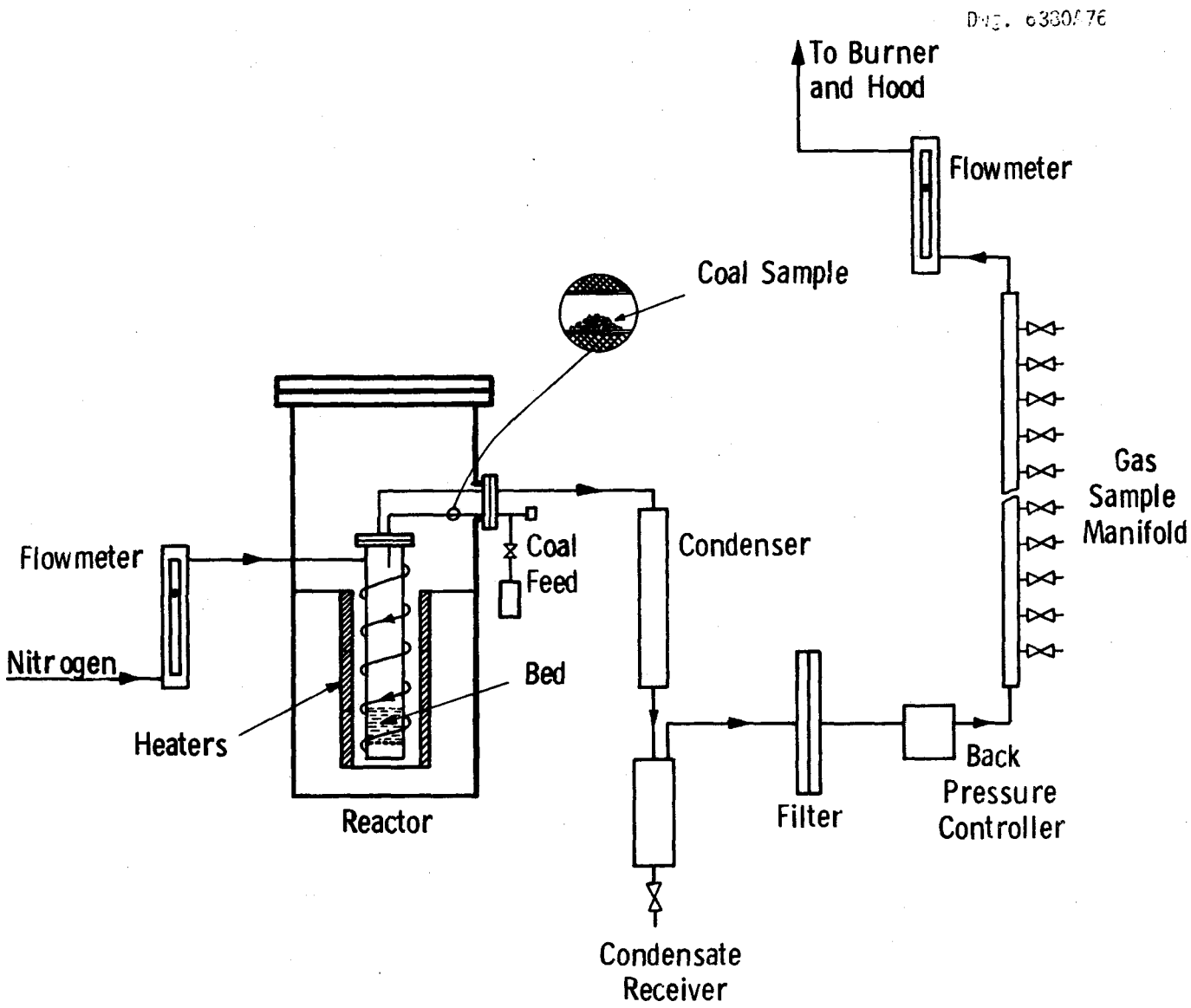

Fig. 2 — Flow diagram of laboratory fluidized bed test unit

MATERIALS

Three coals were studied in the experiments: a noncaking subbituminous C coal from Wyoming, a weakly caking high-volatile C bituminous coal from Indiana, and a highly caking Pittsburgh bed coal from Pennsylvania. These coals were scheduled for testing in the process development unit. The chemical analyses are given in Table 1.

The bed material was a char produced by FMC Corporation from Western Kentucky bituminous coal. In most experiments, the bed particle size was -1.40 mm +1.00 mm. The char analyzed 12% ash and 9.4% volatile matter. Before being used in a test, the char was heated at the test temperature until only a trace of volatile matter could be detected in the off gas.

The char bed was fluidized with nitrogen at a flow rate of 50 ℓ/min (referred to 1 atm, 25°C). When operating at 872°C and 10 atm pressure, which were the usual conditions, the superficial gas velocity in the reactor was 33.5 cm/sec. This was 3.5 times the minimum fluidizing velocity of the char.

Table 1 -- Coal Analyses

	Wt % of Dry Coal		
	Wyoming Subbituminous C	Indiana High Volatile C	Pittsburgh High Volatile A
Proximate			
Volatile Matter	46.1	39.6	41.2
Fixed Carbon	50.4	49.8	49.9
Ash	3.44	10.6	8.89
Ultimate			
Carbon	73.3	72.3	76.5
Hydrogen	5.03	5.00	4.89
Oxygen	16.5	8.11	6.89
Nitrogen	1.23	1.20	0.95
Sulfur	0.49	2.75	1.85
Ash	3.44	10.6	8.89

TEST PROCEDURE

The reactor was charged with FMC char to a depth of 3.5 cm and a 0.25 g sample of coal, dried at 110°C in nitrogen, was placed in the feed tube. The ratio of bed weight to sample weight was approximately 50 to 1.

After heating to the operating temperature, the reactor was pressurized and the gas flow and bed temperature were adjusted and stabilized. The timer was then started and the coal sample was injected into the reactor and onto the fluidized bed. Samples of off-gas were taken at short intervals during gas evolution from the coal. The reactor was then cooled and the char or agglomerates produced by the coal were separated and examined. In most tests, the particles of the char or agglomerate product were larger than the bed particles and a clean separation could be obtained by screening.

RESULTS AND DISCUSSION

Devolatilization

The results of typical devolatilization experiments run with -1.70 mm +1.40 mm coal are presented in Figs. 3, 4, and 5. The curves show the concentrations of the major gaseous products in the off gas plotted against the time after the addition of the coal sample. The time required for the fluidizing gas to travel from the bed to the sample station was deducted. This time was determined experimentally by injecting tracer gases into the bed in place of coal samples.

The quantities of the various gases evolved are represented by the areas under the curves. Although the three coals were different in rank, they emitted the same gaseous products in roughly the same proportions and the same times. The greatest difference was in the quantity of carbon oxides. This quantity varied with the oxygen content of the coal. The subbituminous coal, which had the highest oxygen content, evolved the most CO and CO_2 whereas the Pittsburgh bed coal, which had the lowest oxygen content, evolved the least. Water evolution probably also varied with the oxygen content of the coal but was determined in only one experiment.

With the exception of hydrogen, the evolution of gas was essentially complete in less than 10 sec after the coal sample was added. The peak in the hydrogen curve came at a slightly later time than the peaks of the other gases, and the concentration of hydrogen after the

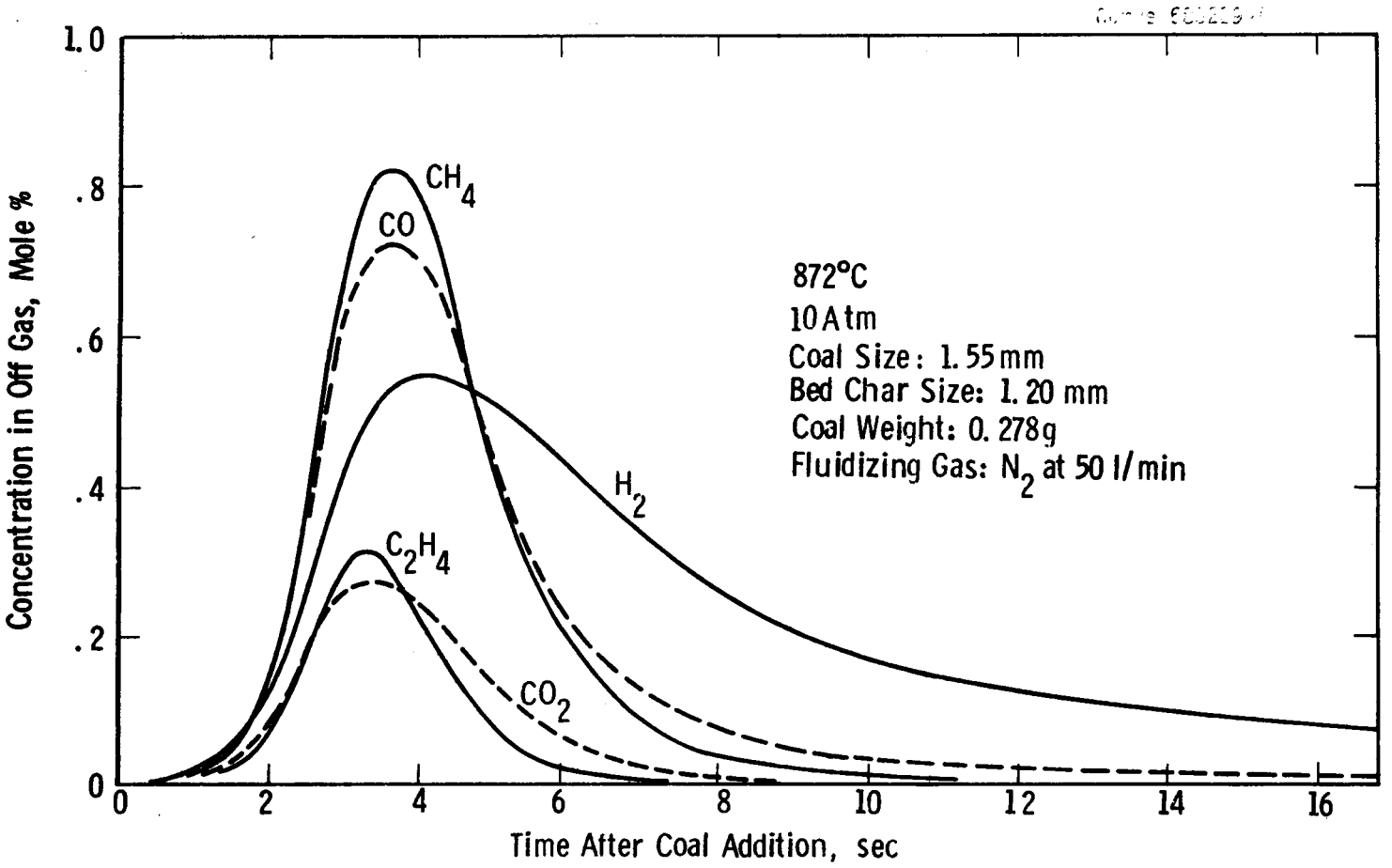

Fig. 3 — Devolatilization of Wyoming subbituminous C coal

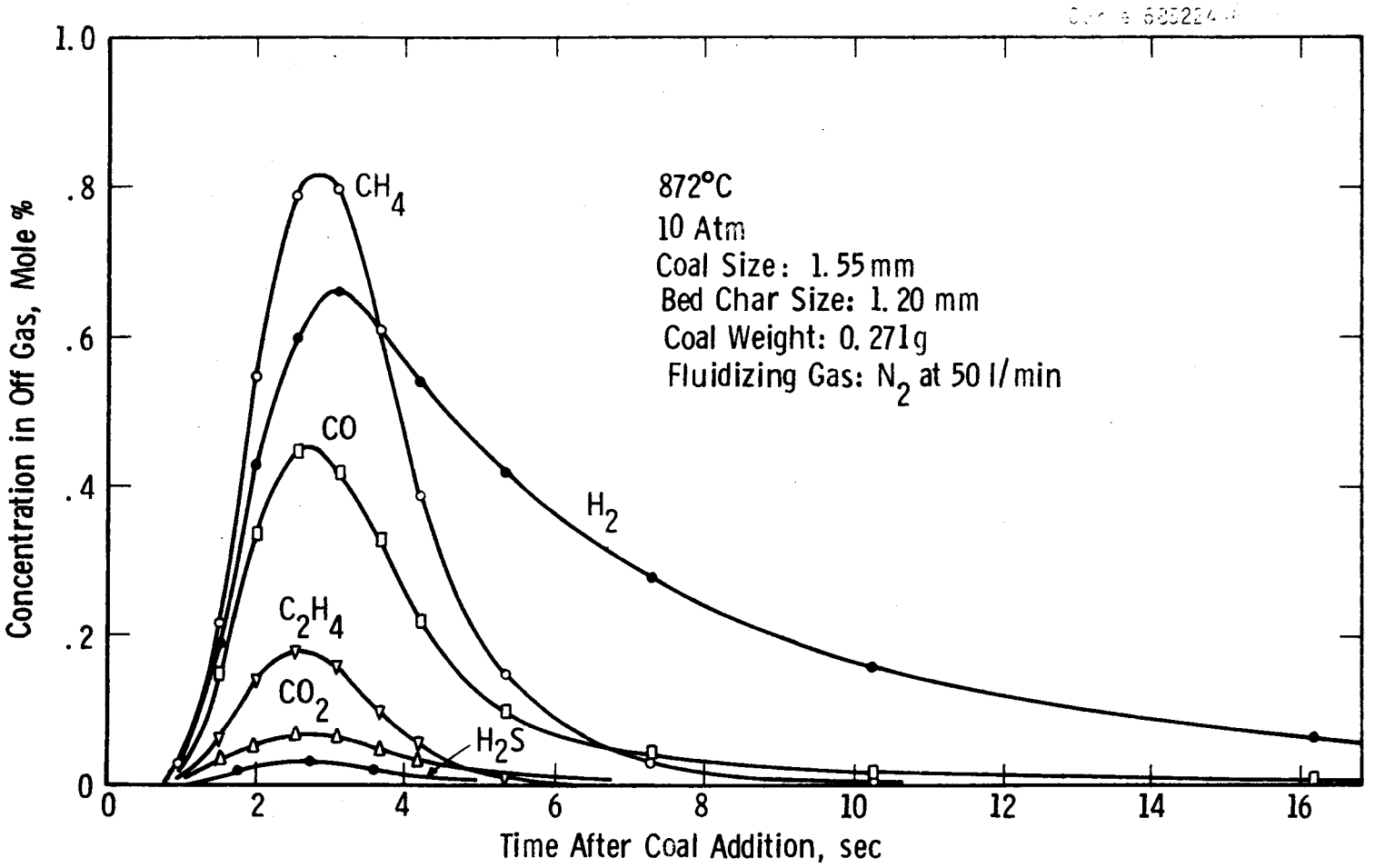

Fig. 4– Devolatilization of Indiana high-volatile C bituminous coal

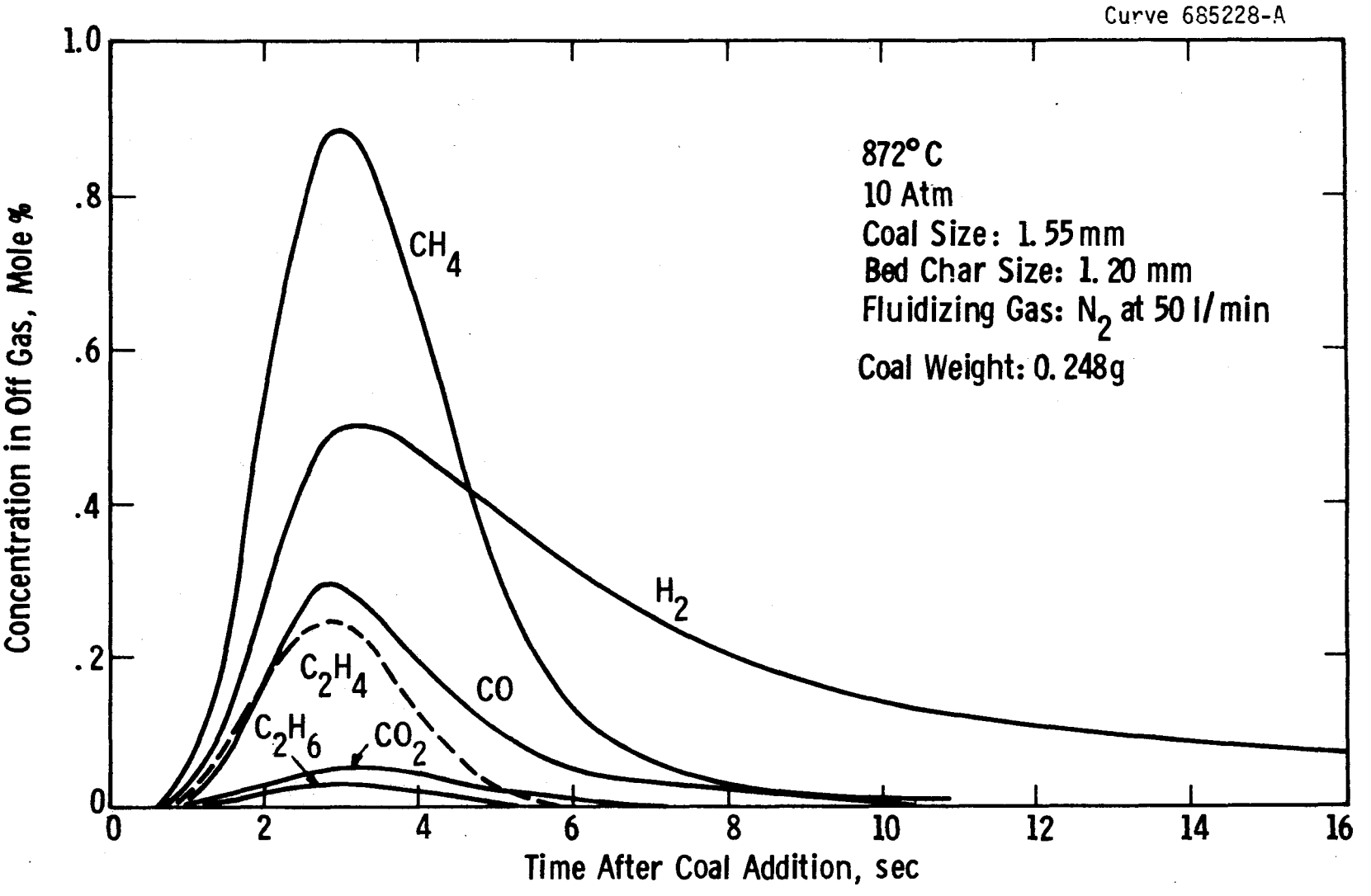

Fig. 5 — Devolatilization of Pittsburgh bed coal

peak declined much more slowly. In one test with Indiana coal, 1.65 min were required for the hydrogen concentration to decrease to 0.01% compared to only 7 sec for methane, and hydrogen could still be detected after 20 min. A residual outgassing of carbon monoxide, lasting about 4 min, was also observed.

These results agree with the generally accepted view that the pyrolysis of coal occurs in two principal stages, the first being a very rapid low-temperature reaction that produces the bulk of the volatile matter and the second being a slow reaction at higher temperature that gives mainly hydrogen.[4,5] Because of the temperature gradient within the coal particle during rapid heating, the two stages overlap, especially for large particles.

Hydrogen sulfide evolution was studied in two tests with different Indiana coals. The gas samples were analyzed for H_2S by the methylene blue method. The results are shown in Fig. 6. Part of the evolved H_2S may have been absorbed by the Inconel reactor; this would not have affected the peak time or the duration of H_2S evolution, however. In these respects, the behavior of H_2S was similar to that of the hydrocarbon gases and the oxides of carbon, strongly suggesting that organic sulfur and not pyrite was the source of the H_2S. Low temperature decomposition of organic sulfur compounds in coal to give H_2S has also been reported by Jones.[5]

The effect of temperature on devolatilization is illustrated in Fig. 7 by the results for methane evolution with the Indiana coal. Tests were run at three temperatures spanning the maximum operating range of the PDU devolatilizer. Increasing the temperature from 872° to 982°C

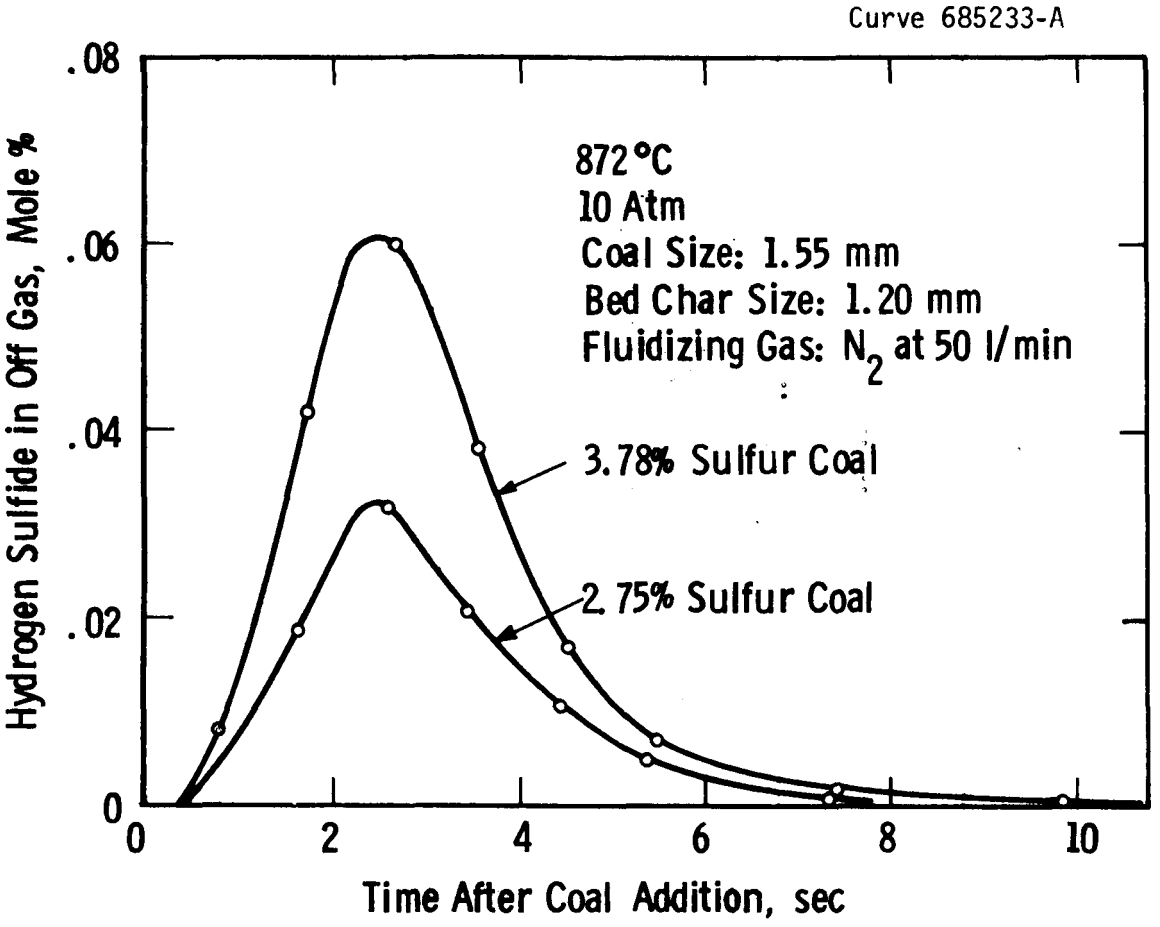

Fig. 6 — Hydrogen sulfide evolution from two Indiana coals

Curve 683457-A

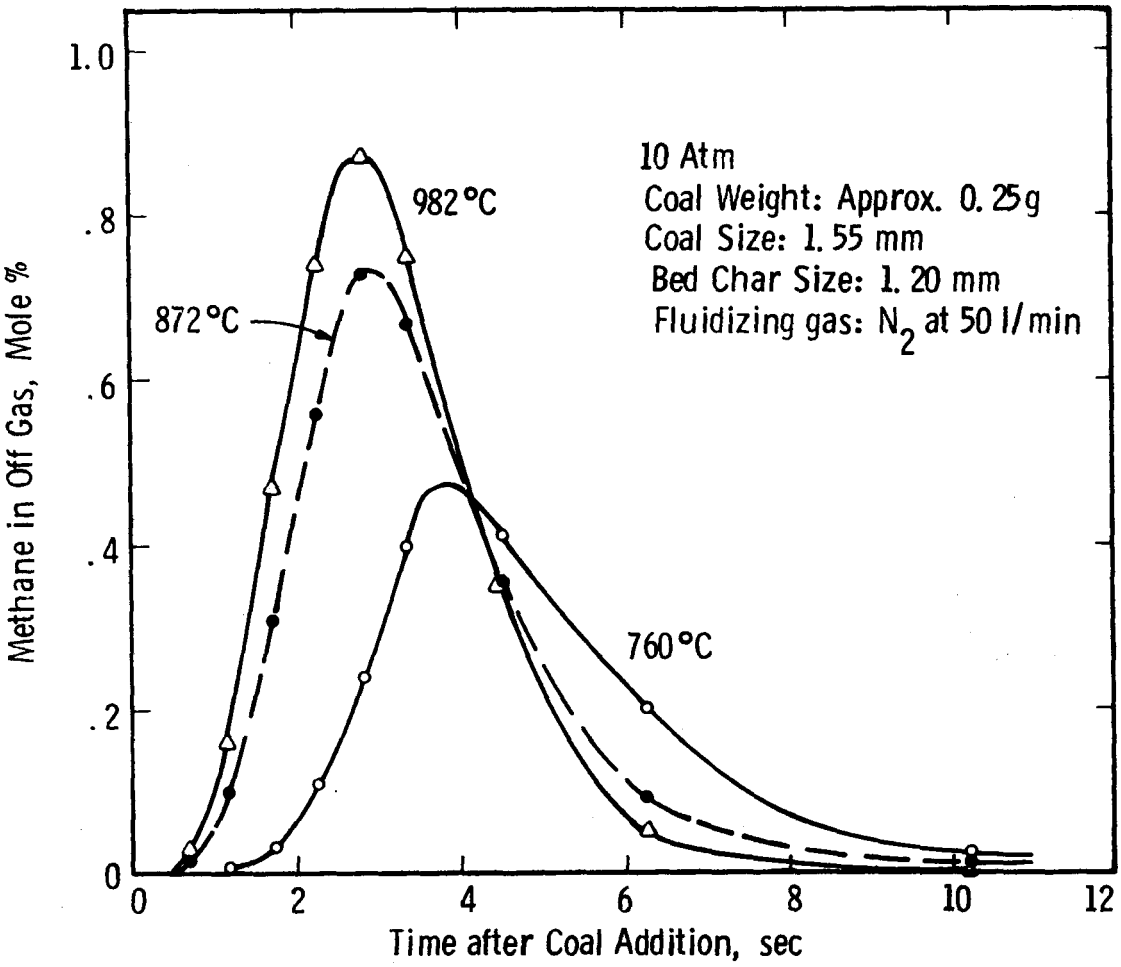

Fig. 7 — Effect of bed temperature on methane evolution from Indiana high-volatile C bituminous coal.

caused little change in the evolution time but there was a moderate increase in the quantity of methane. On lowering the temperature to 760°C, methane production decreased substantially and the evolution time increased.

In the experiments run at 872°C, 7-9% of the coal appeared as tar in the devolatilization products. The tar was recovered from the downstream components of the apparatus, up to and including the filter, by leaching with acetone and benzene. A lower tar production is expected in the PDU operation because the gas residence time in the bed will be much longer and decomposition of tar will occur. Hesp and Waters[6] reported that the major products of thermal cracking of tar, aside from solid carbon, are hydrogen and methane. They found that the maximum yield of methane occurred between 850° and 900°C.

The distribution of the hydrogen and the oxygen in the coal among the decomposition products in the primary stage of devolatilization is illustrated in Table 2. In the first 10 sec after the coal addition, about 42% of the hydrogen was evolved in the form of reducing gases and an equal proportion of the oxygen was evolved as carbon monoxide. During the following 20 min, the coal residue lost an additional 25% of the original hydrogen as molecular hydrogen and an additional 4-5% of the original oxygen as carbon monoxide.

The reducing gases evolved by the coal on heating are important to the gasification process because they add significantly to the heating value of the fuel gas. Methane makes the greatest contribution because of its relative abundance and its high heat of combustion. The methane

Table 2 -- Hydrogen and Oxygen Balances after 10-sec Devolatilization of 1.55 mm Indiana Coal at 872°C, 10 atm in a Fluidized Bed of Char

	Wt % of Dry Coal	
	Hydrogen	Oxygen
In Coal	5.00	8.11
In Products		
H_2	.80	-
CH_4	1.03	-
C_2H_4	.19	-
C_2H_6	.08	-
H_2S	.03	-
H_2O	.40	2.82
CO	-	3.44
CO_2	-	1.07
Tar*	.40	.12
Char (by diff)	2.07	.66
	5.00	8.11

*Tar assumed to contain 5% hydrogen and 1.5% oxygen.

evolved in the laboratory experiments was equivalent to about 1% of the projected production of fuel gas in a commercial system. A higher production of methane in the commercial process is expected, however, because the devolatilizer bed will be fluidized with fuel gas containing hydrogen, which will react with carbon to form methane, and also because methane will be formed by the decomposition of tar.

Current laboratory experiments with Pittsburgh bed coal and a synthetic fuel gas indicate that methane formation may be doubled by the hydrogasification of carbon. The results tend to confirm previous projections of 2-3% methane in the fuel gas.[1,2] The contribution of tar decomposition to methane production could not be studied with the present apparatus.

Effect of Coal Particle Size on Devolatilization Time and Duration of Plasticity

The development of plasticity in coal on heating is the direct result of the decomposition reactions, the initial phase of which generates liquid products.[4] The decrease in fluidity after the initial maximum is due to evaporation and decomposition of these products with the formation of volatile matter and a solid residue. The slow, secondary decomposition producing hydrogen apparently occurs after solidification.

The primary devolatilization period, in which the coal exhibits plasticity, is well defined in the present work by the curves showing methane evolution as a function of time. Using methane evolution as an indicator, the time required to devolatilize the Indiana coal at 872°F was deter-

mined for six particle sizes ranging from 0.5 mm to 4 mm. The methane evolution curves are given in Fig. 8. They follow the expected pattern, namely, large particles heat up more slowly than small particles and therefore take longer to devolatilize.

Because of nonideal gas flow such as back mixing in the reactor and exit train, the curves in Fig. 8 do not give a true concentration-time relationship for the mixture of evolved gas and fluidizing gas at the site of devolatilization in the bed. Nonideal flow disperses the evolved gases so that their concentrations at the point of sampling downstream are decreased and the apparent evolution time is increased.

A correction for dispersion was made mathematically, using the results of gas tracer experiments conducted with hydrogen, carbon dioxide, and fuel gas. A pulse of the tracer was injected just beneath the surface of the bed through eight symmetrically located orifices and the tracer output versus time was monitored at the sampling site. The magnitude of the dispersion effect is illustrated in Fig. 9. Using the results of these tests, corrected methane evolution curves for the six coal sizes were derived. Two of the corrected curves, shown in Fig. 10, illustrate the magnitude of the correction.

Using the corrected curves, the actual times for 50% and 95% devolatilization were calculated for each particle size. (Because of tailing off of the curves, the time for 100% evolution of methane could not be established accurately. Total methane evolution could be estimated with relatively little error, however.) The results, given in Table 3, show that the times for 50% devolatilization ranged from 1.6 sec for the

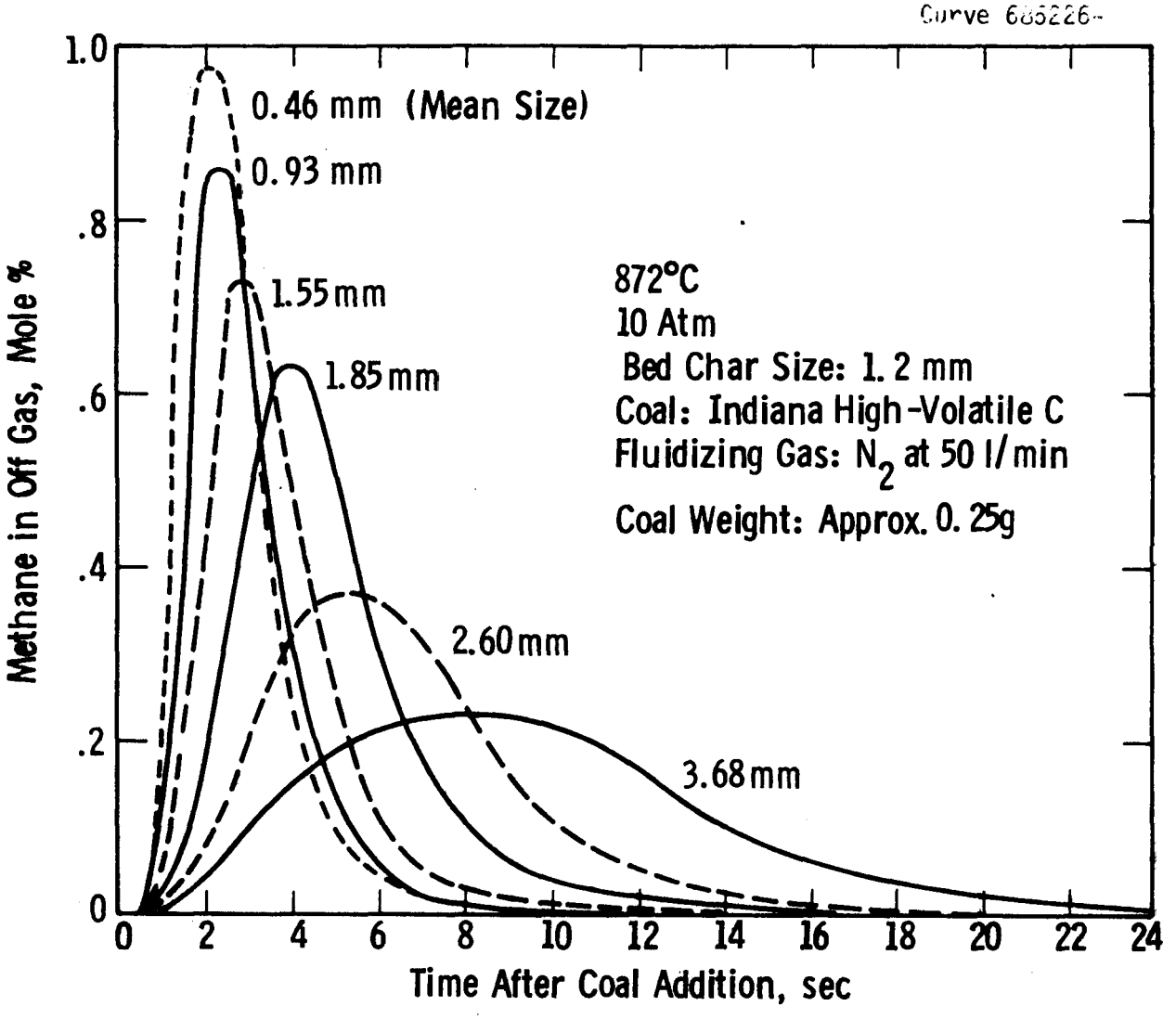

Fig. 8 — Effect of coal particle size on methane evolution time

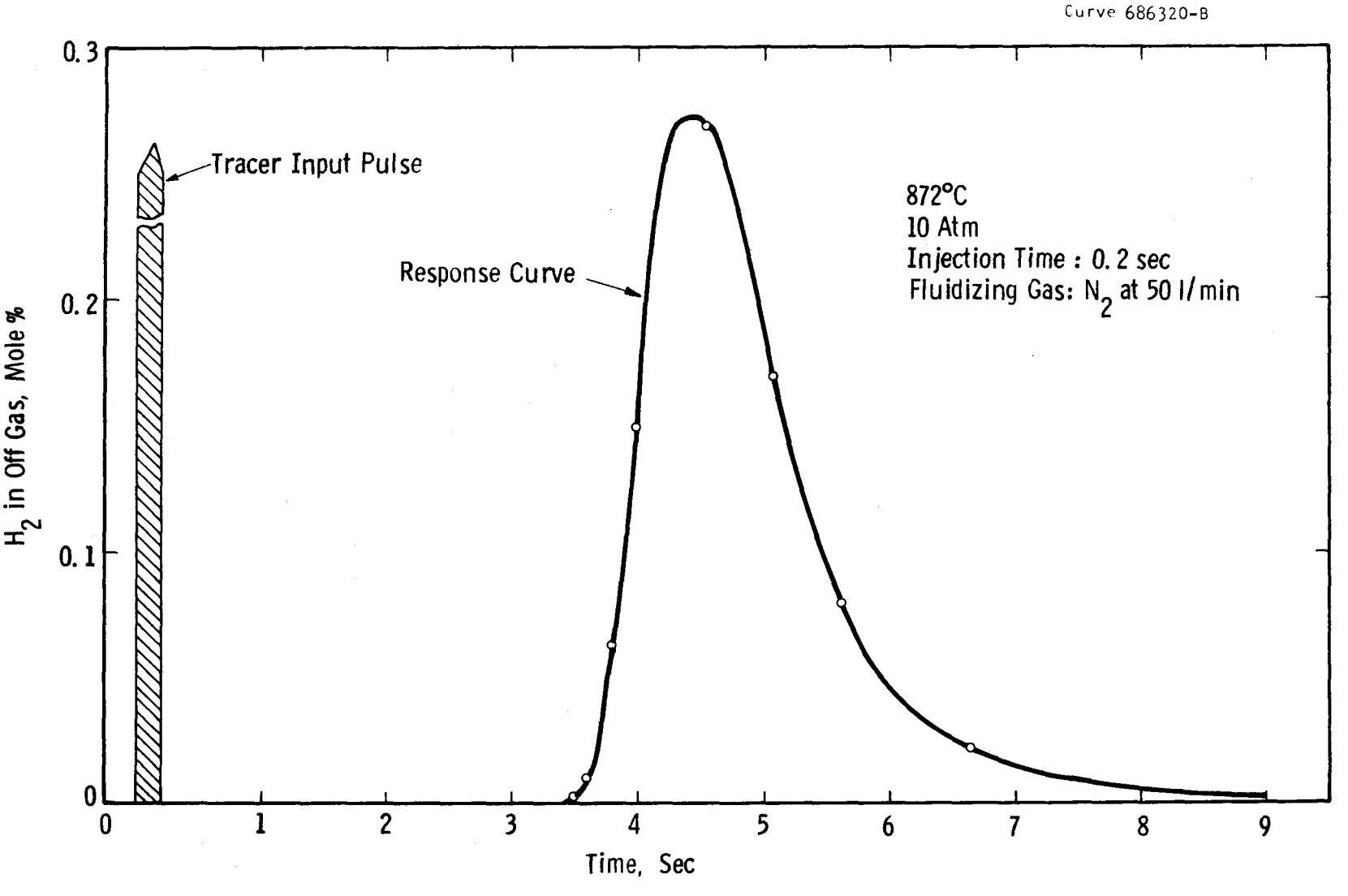

Fig. 9 — Dispersion of hydrogen tracer because of nonideal gas flow

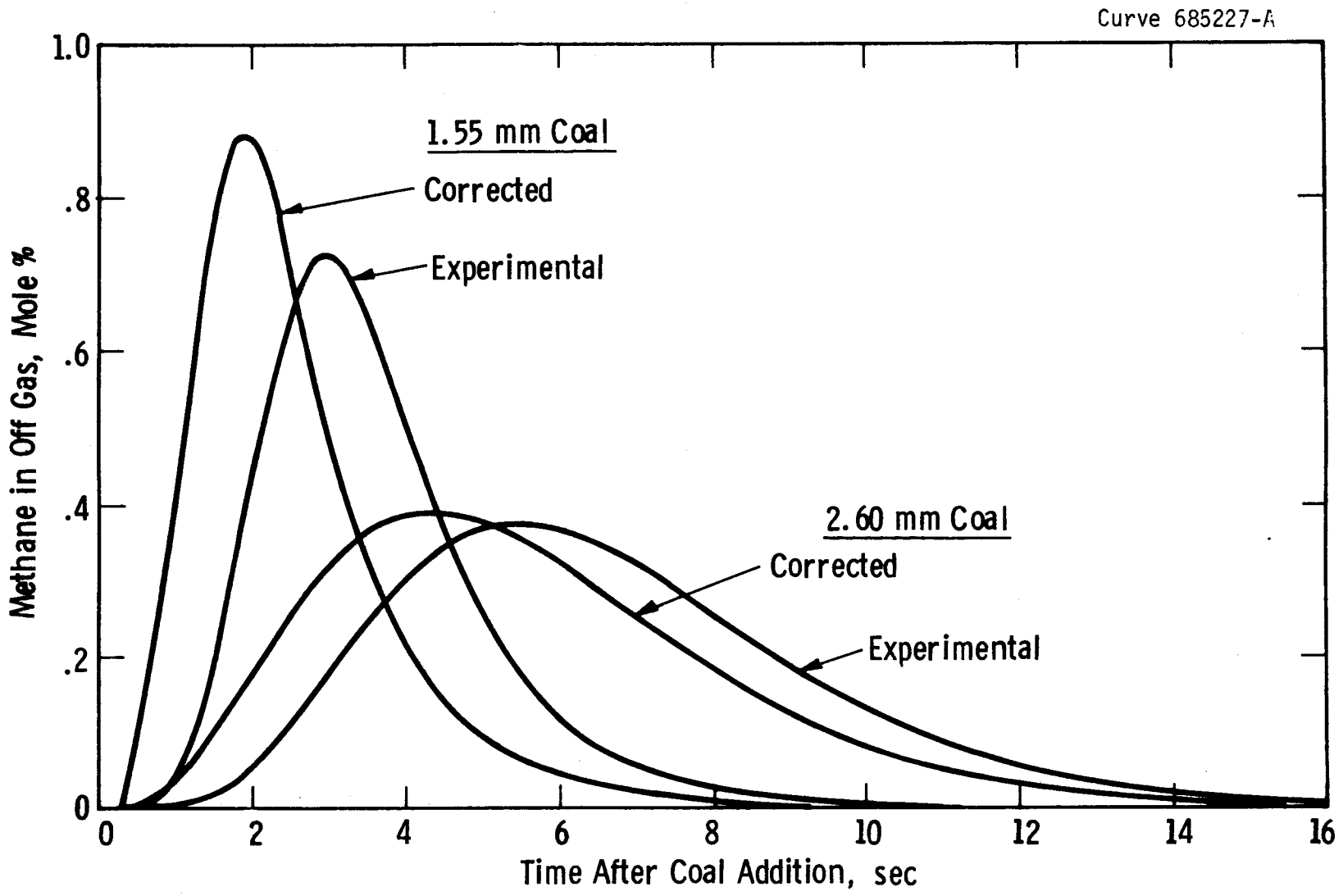

Fig. 10 – Correction of methane evolution for dispersion

Table 3 -- Effect of Coal Particle Size on the Primary Devolatilization Time* of Coal Added to a Fluidized Bed of Char at 872°C

Coal Particle Size, mm	Devolatilization Time, sec	
	50% Completion	95% Completion
- .500 + .425	1.62	4.58
-1.00 + .850	1.82	4.32
-1.70 +1.40	2.43	5.40
-2.00 +1.70	3.60	8.10
-2.83 +2.36	5.16	10.7
-4.00 +3.35	8.15	17.5

*Based on time required for methane evolution.

smallest coal size to 8 sec for the largest size. For 95% devolatilization, the range was 4 to 17 sec.

These times are very long compared to the residence time of the coal feed in the draft tube of the devolatilizer (about 0.5 sec). Therefore, assuming similar heat transfer rates in the devolatilizer and the laboratory reactor, it can be concluded that only the very small coal particles in the devolatilizer feed will become appreciably devolatilized during passage through the draft tube and that large particles may still be capable of causing agglomeration on reaching the upper bed.

The degree of devolatilization required to prevent agglomeration is not clear. Agglomeration did not occur in tests in the process development unit with Wyoming and Indiana coals.[7] Subsequent tests with highly caking coals gave similar results. These facts, considered in conjunction with the data from the laboratory experiments, indicate that a high degree of devolatilization is not required to prevent agglomeration in the recirculating bed draft tube.

Several factors may contribute to the absence of agglomeration in the PDU tests, for example: the dilution of the coal feed by the recirculating char, partial melting of the coal particles followed by crusting over during disperse-phase flow in the draft tube, and a reduction in surface stickiness due to adsorption of fine char and dust. Further work is underway to develop an understanding of the phenomenon.

Characterization of Char and Agglomerates

No agglomerates formed in the experiments with the subbituminous coal. With the two bituminous coals, however, every particle agglomerated

with the bed. The agglomerates consisted of a central carbonized coal particle covered with a layer of bed char. Although the coal swelled during the rapid heatup and the residue was hollow, few particles burst or disintegrated. The extent of swelling ranged from 25% for 3.5-4 mm particles to 100% or more for 1.5 mm and smaller particles. Photographs of typical agglomerates are shown in Fig. 11.

The agglomerates were very uniform in size when made from uniformly sized materials. As the particle size of the bed was decreased, the weight of the coating on the coal particle also decreased although the number of adhering particles increased. This is illustrated by the following data from three tests run at 872°C with -1.70 mm +1.40 mm Pittsburgh bed coal:

Particle Size of Bed Char, mm	Weight of Char Coating, g per g of feed coal	Number of Adhering Bed Particles per Particle of Feed Coal
-1.40 +1.00	1.66	8
-0.500 +0.425	.90	65
-0.149 +0.125	.48	876

Estimation of the relative areas of the surface of the coal residue and the char cross sections shows that these coatings were essentially monolayers. The fact that a single surface layer of rather fine char was able to neutralize the stickiness of the coal suggests the possibility that a coating of char dust would have a similar effect. The absence of agglomeration with caking coals in the experiments conducted in the process development unit may have been due in part to the presence of dust which coated the coal particles as they passed through

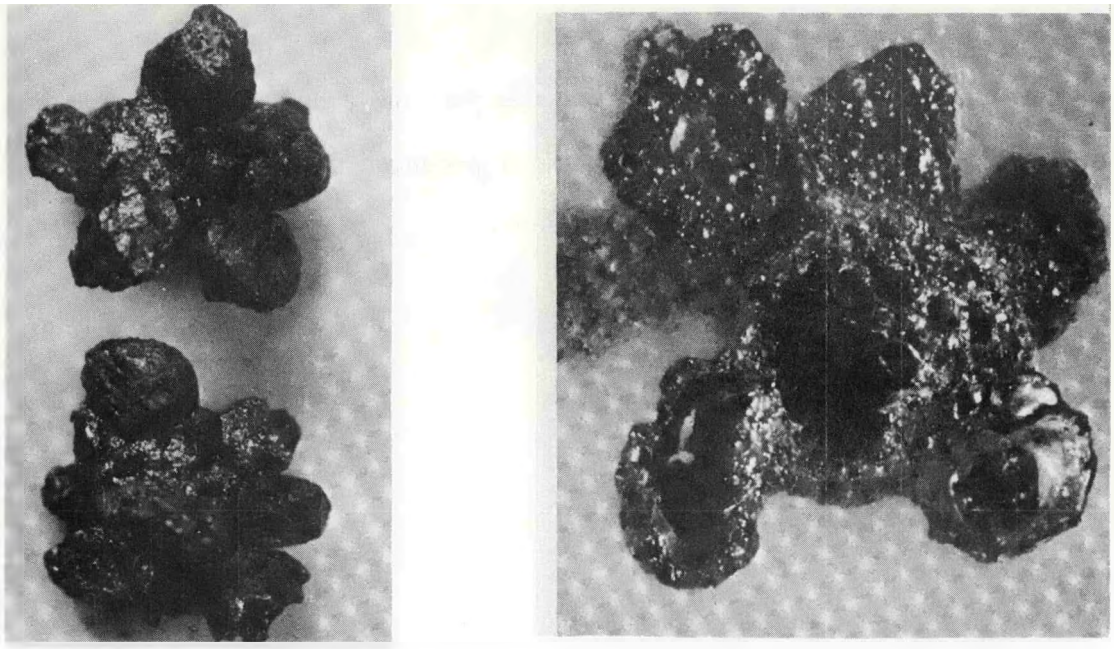

1.2 mm Char Bed

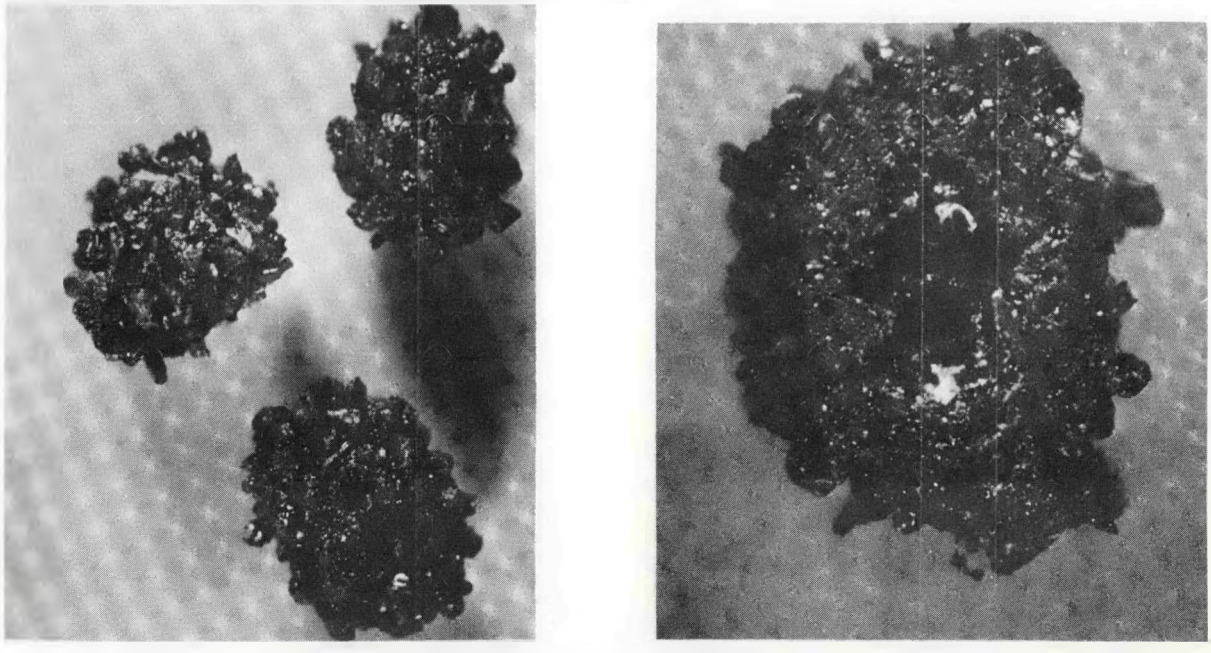

0.37 mm Char Bed

Fig. 11 - Coal-char agglomerates made in fluidized beds from 1.55 mm Pittsburgh coal and two sizes of bed char. Overall views at left, 10x. Cross sections at right, 20x.

the draft tube. The structure of the char produced in the devolatilizer was similar to that of the laboratory produced char except that the coating of coarse bed char was absent.

SUMMARY

The pressurized fluidized bed test facility was an effective tool for investigating the devolatilization of caking and noncaking coals. The results of the tests show:

- The principal gases evolved by the three coals tested are hydrogen, methane, carbon monoxide, water, ethylene, carbon dioxide, ethane, and hydrogen sulfide.
- Devolatilization occurs in two principal stages: (1) a rapid, low-temperature evolution of the bulk of the volatile matter, and (2) a slow, high-temperature evolution of gas that is mainly hydrogen.
- During the low-temperature devolatilization stage, hydrogen sulfide follows the same evolution pattern as carbon-bearing gases, implying that the sulfur involved is organic in origin rather than pyritic.
- The time required for the coal to pass through the plastic phase on heating in a fluidized bed of char at 872°C varies from about 4.5 sec for 0.5 mm particles to more than 17 sec for 4 mm particles.
- More than two-thirds of the hydrogen in the coal is evolved as molecular hydrogen and hydrocarbon gases and about 8% is evolved in the tar.
- The coal particles swell on rapid heating in the fluidized bed but do not generally burst or disintegrate. The residues of the caking coals are hollow.
- Caking coals agglomerate with the bed char. The adhering char particles form a monolayer on the surface of the carbonized coal, suggesting that fine char or dust may coat the coal particles while in the draft tube of the devolatilizer and contribute to the prevention of agglomeration.

REFERENCES

1. Archer, D. H., E. J. Vidt, D. L. Keairns, J. P. Morris, J.L.P. Chen, "Coal Gasification for Clean Power Generation," Proceedings Third International Conference on Fluidized Bed Combustion, November 1972 (NTIS Number PB-231 977).

2. "Advanced Coal Gasification System for Electric Power Generation," Westinghouse Electric Corp., Contract reports to ERDA/FE:
   a) Interim Report No. 1, NTIS No. PB-236 971
   b) Interim Report No. 2, NTIS No. FE-1514-T-4
   c) Interim Report No. 3

3. Keairns, D. L., R. A. Newby, E. P. O'Neill, D. H. Archer, "High Temperature Sulfur Removal System Development for the Westinghouse Fluidized Bed Coal Gasification Process," Preprints Fuel Chemistry Division, ACS San Francisco Meeting, Aug. 29-Sept. 3, 1976.

4. Lowry, H. H., editor, Chemistry of Coal Utilization, John Wiley & Sons, New York, 1963, pp. 188, 381, 385.

5. Jones, W. Idris, "Recent Developments in the Thermal Treatment of Coal," Journal of the Institute of Fuel, Vol. 24, March 1951, pp. 69-75.

6. Hesp, W. R., P. L. Waters, "Thermal Cracking of Tars and Volatile Matter from Coal Carbonization," Ind. Eng. Chem. Prod. Res. Develop., Vol. 9, No. 2, 1970, pp. 194-202.

7. Shah, R., P. J. Margaritis, L. K. Rath, P. Cherish, L. A. Salvador, "Operation of the Westinghouse Coal Gasification Process Development Unit," Proceedings Eleventh Inter-Society Energy Conversion Engineering Conference, September 1976.

SECTION 5.4

APPENDIX D

APPENDIX D

Paper presented at session on Purification of Low Btu Gas during ACS meeting, August 29-September 3, 1976, San Francisco

HIGH TEMPERATURE SULFUR REMOVAL SYSTEM DEVELOPMENT FOR THE WESTINGHOUSE FLUIDIZED BED COAL GASIFICATION PROCESS

D. L. Keairns, R. A. Newby, E. P. O'Neill, D. H. Archer
Westinghouse Research Laboratories
Pittsburgh, Pennsylvania 15235

ABSTRACT

High temperature sulfur removal can be achieved with calcium based sorbents (e.g. dolomite) in fluidized bed coal gasification systems now being developed for power generation. The use of dolomite offers the opportunity to meet environmental emission standards, to minimize energy losses, and to reduce electrical energy costs.

In addition to achieving the removal of sulfur from the low Btu gas, the complete sulfur removal system must be integrated with the total power plant and environment to assure compatibility. Critical requirements to achieve a commercial system include establishing criteria for "acceptable" sorbents, establishing integrated sulfur removal/gasification process design parameters, predicting trace element release, predicting sorbent attrition, developing an economic regeneration and/or once-through process option, developing a spent sorbent processing system, and establishing safe and reliable disposition options for spent sorbent. Design and operating parameters are being developed and potential process limitations identified.

This work is being performed as part of the Westinghouse Coal Gasification Program. The project is being carried out by a six-member industry/government partnership comprising ERDA, Public Service of Indiana, Bechtel, AMAX Coal Co., Peabody Coal Co. and Westinghouse. This work has been funded with federal funds from the Energy Research and Development Administration under contract E(49-18)-1514. The content of this publication does not necessarily reflect the views or policies of the funding agency.

INTRODUCTION

The production of a low Btu fuel gas from coal for combined cycle electric power generation provides the potential for improved thermal efficiency and reduced power costs compared with conventional power plants with flue gas desulfurization and can provide acceptable environmental impact. The ability to produce the low Btu gas at elevated pressure (e.g. 1500 kPa) with removal of sulfur and particulates from the high temperature gas (e.g. 800-900°C) will enable the maximum thermal efficiency to be achieved. Calcium-based sorbents, such as limestone and dolomite, have been proposed for the high temperature sulfur removal.

Westinghouse has been working on the development of a multi-stage fluidized bed gasification process for combined cycle power generation since 1970.[1,2] The goal of the program is the integration and operation of a gasifier/power-generating plant on a scale which will demonstrate the commercial operation of the process. An integrated program is underway to proceed from bench-scale laboratory research through pilot scale development and system design and evaluation to the operation of a demonstration plant. The pilot development is now being carried out in a 15 ton/day process development unit.

Westinghouse is investigating gas cleaning systems for high temperature operation (800-900°C), intermediate temperature operation (e.g. 650°C), and low temperature operation. Work has been carried out on both sulfur removal and particulate control systems. This document is limited to an overview of the high temperature sulfur removal system development work on calcium-based sorbents. This system was selected for the base concept based on the potential for high system efficiency and the high kinetic efficiency of removing hydrogen sulfide under the proposed operating conditions with an economically available sorbent. Alternate systems, such as the use of iron oxide or low temperature processes, have not been excluded as candidates for the demonstration plant and are also being studied. An intermediate temperature process is attractive in that it reduces the materials problems while maintaining a relatively high plant efficiency.

The approach to the development of the calcium-based sulfur removal system includes laboratory experimental programs utilizing pressurized thermogravimetric analysis, pressurized fluidized bed reactors, and physical and chemical characterization to develop basic data and to develop screening techniques; data analysis to develop design criteria; systems analyses to assess the technical,economic, and environmental impact of alternate sulfur removal system concepts and to assess the impact of these alternatives on the total power plant.

SULFUR REMOVAL SYSTEM

The basic gasification process utilizing the high temperature calcium-based sorbent system is illustrated in Figure 1. The gasification process has been described.[1,2] The sulfur removal process options are indicated in Figure 1: in-bed desulfurization and external desulfurization. In situ desulfurization of the fuel gas within the recirculating bed devolatilizer combines the sulfur removal and coal devolatilization in a single vessel. This approach requires compatible coal and sorbent behavior and the ability to separate sorbent and char. The external desulfurizer requires a separate vessel and associated components but provides greater flexibility. Both systems are being assessed through process simulations, PDU operation, and engineering analyses.

Two basic sulfur removal systems have been identified and investigated: once-through sorbent operation and regenerative operation. The reference once-through system and regenerative system concepts are illustrated in Figure 1. An alternate once-through system concept is also indicated which has been considered. A number of spent sorbent processing and regeneration processes have been investigated. Similarly, a number of disposal and utilization options are available. These process alternatives will be discussed in the following sections. Other options such as pretreatment of the sorbent to improve its attrition behavior or sulfur capacity and the addition of "getters" to remove alkali metals to prevent gas turbine corrosion are also being considered.

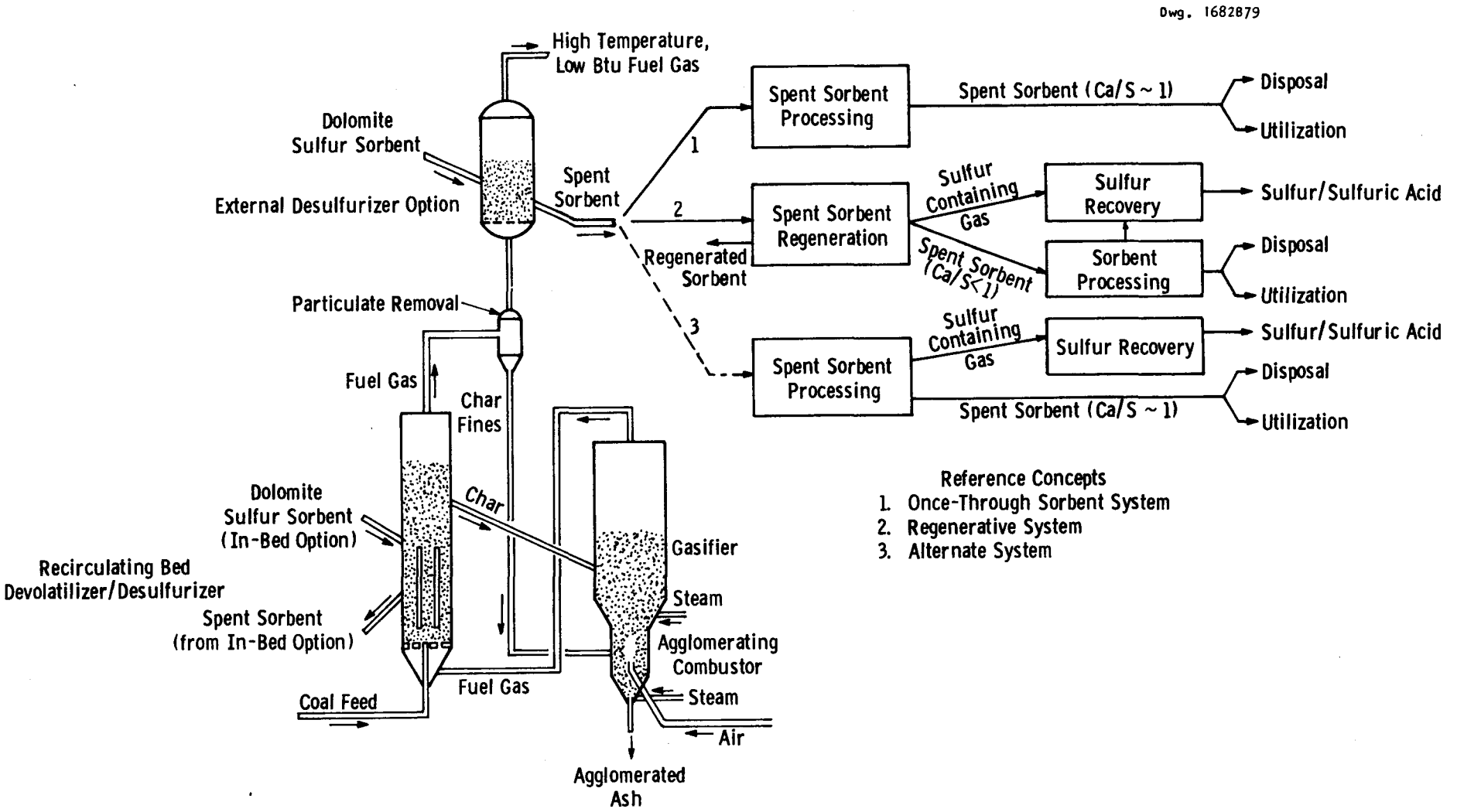

Fig. 1—Westinghouse multistage fluidized bed gasification/desulfurization process utilizing calcium-based sulfur removal system

SULFUR REMOVAL

Laboratory and engineering studies are being carried out to evaluate two areas critical to sulfur removal: sulfur removal process options and sorbent selection. These efforts parallel development work planned for the process development unit related to these areas.

Process Options

The technical and environmental performance and economic aspects of sulfur removal process options are being evaluated in order to provide a basis for selection and to define process development requirements. Two major options have been identified: once-through sorbent operation versus regenerative sorbent operation and in situ (devolatilizer) desulfurization versus external desulfurization.

Both once-through sorbent and regenerative sorbent desulfurization behavior are being developed. The PDU is currently designed for once-through sorbent operation. Trade-offs between once-through and regenerative sulfur removal exist with factors such as sorbent consumption, sorbent attrition, trace element release, and system complexity and operability being important considerations.

Sorbent Selection

Both limestone ($CaCO_3$) and dolomite ($MgCa(CO_3)_2$) can be used as sulfur sorbents under full gasification conditions at high fuel temperatures, but laboratory studies show that there are several factors which restrict their use under specific design conditions, and which impact on both the desulfurization process, and the overall power generation plant.

Limestone reacts with hydrogen sulfide only when it has calcined, a kinetic rather than a thermodynamic restriction.[3] For atmospheric pressure applications, calcined limestone should achieve 90% desulfurization of fuel gases at calcium to sulfur molar feed ratios of $\sim$1.8/1.[4] Recent fixed-bed tests by the Bureau of Mines confirm this projection.[5] However for desulfurizing low Btu gas at pressure, calcium carbonate is the stable form of the reacting sorbent, and limestone is inactive.[6]

For dolomite, at Ca/S feed ratios of < 1.2/1.0, projections from laboratory data show that almost complete reaction of the calcium content may be attained while fixing 90% of the fuel sulfur in solid form, for particle sizes up to 2000 microns.[7] For larger particle sizes reaction is apparently limited by diffusion of reactant into the solid. No significant variation was noted in testing dolomites ranging from the relatively pure massive-grained Canaan dolomite (Connecticut), through the sucrose-type dolomites (Glasshouse, Ohio), to the impure Tymochtee dolomite (Ohio).[2c] Fluidized-bed tests by Conoco Coal Development Co.* have demonstrated the excellent sulfur capture abilities of dolomite with simulated fuel gases.[8] The Bureau of Mines tests showed that half-calcined dolomite demonstrated improved sulfur removal at 1500°F over that noted at 1400°F.[5] However when they increased the desulfurizing temperature to 1600°F, they noted a drastic loss of desulfurizing action as the dolomite decomposed to the fully-calcined state. While this test has not been simulated in laboratory tests, precalcined dolomites have shown similar sulfidation reaction rates to those noted with half-calcined dolomite. Further tests are evidently required to explore this discrepancy.

The major limitations on using dolomites arise from trace-element emissions, attrition rates, and suitability for processing by direct air oxidation for disposal.

One of the major concerns in operating a gas turbine with the low Btu gas is the extent to which corrosion and erosion will limit the lifetime of the metal alloys used in the blades and stators.[2c] The alkali metals, particularly sodium, induce hot corrosion (accelerated oxidation or sulfidation attack of the metal) by depositing oxygen-excluding liquid films of sulfates on the metals. Dolomites contain sodium and potassium as impurities, and they are found both as clay mineral components, and as more volatile compounds - probably chlorides, in the carbonate rock. The range of these impurities in dolomites is enormous, e.g. Na (5-330 ppm), and K(5-6,500 ppm).[2c] Recent studies

---

* Conoco Coal Development Co. and Consolidation Coal Co. are used in this paper. Consolidation Coal Co. is used when work was performed under that organizational name.

of the release of alkalis from dolomites into fuel gas have demonstrated that significant fractions of the alkali can enter the gas stream, and that this release is essentially complete within a short fraction of the expected sorbent residence times.[2c] The resulting alkali level in the turbine feed gas is substantially in excess of that permitted by current empirical specifications for oil-fired turbines (~10 ppb Na). There are several approaches which may be taken to avoid this problem. First of all, a low-alkali dolomite may be chosen as sulfur sorbent. This is likely to be the result of an unusually fortuitous selection of power plant site. Although the available analysis of dolomites show significant variations in alkali content within a particular geological stratum from quarry to quarry and from stratum to stratum within a quarry, the majority of the analyses are of sufficient vintage to be suspect. However we have noted a consistant increase in alkali content with increasing quarry depth, so that material quarried at a depth of 100 ft may contain one order of magnitude more alkali than that quarried near the surface.[9]

An alternative to selecting a "clean" dolomite, is to pre-heat the material to release the alkalis before using the stone as a sulfur sorbent. The bulk of the alkali release occurs within 20 minutes of heating the stone to ~870°C, and after this initial release the rate of alkali loss is extremely low. The third possibility is to add materials such as aluminosilicates to the sorbent bed, or at a particulate filtration stage to getter the alkalis. It should be emphasized that several critical questions cannot be satisfactorily answered without further research. The extent to which chlorine from the coal may strip alkalis from dolomite and coal char must be investigated. In addition the turbine tolerance to the combined presence of sodium and potassium requires further experimental and theoretical investigation.[2c] The chemical fate of minor elements such as the alkalis in coal gasification is not well known. Recent studies at the Bureau of Mines show considerable

release of chlorine to the gas phase - presumably as HCl.[2c] However the mass balance for alkalis in the input and output solids was not sufficiently precise to estimate the levels of alkali in the gas phase.

It should also be noted that the turbine tolerance to alkalis is theoretically a function of total chlorine (as HCl) levels in the gas phase. The combination of high chlorine and high alkali levels may avoid corrosive sulfate deposits. This apparent advantage will be limited by direct gaseous attack of the protective oxide scales on the turbine alloys.

SORBENT REGENERATION

The consumption of sorbent by the power plant sulfur removal system may be minimized by utilizing a processing step to regenerate the utilized sorbent to an active form. Ideally the sorbent would be entirely reconstituted by the regeneration process, but in reality fresh sorbent will be required due to deactivation of the regenerated sorbent and attrition losses. Regeneration of the sulfided sorbent requires that the captured sulfur be converted to some other form, preferably elemental sulfur of commercial quality. The purge stream of spent sorbent must be processed to some environmentally acceptable or useful form. This combination of functions, sorbent regeneration-sulfur recovery-spent sorbent processing, must result in an integrated process which is compatible with the coal gasification process and is economically and environmentally acceptable.

Regeneration Process Options

A variety of potential regeneration process concepts have been evaluated for technical feasibility. Two concepts have been selected for further engineering assessment: (1) Sorbent regeneration by reaction of sulfided sorbent with steam and carbon dioxide to generate carbonated sorbent and a hydrogen sulfide gas stream; (2) sorbent regeneration by reaction of sulfided sorbent with oxygen to generate the oxide form of the sorbent and a sulfur dioxide gas stream. The chemical reactions are written, respectively.

$$CaS + H_2O + CO_2 \rightleftharpoons CaCO_3 + H_2S \qquad (1)$$

and

$$CaS + 3/2\ O_2 \rightleftharpoons CaO = SO_2 \qquad (2)$$

Steam and CO_2 Regeneration Scheme

A schematic flow diagram for the sorbent regeneration system based on the steam and CO_2 regeneration reaction is shown in Figure 2. This process is also being evaluated by Consolidation Coal.[8]

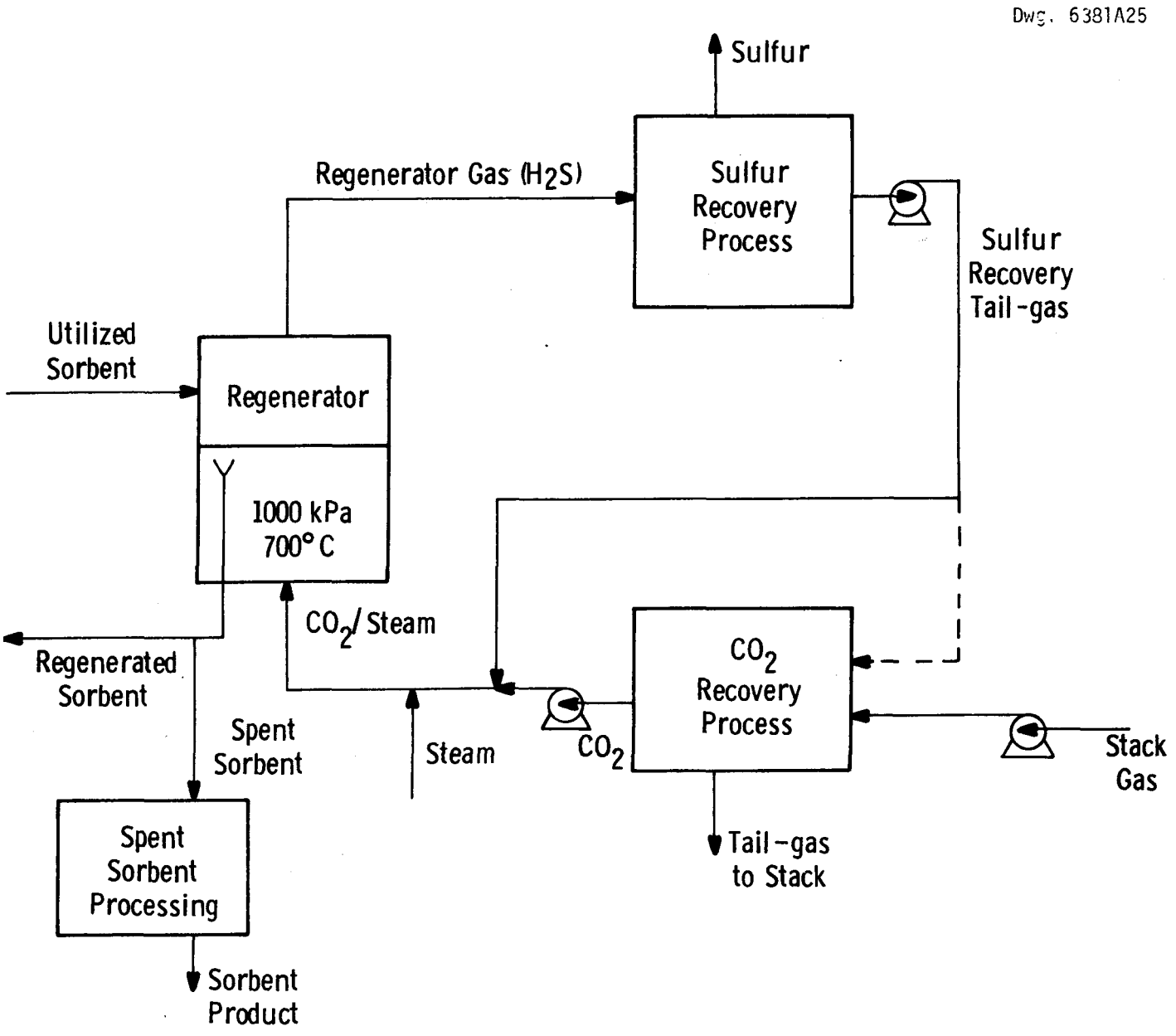

Fig. 2 — Sorbent regeneration by steam and CO_2 reaction

Three major components are involved in the sorbent regeneration system: the regenerator reaction vessel, the sulfur recovery process and the CO_2 recovery process. A number of commercial processes are available for sulfur recovery from H_2S gas streams. The specific process selection will depend largely on two factors - the level of H_2S in the regenerator gas and the optimum scheme for steam and CO_2 utilization. An H_2S volume percent of about 15% will permit the application of conventional Claus process technology. Lower H_2S concentrations will require either preliminary concentrating of the H_2S-gas, followed by Claus sulfur recovery, concentrating and recycle of the Claus plant tail-gas, or application of alternate sulfur recovery processes suitable for low H_2S concentrations such as the Stretford process (Ralph M. Parsons Co. and Union Oil Co. of California).

Make-up CO_2 for the regeneration reaction can be supplied by power plant stack gas purification. A portion of the sulfur recovery tail-gas may also require purification in order to maintain low levels of impurities (N_2, O_2, etc.) in the CO_2/steam reactant stream. Numerous commercial processes are available for CO_2 recovery - Selexol, Benfield, Catacarb, Sulfinol, and many others. The economics and environmental performance of each of these processes will differ for this application and require evaluation.

The single most important factor influencing the economics and performance of this regenerative scheme is the regenerator gas H_2S concentration. The size of the regenerator reaction vessel, the size and complexity of the sulfur recovery process, and the rate of steam consumption and auxiliary power usage all increase as the H_2S concentration is reduced. Estimates of the H_2S concentration based on reaction kinetics and thermodynamics are about 3-5 volume %.

Other factors such as regenerated sorbent activity, the required rate of sorbent circulation, the effect of the regeneration process on the power plant availability, etc., are also important to the process feasibility.

Oxygen Regeneration Scheme

A schematic flow diagram of the sorbent regeneration system based on the oxygen regeneration reaction is shown in Figure 3. An atmospheric pressure version of this process has been applied by Esso (U.K.) for their CAFB gasification process.[10]

This regeneration process is conceptually simpler than the steam/CO_2 regeneration process since only two major process components are involved: the regenerator reaction vessel and the sulfur recovery process. On the other hand, the oxygen regeneration process is necessarily a higher temperature regeneration scheme with the potential for greater sorbent deactivation. The regenerator could be operated at pressures of 200 to 1000 kPa (2 to 10 atmospheres) and temperatures of 1000 to 1100°C with SO_2 volume percents of 2 to 4 expected for the high pressure system and up to 10% for the low pressure system.

Sulfur recovery from dilute SO_2 streams is generally more expensive and complex than from dilute H_2S streams. The most highly commercialized sulfur recovery process for this application is the Allied Chemical direct reduction process (using methane or clean liquid fuels as reductant) which will work effectively on SO_2 streams down to about 4 volume % SO_2 depending upon the oxygen content of the gas.[11] For lower SO_2 concentrations a commercial concentrating step such as the Wellman-Lord process must be used. Other sulfur recovery processes applicable to SO_2 streams which are in early stages of commercialization are the Foster Wheeler RESOX process (which uses coal as the SO_2 reductant), the ASARCO-Phelps Dodge process, the Bureau of Mines Citrate process, the Westvaco activated carbon process, and the Stauffer Aquaclaus process.

While the low pressure oxygen regeneration results in a much greater SO_2 concentration in the regenerator gas, the technological and reliability problems involved in circulating the hot sorbent between vessels with greatly different operating pressures may not be easily overcome. Again, as in the steam/CO_2 regeneration process,

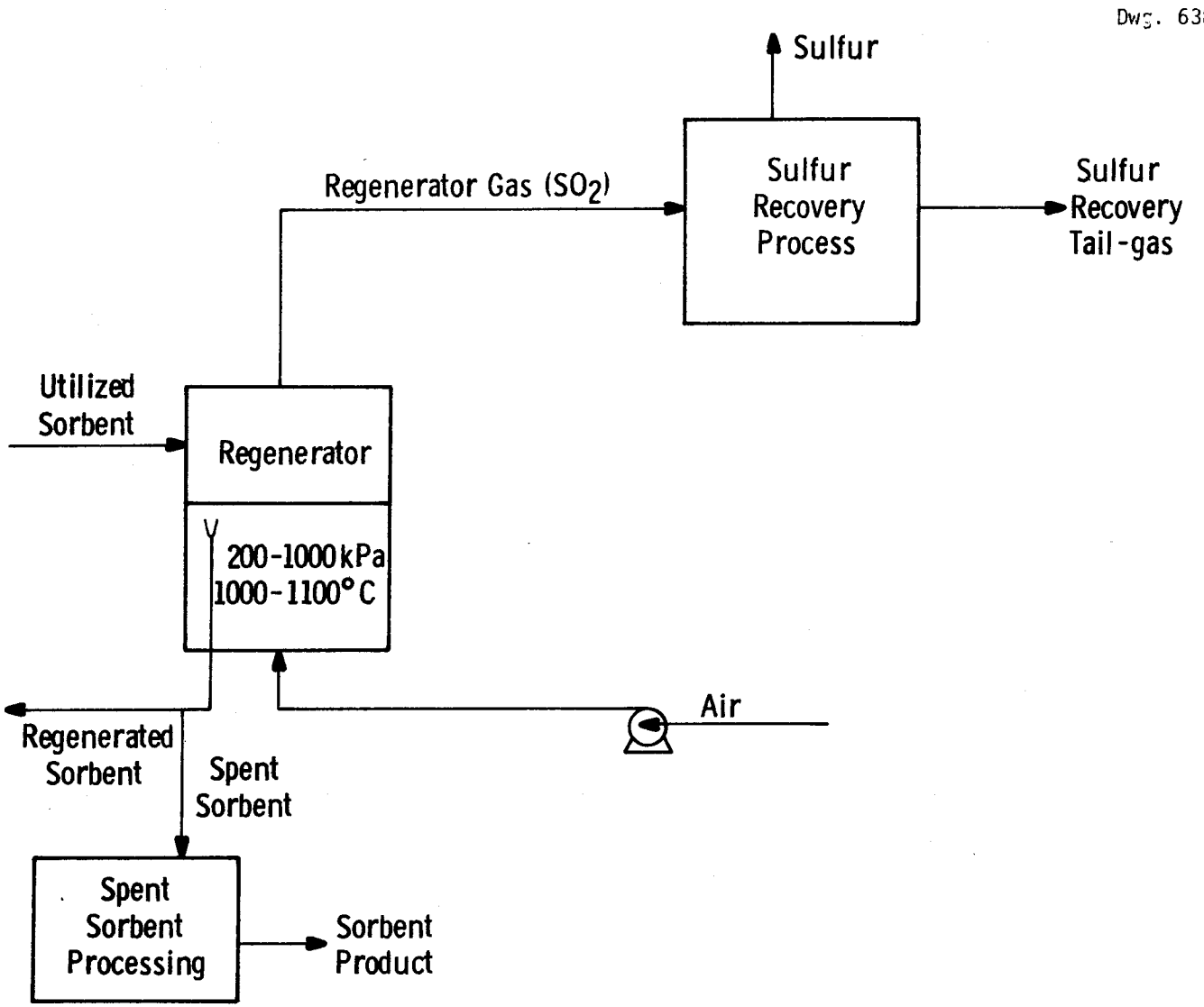

Fig. 3 – Sorbent regeneration by oxygen reaction

the concentration of the sulfur-bearing species in the regenerator gas has a dominant influence on the economics and performance of the regeneration system. Increased operating temperatures will provide greater SO_2 concentrations (thermodynamically) but may increase sorbent deactivation.

The overall economics, technical performance and environmental impact of these two sorbent regeneration concepts must be evaluated in order to determine the feasibility of sorbent regeneration, in order to select the most promising regeneration scheme and in order to identify the optimum components to be utilized in the regeneration scheme. The critical interfaces between the coal gasification system, the power generation system, the spent sorbent processing system and the sorbent regeneration system are being considered in the evaluation.

Regeneration Chemistry

It was noted by Mellor[12] that the equilibrium $CaS + H_2O + CO_2 \rightleftharpoons CaCO_3 + H_2S$ cannot be used to reform calcium carbonate, because of the low concentration of hydrogen sulfide produced. This problem may be overcome by carrying out the reaction at pressure.[13] However the early work by Pell[14] showed that calcium sulfide is rapidly deactivated, and TG studies show that only 20% of the calcium sulfide is readily converted to calcium carbonate after 10 cycles of sulfidation/regeneration, at 704°C.[b]

An encouraging feature is that the rate of sulfidation decreases very slowly as the stone is recycled and the regenerated sorbent is almost as reactive as fresh stone.[6]

The initial rate of regeneration is very fast and is apparently limited by production of the equilibrium level of hydrogen sulfide, since the initial rate increases on dropping the temperature from 700°C to 650°C. However, when the regeneration has proceeded to a certain stage (50% after 2 cycles, or 20% after 10 cycles), the rate

falls off by more than one order of magnitude. At this stage the rate can be increased by increasing the reaction temperature, so that at 870°C, all the sulfide is readily regenerated. However, the equilibrium concentration of H_2S becomes so unfavorable that this is not a technically feasible solution.

The deactivation of calcium sulfide thus becomes a chemically limiting step in regeneration. An additional clue to the mechanism of deactivation is given by the fact that when calcium sulfide is prepared by reduction of calcium sulfate, at 820 or 850°C, for 2 hours, only 26% of the calcium sulfide is regenerable.[15] This increased deactivation may be partly due to the longer residence time at higher temperatures than is customary in sulfidation reactions, since sulfidation takes about 15 minutes. Recent studies by Sun[16] have shown that longer exposure at high temperatures (871°C) during sulfidation, reduces the extent of regeneration, as does increasing the temperature of sulfidation to 950°C, while lowering the sulfidation temperature to 750°C increases the extent of regeneration. The deactivation of the calcium sulfide is always accompanied by some growth of calcium sulfide particle size, and by extensive growth of magnesium oxide crystallites in proximity to the calcium sulfide as determined by X-ray diffraction line-widths.

It can be concluded that a continuous regeneration system must operate with a low sulfur differential between the calcium sulfide content of the desulfurizer and regenerator exit streams.

Squires[17] has demonstrated that the extent of regeneration improves dramatically with partial pressures of steam of 15 atmospheres, and that 50% of the calcium sulfide is regenerable. While his sulfidation reaction conditions (700°C) may not have been severe enough to cause growth of the magnesium oxide around the calcium containing crystallites, the improved diffusivity of the reactant gases through the solid caused by raising the H_2O/CO_2 ratio may significantly improve the extent of regeneration before the reaction rate dwindles. Pell's

experiments carried out at a 1/1 ratio at 15 atm indicate little if any improvement over the TG value for extent of regeneration. The average extent of regeneration for 20 cycles is ∿13%, so that each mole of calcium will remove 2.7 moles of sulfur via the regenerator, and one mole of sulfur via the spent sorbent stream.

The calcium to sulfur molar make-up feed rate required is therefore 0.25/1 unless attrition losses are greater than 5% of the total calcium per cycle, in which case reducing the attrition loss becomes more important than improving the regenerability of the stone. Consolidation Coal Co.[8] have reported attrition loss rates of less than 1% per cycle; however it is not known if such performance can be projected to large scale units.

SPENT SORBENT DISPOSITION

The once-through and regenerative process options will produce a dry, partially utilized dolomite or limestone with particles up to 6 mm in size. In addition, fine particles of sorbent (with some ash and char) will be collected in the gas particulate collection systems. The composition of the sorbent for disposition will depend on the characteristics of the original stone, the coal feed, the selection of the sorbent processing system, and the process operating conditions. The major compounds in the waste stone from the desulfurizer or regenerator utilizing dolomite are calcium carbonate ($CaCO_3$), magnesium oxide (MgO), and calcium sulfide (CaS). Trace elements from the sorbent and coal will also be present.

Direct disposal or utilization of this material is not considered to be an option which will be generally available. Thus, processing of the spent sorbent has been incorporated in the sulfur removal system. The ultimate selection and development of a spent sorbent processing scheme will depend on many factors related to the development of the desulfurization system and the regeneration system. These factors will determine the nature of the spent sorbent and the processing required for the spent sorbent processing system. Among the factors that will affect the disposition of the sorbent are the quantity of spent sorbent, its chemical characteristics, regulations, geographical location, and the market size in the case of utilization.

Processing

A variety of spent sorbent processing schemes have been identified which could potentially convert the spent sorbent produced in a once-through or regenerative operation into a material suitable

for direct disposal or utilization.[4,19] Processing alternatives have been developed to convert calcium-based sorbents containing calcium sulfide to environmentally acceptable forms for disposal or utilization. Work by Westinghouse on the CAFB fluidized bed gasification/ desulfurization process, under contract to EPA, has identified spent sorbent processing options.[4] Experimental programs are now being carried out as an extension of this work to permit technical and economic assessments of these processes. These tests will provide information directly applicable to the subject coal gasification/ desulfurization process. Spent sorbent processing systems being considered include dry oxidation, oxidation plus carbonation, deadburning, slurry carbonation, dry sulfation, high temperature processing with coal ash, and low temperature processing with coal ash.

A dry oxidation process which converts the spent sorbent (calcium sulfide) from a once-through or regenerative operation into a calcium sulfate material has been selected as the base spent sorbent processing scheme. Experimental studies and process studies for the dry oxidation process are being performed as part of the current program.

Thermogravimetric studies of the direct oxidation of calcium sulfide to calcium sulfate have revealed some important features of the reaction which must be considered in process evaluation.

First, in most dolomitic stones, complete oxidation of the sulfided stone occurs rapidly in air at 800°C, while sulfided limestones containing more than 30 molar % CaS and the sulfides of large-grained dolomites are oxidized incompletely.

Secondly, the reaction is extremely exothermic, $\Delta H_{298} = -912$ kJ mole^{-1}, and if the temperature of the reacting solid is permitted to rise to higher temperatures, sulfur dioxide will be

emitted by one of two mechanisms. In the first mechanism direct oxidation to the oxide may occur: $CaS + 3/2\ O_2 \rightarrow CaO + SO_2$. However if low partial pressures of oxygen are developed in the system as a result of the primary reaction, then calcium sulfide and calcium sulfate interact to reject sulfur dioxide according to the reaction

$$3\ CaSO_4 + CaS \rightarrow 4\ CaO + 4\ SO_2.$$

By carrying out the oxidation reaction in a fluidized bed reactor at 800°C in excess air, both of these competing reactions may be avoided. In thermogravimetric tests at 800°C, sulfur dioxide transients in the exit gas stream were accompanied by temperature excesses. Typically 32 moles of cold air per mole of calcium are required for heat balance in a system operating at a 2/1 calcium to sulfur mole ratio in the desulfurizer. Because of the large excess of air entering the system, >3X stoichiometric, the particles should oxidize at much the same rate as they do in the TG apparatus; stone residence times greater than 30 minutes are projected to ensure that oxidation is almost complete (>90%).

The third feature of this reaction is that regenerated stone which has experienced multiple sulfidation/regeneration cycles is not completely oxidizable. A function of the calcium sulfide which is inert in the regeneration reaction is also inert in the oxidation reaction.

Based on the information available, the dry oxidation process is considered attractive for once-through operation with most dolomites. This process does not appear as attractive for once-through operation with limestones or for regenerative operation. The primary concern is the environmental impact from sorbent disposal. Further work is required to permit a comprehensive assessment of dry oxidation. Work is proceeding to investigate other processing options.

Disposal

The environmental impact of any disposed material is a function of its physical and chemical properties and the quantity involved. Two disposal alternatives will be investigated: land and ocean dumping. Environmental impact tests are planned to study the direct disposal of material from the spent sorbent processing system. These tests will be carried out using material produced in laboratory units to investigate the affect of operating conditions and in the process development unit to determine the environmental impact from material produced in the integrated process.

Westinghouse has carried out environmental impact tests on related materials as part of the CAFB fluidized bed gasification and the fluidized bed combustion programs being carried out under contract to EPA.[4,18,19,20] Leaching and activity tests have been developed at Westinghouse to assess the potential water contamination and heat release from disposing a spent bed limestone directly from a gasification process and from the spent limestone after further processing. These studies indicate the leachability and activity can be significantly reduced by further processing. Spent dolomite from fluidized bed combustion processes has also been tested[18] which indicates that if the calcium sulfide in the dolomite can be converted to calcium sulfate through the dry oxidation process, the material will be environmentally acceptable.

Utilization

The direct disposal of sorbent may not be possible or permitted in all cases. Utilization of spent sorbent is an alternative which has the potential to provide technically and economically attractive by-product. Potential applications of processed or unprocessed spent sorbent include soil stabilization, land fill, concrete, refractory brick, gypsum, municipal waste treatment. Preliminary work has been carried out in this area.[4,20,21]

ASSESSMENT

High temperature sulfur removal with a fluidized bed coal gasification system appears attractive based on available information. A number of processing options are being developed which consider integration of the sulfur removal system with a low Btu gasification - combined cycle power plant and consider the total sulfur removal system from sorbent selection to sorbent disposition. Assessment of the sulfur removal system includes:

Sulfur Removal: Dolomites are the preferred sorbent for the Westinghouse coal gasification process. Sulfur removal efficiencies of 90% are projected with mean particle sizes between 1000 and 2000 μ and a calcium to sulfur molar ratio of 1.2/1.0 for a once-through system. Combined devolatilization/desulfurization is considered attractive but compatibility must be demonstrated. The external desulfurizer option offers an alternative with greater flexibility. There appear to be ample supplies of dolomite available.

Sorbent Regeneration: Two regeneration concepts have been selected for further study. Regeneration by carbon dioxide and steam is technically feasible and is the preferred option. Calcium to sulfur molar feed make-up is projected to be 0.25/1 based on attrition losses < 5% of the sorbent per cycle. Commercial technology is available for sulfur recovery from dilute H_2S or SO_2 gas streams and for CO_2 recovery. Advanced systems, which may reduce costs, are not being incorporated into the current development effort.

Spent Sorbent Disposition: In general, spent sorbent processing will be required for once-through or regenerative operation due to the calcium sulfide present in the sorbent. Alternate processing schemes are under investigation to permit disposal or utilization of the material.

A dry oxidation process is attractive for once-through operation with most dolomites. Preliminary oxidation tests and environmental impact tests indicate this processing option will be economic and environmentally acceptable. Preliminary tests on related materials indicates utilization of the spent sorbent may be practical.

Sorbent Selection: General factors to be considered in the selection of a sorbent are the desulfurization performance, the sorbent regenerability, the spent sorbent properties, sorbent attrition behavior and trace metals release behavior. Sodium, potassium, and chlorine release is of particular importance to control gas turbine corrosion. Trace metals release to the fuel gas may be controlled by selecting a "pure" sorbent, pretreating the sorbent or utilizing a getter in the fuel gas cleaning system. Available data indicate the trace elements can be controlled to meet turbine protection requirements. Further work is required to specify the preferred method of operation.

A once-through sulfur removal system utilizing dolomite with a dry oxidation spent sorbent processing system has been selected for the reference design. Further development evaluation of the technical performance, economics, and environmental impact of the alternative sulfur removal systems under consideration must be carried out to select the most promising system. The integration of the alternative processing schemes into an optimum high temperature sulfur removal system which is compatible with the coal gasification power plant is the object of the development effort.

REFERENCES

1. Archer, D. H., E. J. Vidt, D. L. Keairns, J. P. Morris, J. L. P Chan, "Coal Gasification for Clean Power Generation," Proceedings Third International Conference on Fluidized Bed Combustion, November 1972 (NTIS Number PB-231 977).
2. "Advanced Coal Gasification System for Electric Power Generation," Westinghouse Electric Corp., Contract reports to ERDA/FE:
   a) Interim Report No. 1, NTIS No. PB-236 971;
   b) Interim Report No. 2, NTIS No. FE-1514-T-4;
   c) Interim Report No. 3
3. O'Neill, E. P., D. L. Keairns, and W. F. Kittle, "Kinetic Studies Related to the Use of Limestone and Dolomite as Sulfur Removal Agents on Fuel Processing," Proceedings Third International Conference on Fluidized Bed Combustion, November 1972, NTIS No. PB-231 977
4. Keairns, D. L., R. A. Newby, E. J. Vidt, E. P. O'Neill, C. H. Peterson, C. C. Sun, C. D. Buscaglia, and D. H. Archer, "Fluidized Bed Combustion Process Evaluation - Residual Oil Gasification/Desulfurization Demonstration at Atmospheric Pressure," two volume contract report to EPA, March 1975, EPA report number EPA-650/2-75-027 a and b, NTIS No. PB-241 834 and PB-241 835.
5. Abel, W. T., and E. P. Fisher, "Limestone to Reduce Hydrogen Sulfide from Hot Produced Gas." U.S.E.R.D.A., MERC/RI-75/3, January 1976.
6. Keairns, D. L., E. P. O'Neill and D. H. Archer, "Sulfur Emission Control with Limestone and Dolomite in Advanced Fossil Fuel Processing," Symposium Proceedings - Environmental Aspects of Fuel Conversion Technology, EPA-650/2-74-118, October 1974.
7. O'Neill, E. P. and D. L. Keairns, "Selection of Calcium-Based Sorbents for High-Temperature Fossil Fuel Desulfurization," Paper presented at the 80th National A.I. Ch. E. Meeting, Boston, September 1975, to be published in AIChE Symposium Series Volume.

8. Carran, G. P., J. T. Clancey, B. Pasck, M. Pell, G. D. Rutledge and E. Gorin, "Production of Clean Fuel Gas from Bituminous Coal," Consolidation Coal Co. report to EPA, EPA-650/2-73-049, December 1973.
9. Data Supplied by the Indiana Geological Survey.
10. Esso Research Centre, England, "Chemically Active Fluid-Bed Process for Sulfur Removal During Gasification of Heavy Fuel Oil," EPA-650/2-74-109, November 1974.
11. Hunter, W. D., Fedoruk, J. C., Michener, A. W., Harris, J. E., "The Allied Chemical Sulfur Dioxide Reduction Process for Metallurgical Emissions," in Sulfur Removal and Recovery from Industrial Processes, J. B. Pfeiffer, ed., American Chemical Society, Washington, D. C., 1975.
12. Mellor, J. W., "A Comprehensive Treatise on Inorganic and Theoretical Chemistry," Vol. III, Longmans, London, 1923.
13. Squires, A. M., "Cyclic Use of Calcined Dolomite to Desulfurize Fuels Undergoing Gasification," in "Fuel Gasification" Advances in Chemistry Series NO69, American Chemical Society, Washington, D. C., 1967.
14. Pell, M., Ph. D. Thesis, Chemical Engineering Department, The City University of New York, 1971.
15. Keairns, D. L., D. H. Archer, R. A. Newby, E. P. O'Neill, E. J. Vidt, Evaluation of the Fluidized Bed Combustion Process, Vol. I. Environmental Protection Agency, Westinghouse Research Laboratories., Pittsburgh, Pa., EPA-650/2-73-048 a. NTIS PB-231 162/9. December 1973.
16. Sun, C. C., Unpublished work, Westinghouse, 1976.
17. Squires, A. M., "Programs for Gasification of Coal in High Velocity Fluidized Beds and Hot Gas Cleaning," paper presented at Symposium "Clean Fuels from Coal", Institute of Gas Technology, Chicago, Illinois, June 1975.

REFERENCES (continued)

18. Sun, C. C. and D. L. Keairns, "Environmental Impact of Solid Waste Disposal from the Fluidized Bed Coal Combustion Process," paper presented at the San Francisco ACS Meeting, August 29 - September 3, 1976.

19. Keairns, D. L., C. H. Peterson, and C. C. Sun, "Disposition of Spent Calcium-Based Sorbents Used for Sulfur Removal in Fossil Fuel Gasification," paper for presentation at the Annual AiChE Meeting, Chicago, Illinois, November 1976.

20. Keairns, D. L., D. H. Archer, J. R. Hamm, S. A. Jansson, B. W. Lancaster, E. P. O'Neill, C. H. Peterson, C. C. Sun, E. F. Sverdrup, E. J. Vidt, and W. C. Yang, "Fluidized Bed Combustion Process Evaluation - Pressurized Fluidized Bed Combustion Development," contract report to EPA, September 1975; EPA report No. EPA-650/2-75-027c, NTIS No. PB-246 116.

21. Peterson, C. H., M. Gunnasekaran, and S. M. Ho, "Utilization of Spent Limestone from a Fluidized Bed Oil Gasification/ Desulfurization Process on Concrete," Proceedings Fifth Mineral Waste Utilization Symposium, Chicago, Illinois, April 1976.